Final Report to

Electric Power Research Institute
Contract EP-P3883/C1886
for

MM5 Modeling
in support of
The Big Bend Regional Aerosol and Visibility Observation Study (BRAVO)

From

Nelson L. Seaman, PI
and
David R. Stauffer, Co-PI

The Pennsylvania State University
Department of Meteorology
503 Walker Building
University Park, PA 16802

To

Naresh Kumar
Environment Division
Electric Power Research Institute
3412 Hillview Avenue
Palo Alto, CA 94304-1395

1 August 2003

Disclaimer

The statements and conclusions in this Report are those of the contractor and do not necessarily reflect those of the Electric Power Research Institute or the U.S. National Park Service. The mention of commercial products, their source, or their use in connection with material reported herein is not to be construed as actual or implied endorsement of such products.

Acknowledgements

The work performed under this project by Penn Sate University was part of a team effort that involved scientists from many institutions. We acknowledge the many helpful discussions with Dr. Christian Seigneur of AER, Inc., and other BRAVO project scientists on meteorological and chemical data pertaining to the Big Bend National Park and its surroundings over North America and the Gulf of Mexico. We also wish to acknowledge Desert Research Institute for supplying special meteorological data sets collected during the BRAVO field campaign of July-October 1999.

This report is submitted in fulfillment of the EPRI Contract EP-P3883/C1886 (PSU Ref. No. 51412).

TABLE OF CONTENTS

List of Figures

List of Tables

Abstract

The MM5 model with four-dimensional data assimilation (FDDA) has been applied to the region surrounding the Big Bend National Park as part of the BRAVO study on three nested-grid domains having grid resolutions of 36-, 12- and 4-km. The 36- and 12-km domains were run for the period from 1 July to 31 October 1999. Additional runs were made using the 4-km domain for two 10-day Intensive Periods in mid-August and mid-October. Data were assimilated into each model run using analysis-nudging on the 36-km and 12-km domains and obs-nudging on the 12-km and 4-km domains. Model output was validated by visual inspections and by statistical evaluations. Evaluation of the statistics in comparison with standard targets for accuracy led to the conclusion that the wind, temperature and mixing ratio fields are of suitable accuracy for use in regional and inter-regional transport studies and for other air-quality applications. For most variables and levels, the 12-km solutions were found to have lower errors than the 4-km and 36-km solutions.

Executive Summary

The MM5 model with four-dimensional data assimilation (FDDA) has been applied to the region surrounding the Big Bend National Park as part of the BRAVO study on three nested-grid domains having grid resolutions of 36-, 12- and 4-km. The 36- and 12-km domains were run for the period from 1 July to 31 October 1999. All grids were configured with 35 layers in the vertical direction, having greater resolution near the surface and in the boundary layer, with deeper layers aloft. Additional runs were made using the 4-km domain for two 10-day Intensive Periods in mid-August and mid-October. The study period was modeled using 5 1/2 day segments, with the model being restarted with initial conditions and lateral boundary conditions supplied from NCEP analyses. Data were assimilated into each model run using analysis-nudging on the 36-km and 12-km domains and obs-nudging on the 12-km and 4-km domains. Special observations available during the BRAVO study consisted mostly of hourly radar wind profiler data at 10 sites in the 12-km domain. Two of these profilers were located within the 4-km domain at Eagle Pass and Big Bend. Additional observations from surface sites and radiosondes were also assimilated. All data fed to the FDDA system were carefully quality checked before being assimilated and questionable data were discarded.

Model output was validated by visual inspections of plotted fields for all predictive variables and selected diagnostic variables, plus extensive statistical evaluation. Given the length of the BRAVO study period, the emphasis was placed on statistical evaluations for the root mean square error (RMSE), mean absolute error (MAE) and mean error (ME), (or bias). The statistics were calculated over the 36-km, 12-km and 4-km domains for each 5 1/2-day segment and were compiled in tables by segment, intensive period, month and for the full four-month BRAVO study period.

Evaluation of the statistics in the tables, along with examination of plotted hourly statistics and spatial fields of the model variables led to the following major conclusions:

1. Examination of results from the August and October Intensive Periods indicates that the MM5 simulations for the 12-km domain have consistently smaller errors than those occurring on the 4-km domain.

   This result is partly due to the different size of the domains and the fact that the 4-km domain contains terrain that is on average much more complex, while the 12-km domain includes wide areas of the Great Plains. Also, the greater resolution of the 4-km grid allows considerably more fine-scale structure to develop in the model solutions, especially near the surface.

   Temperature and moisture errors on the 4-km domain are larger than on the 12-km domain, in part, because the land-use types in the former are heavily dominated by arid and semi-arid climates. While the MM5 recognizes these land-use categories, it can be inferred from the results that the soil moisture availability for arid land-use types was specified to be too high, resulting in a pattern of

higher-than-observed mixing ratios in the surface layer over avid areas and cooler temperatures.

2. The model simulations of the Intensive Periods indicate that having only 12-km and 36-km MM5 solutions for the full four-month BRAVO period is not a handicap. The 12-km fields have generally lowest errors for wind, temperature and mixing ratio, and they contain sufficient detail to capture the regional flow.

3. The four-month MM5 simulations on the 12-km domain have errors for surface temperature and moisture that are well within the standard targets for accuracy established independently by ENVIRON Corp. Consequently, these fields should be suitable for use in air-quality studies.

4. The biases (MEs) found on the 12-km domain in the wind speed and direction for all layers and in all model run segments are small and fall within the standard targets for accuracy. This demonstrates that the 12-km wind fields are suitable for air-quality studies, including regional and inter-regional transport investigations.

5. For the 12-km domain, the small values of MAE for wind direction and RMSE for wind speed in the nominal PBL (30-1500 m AGL) and the lower free troposphere (1500-5000 m) are well within the standard targets for accuracy at all levels.

   The RMSE and MAE wind speed and direction statistics reveal that the instantaneous local wind errors remain quite modest over all averaging periods from 5 1/2 days to 4 months. This is a favorable result for modeling regional and inter-regional transport because the majority of trace gases and aerosols are transported in these layers.

6. On the 36-km domain, evaluation of errors within the same region covered by the 12-km domain indicates that wind speed and wind direction errors generally are larger than those found in the 12-km solutions. The differences are substantial and definitely are not due solely to the lack of an independent data set for validating the 12-km solutions (which use obs-nudging based on wind data that are assimilated on that domain).

   The loss of accuracy in the 36-km solutions is rather large for both wind speed and direction. Nevertheless, the directions simulated on the 36-km domain are accurate enough to fall within the benchmark values for most layers and most segments. Wind speed MEs and RMSEs above the surface in the 36-km solutions are greater than the benchmarks, so that the effect on regional and inter-regional transport must be considered significant. In the surface layer, however, the 36-km RMSE for speed is within the benchmark. Therefore, the 36-km winds are only marginally suitable for use in air-quality applications. In general, the 12-km wind fields should provide more accurate solutions for transport calculations.

7. The 36-km temperature fields have, in general, somewhat larger errors than those found in the 12-km temperature fields. However, the 36-km solutions have slightly smaller errors for the water-vapor mixing ratio. The differences are not significant in either field.

   Since the differences in the 36-km and 12-km solutions are not very large for temperature or mixing ratio, it is concluded that both are acceptable for air-quality applications. However, the 12-km solutions are preferred because of the impact of temperature on air chemistry and they should have more fine-scale detail than the 36-km solutions.

1. INTRODUCTION

1.1 Background

The U.S. National Park Service has been entrusted with the management and care of many of the most priceless natural treasures of the nation. As population and development pressures grow, the value of these treasures and the importance of protecting them for the enjoyment of future generations become ever greater. The National Park Service (NPS) has a long history of providing necessary but controlled public access, careful development of facilities, and protection of the delicate ecosystems and geologic formations within the parks. The Electric Power Research Institute (EPRI) has long been a partner with federal, state and local governments and private sector stakeholders to support high-quality environmental research aimed at improving our understanding of how natural and anthropogenic trace emissions affect the environment and how humans can develop effective and low-cost methods to sustain these natural treasures.

Traditionally, protection of the national parks concentrated primarily on local activities associated with their use (roads, trails, displays, food and lodging, wildlife and forest management, etc.). However, over the past several decades it has become increasingly evident that a serious non-local threat to the health and beauty of the parks has emerged in the form of worsening air quality. Perhaps the most visible evidence of this threat has been found increasingly across the Southwest U.S., where the breathtaking pristine vistas that have always been a key part of the region's natural beauty have been degraded by haze that seems to grow more ubiquitous year by year. The more reactive chemicals in these haze aerosols, which are composed largely of sulfates, nitrogen oxides, hydrocarbon particulates, and ozone (the most serious species can vary from region to region), can also upset the delicate balances of vegetation and streams, and can attack vulnerable archeological sites. Consequently, EPRI and NPS, along with other government agencies and private stakeholders, have sought to identify the primary sources of air pollution affecting the parks and to develop strategies to reduce the emissions that pose a threat to their ecological health.

The Big Bend National Park (BBNP) along the upper Rio Grande in west Texas is one of the parks that has come under serious attack from non-local air pollution in recent decades. A detailed source attribution study to identify specific emitters affecting the Park is a difficult subject and is not the subject of this report. However, it is clear that, while BBNP lies in a generally undeveloped area, distant sources of emissions that might affect it have multiplied rapidly as industrialization intensifies in East Texas, northern Mexico and more distant regions. Emissions from these regions can become a threat to air quality in BBNP hundreds of kilometers away through a combination of regional meteorology and complex air chemistry. The climatology of the region is especially favorable for transport from these potential source regions to the park during the summer and early autumn.

The resultant haze over BBNP is believed to consist of aerosols composed primarily of sulfates and hydrocarbon particulates. The aqueous chemistry largely responsible for secondary aerosol formation in this region is promoted by the rich source of water vapor over the Gulf of Mexico, which lies upwind during the typical warm-season flow patterns often associated with haze

events. This general assessment, however, is much too imprecise to be the basis for either a scientific understanding of the problem, or for developing an effective and economical regional control strategy. Therefore, the Big Bend Regional Aerosol and Visibility Observation (BRAVO) Study was been undertaken with the ***primary objectives*** being (a) *to understand the long-range, trans-boundary transport of visibility-reducing particles for the regional sources in the U.S. and Mexico, and (b) to quantify the contributions of U.S. and Mexican source regions and source types responsible for poor visibility at BBNP.*

Expanding on these primary objectives, additional goals that are a part of BRAVO include:

- Determination of the chemical constituents of the fine particles responsible for regional hazes along the U.S.-Mexico border, inclusive of BBNP;
- Determination of the effects of meteorology, including moisture from the Gulf of Mexico on visibility-reducing particles;
- Evaluation and improvement of accuracy of atmospheric models and source-attribution methods through the use of atmospheric tracers and updated source emissions profiles.

1.2 BRAVO Activities and Modeling

In its Solicitation of Interest distributed 8 June 2000, the BRAVO science committee presented a summary of activities then underway that outlined the activities in support of these objectives. Of central importance, the BRAVO field study was conducted from July through October of 1999 to obtain the necessary observational database from which to improve our understanding of the air pollution affecting the BBNP. **Figure 1** shows the locations of the upper-air meteorological network and the tracer-release sites operated during the field study. Monitoring of the aerosols and evaluation of their constituents was an extensive important part of the BRAVO field program, but will not be discussed in this report. Rather we focus on the meteorology of the BRAVO study period and its simulation using numerical modeling techniques.

Figure 1 indicates that the upper-air network had fairly reasonable density for defining the mesoalpha-scale (200 - 2000 km) wind flow over the BRAVO study region. The average spacing of the upper-air sites over Texas, Oklahoma and Louisiana was about 300 km, and included 10 radar wind profilers. The profilers are particularly helpful for resolving the mesoscale wind patterns because they monitor the atmosphere continuously, rather than once every 12 h, as is the case for the standard National Weather Service (NWS) radiosonde network. Six of the profilers were located within 500 km of BBNP. Thus, the regional-scale transport of airborne pollutants over Texas should be defined rather well.

However, this does not mean that sufficient observations are available to adequately define all aspects of the meteorology associated with poor visibility in the region. For example, a glance at

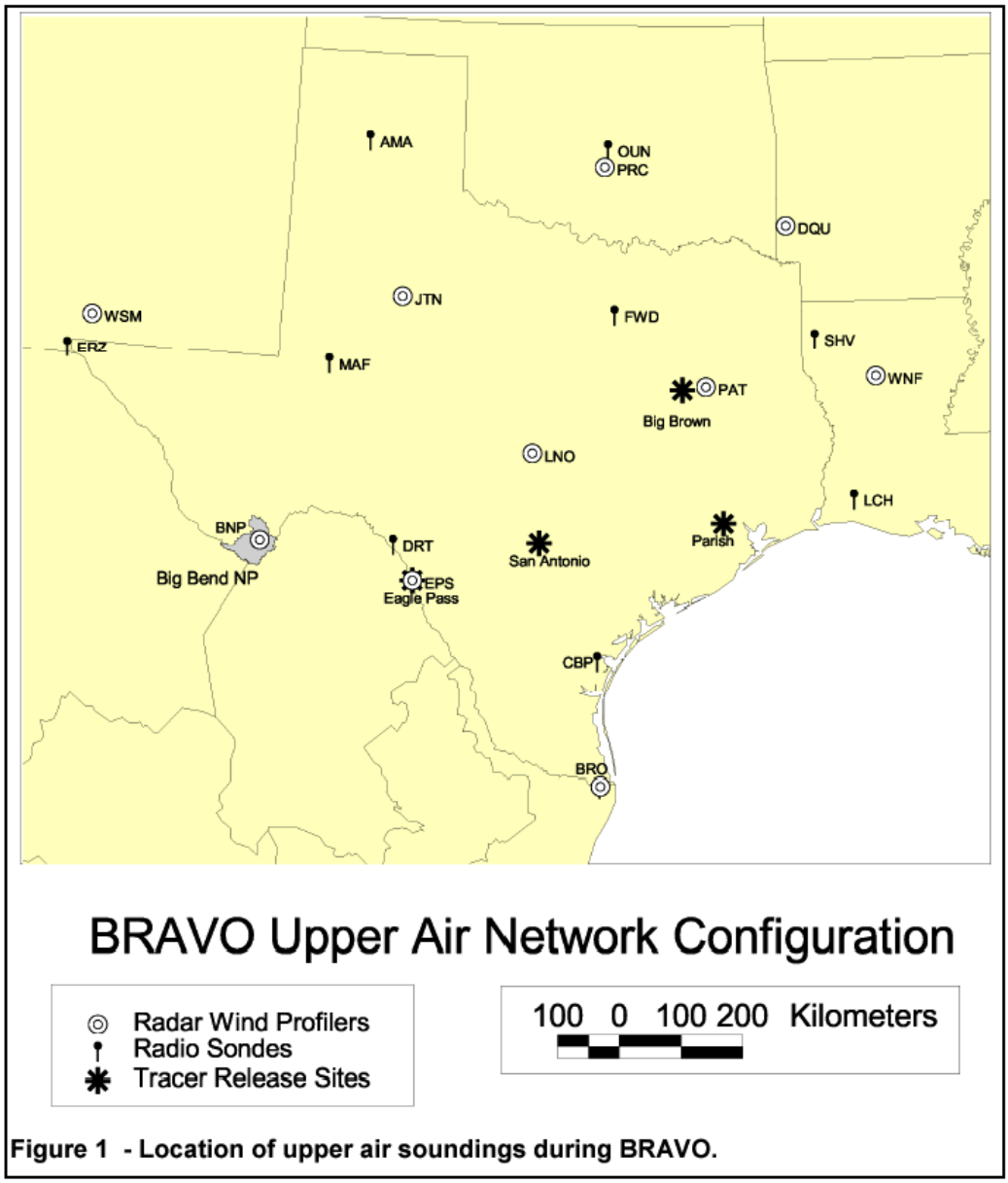

Figure 1 - Location of upper air soundings during BRAVO.

Figure 1. Location of upper air sounding network operated during BRAVO.

Figure 1 reveals that the enhanced observing network stops abruptly at the Rio Grande. Without similar detailed observations in Mexico, there exists a critical gap in the data necessary to define the regional and inter-regional transport. Furthermore, the meteorological impacts on aerosol formation and concentrations over BBNP are not limited to the winds. Thermodynamics, moisture and turbulent mixing are also important, but it appears that there are no supplemental mass-field measurements to assist in defining these variable fields. Because of these limitations in the database, the BRAVO committee recognized that 3-D numerical meteorological modeling is important in order to fill in the gaps in the observations.

The Solicitation of Interest identified the MM5 mesoscale model as a potentially useful numerical tool to perform the meteorological modeling needed to support the BRAVO goals. Among the MM5's benefits are its widespread prior use and evaluation for air-quality applications (including extensive peer review of results), capability for four-dimensional data assimilation (FDDA) for either analyses or individual special observations, a wide range of well-tested physical parameterizations, availability in the public domain, and ongoing user support through the National Center for Atmospheric Research (NCAR). Also, several groups of scientists using MM5 have extensive experience with both its internal structure and with air-quality applications. The BRAVO science committee has proposed that MM5 be used on three nested domains having resolutions of 36-, 12- and 4-km (**Figure 2**). The terrain for the 12-km and 4-km domains are shown in **Figures 3 and 4**. We agree that MM5 is the best choice for meteorological modeling in support of BRAVO and that the domains proposed by the committee are reasonable for this study.

1.3 Meteorological Influences Affecting Air Quality of BBNP

The meteorological processes affecting the chemistry of haze production and its arrival at BBNP are far more complex than simple horizontal advection by the winds. Before discussing the design of the modeling system, it is worthwhile to review some of the important meteorological processes that are expected to be relevant for BRAVO.

First, as noted above, the climatology of the region in summer and early autumn includes a fairly common transport corridor from the Gulf of Mexico to the upper Rio Grande Valley. These conditions are often initiated by the westward extension of the Bermuda High over the southeastern U.S. and low pressures over the Mexican Plateau during the early summer. The Bermuda High is a very large quasi-stationary synoptic-scale feature whose east-west axis frequently lies between 30-40 N during this time of year. It leads to strong surface moisture fluxes over the Gulf of Mexico and generally northward transport of that moisture over the continent. The onshore low-level advection often carries the moist air over land from the Gulf toward the north-northeast to the Great Plains and up the Mississippi and Ohio Valleys. However, in some cases, the flow from the western Gulf is toward the west-northwest in the direction of the BBNP. This scenario may occur when the axis of the Bermuda High builds westward and northward or when pressures over the Mexican Plateau are lower than normal. For example**, Figure 2** shows the sea-level pressure analysis for 25 July 2000 from the National Centers for Environmental Predictions (NCEP). The figure indicates light southeasterly winds at the surface across East and Central Texas and east-southeasterlies in the Rio Grande Valley

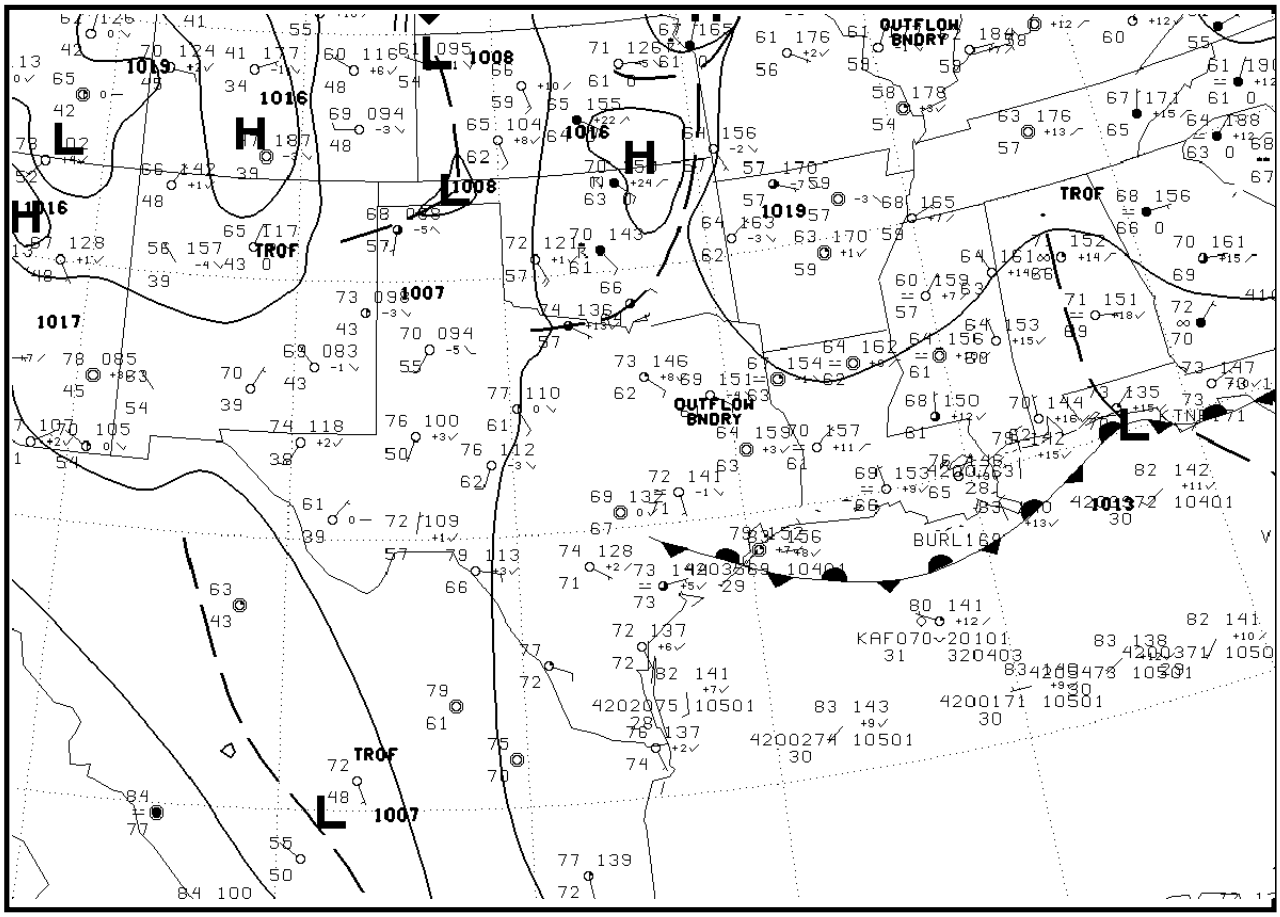

Figure 2. **NCEP analysis of observed sea-level pressure (mb) for 1200 GMT, 25 July 2000. Isobar interval is 4 mb.**

associated with a northward shift of the surface Bermuda Ridge into the Ohio Valley. At the same time, the winds near 3 km (700 mb) over Texas are from the northeast (**Figure 3**) in response to a strong upper-level ridge over Northwest Mexico.

While the synoptic conditions described above demonstrate a common scenario for the advection of moist air from the Gulf across the emissions source areas in Texas and Mexico, there are a number of other physical processes that also can have significant effects on the production and concentrations of aerosols leading to poor visibility in the vicinity of BBNP. For example, the formation of some of the more important secondary aerosol species from the original emissions is accelerated by aqueous chemistry. In particular, sulfates can form rapidly from SO_2 as a result of the chemical reactions occurring in cloud droplets. These sulfates can also be removed efficiently from the atmosphere by precipitation due to their high solubility in water. Furthermore, in the typically unsaturated region around BBNP, haze is highly dependent on the hygroscopic nature of the sulfate particles and other secondary species left over from these aqueous chemistry reactions after the clouds dissipate. Thus, cloud formation and humidity in the upstream air mass that eventually reaches the BBNP are extremely critical to the development of hazy conditions.

In addition to the moisture source over the Gulf of Mexico, horizontal winds, and emissions contributed from East Texas and northern Mexico, several other factors help to control the moisture content and pollution concentrations in air streams transported in the direction of BBNP. Perhaps the most important factors involve the mixed-layer depth and related processes at its upper and lower boundaries. Typically, the mixed-layer depth during the warm season may average about 1 - 1.5 km along the Gulf Coast, but it can easily reach 3 km deep over the arid regions of West Texas. That means that during its transport from the Gulf, the moist air of the coastal boundary layer will undergo sensible heating and entrainment of dry air from aloft. For example, in the case shown in **Figures 2 and 3**, notice that the dew-point depression at 700 mb over most of Texas is more than 20 C. Entrainment of this dry air into the planetary boundary layer (PBL) tends to lower the mean relative humidity. The result is a decrease of the mean cloudiness toward the west. Thus, the visibility in a given case will depend not only on the particulate load and species content, but also on whether the humidity remains high enough to cause deliquescence of the hygroscopic particles. On the other hand, if the air farther aloft above the moist boundary layer is extremely warm (perhaps advected eastward from the Mexican Plateau), then a strong stable layer will exist that caps the boundary-layer air and inhibits mixed-layer growth and entrainment. This elevated "lid" is especially frequent over TX and OK in the spring and early summer, and can be associated with outbreaks of severe thunderstorms and tornadoes from TX to the Midwest. Thus, the stability of the air column, the growth of the mixed-layer depth from the Gulf toward the west, and entrainment of dry air from aloft are all important factors affecting boundary-layer humidity and the opportunity for deliquescence of hygroscopic particles.

The land surface is a further source of moisture through direct surface evaporation and transpiration, even over the semi-arid regions of Mexico and West Texas. If surface moisture fluxes are larger than normal, as may occur following an outbreak of thunderstorms or

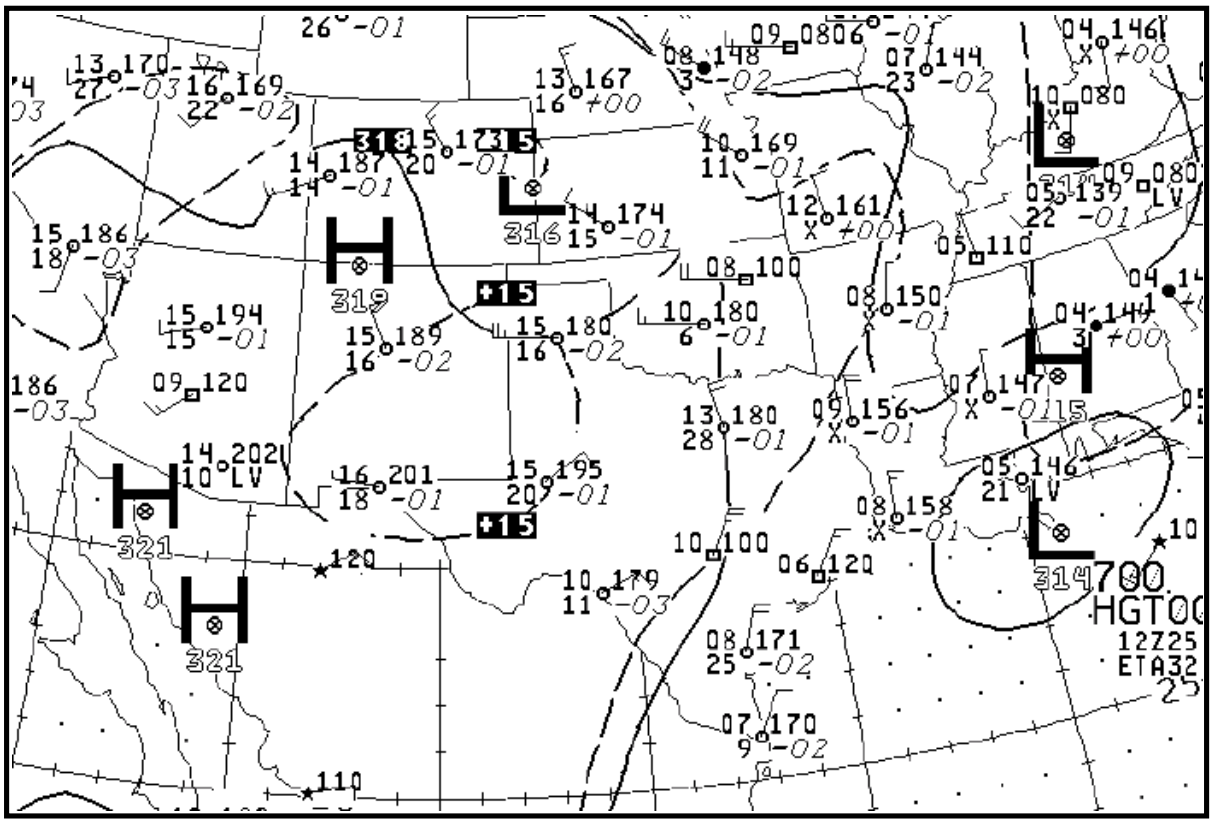

Figure 3. NCEP analysis of 700-mb heights (dm) and temperatures (C) for 1200 GMT, 25 July 2000. Contour interval is 30 m. Isotherm interval is 5 C.

the passage of a tropical storm, they may result in a more moist, shallower and cooler boundary layer. Post-precipitation cases, therefore, can be conducive to lowered visibilities as well.

Except for a few research sites, there are very few direct measurements of evapo-transpiration or soil moisture in the U.S. or Mexico. Meteorologists have had to develop alternative methods to estimate soil moisture in order to estimate the surface moisture flux. The vegetation type, in general, is a strong function of the average soil moisture. Therefore, meteorologists often estimate the mean soil moisture on the basis of the vegetation cover, or the "land use" category. Although the mean or climatological value of soil moisture is valuable, the actual soil moisture on a given day can vary considerably due to the antecedent rainfall and evaporation rates over the previous days and months. In recent years, progress in estimating soil moisture has been made by the implementation of "off-line" soil-hydrology models, such as the Noah land-surface model at NCEP, which uses as estimates of observed surface temperatures, humidities, clouds and rainfall derived from the NOAA network of NEXRAD WSR-88D radars (corrected with rain-gauge data) as its inputs. Although imperfect, these time-dependent soil-moisture products are valuable for reducing uncertainties in calculations of the surface moisture flux in numerical weather prediction models. However, correct use of these land-surface model estimates of soil moisture in weather prediction modeling systems requires that the same land-surface model be embedded in the weather model, or else serious imbalances in the surface fluxes can develop.

In addition to the thermodynamics associated with the land surface, several other mesoscale factors can have significant influence on the aerosol concentrations, as well. Among these are the development of nocturnal low-level jets. These high-speed winds develop at night in the middle and upper regions that had been part of the previous day's convective PBL. Existing in relatively thin layers often less than a kilometer in depth, they can lead to very rapid transport of airborne pollutants over long distances. Also, the complex mesobeta-scale (20-200 km) terrain of the Big Bend region can induce channeling of the winds, particularly in stable conditions. The terrain also can induce buoyancy-driven mountain-valley breezes, causing pollutants to be carried vertically upslope or downslope, depending on the stability regime. Precipitation, although generally not widespread in West Texas, can be important in certain cases. As discussed above, sulfates are highly soluble and wet deposition can be a dominant removal mechanism. During the summer and early autumn, individual thunderstorms (often induced in part by the irregular heated terrain) and an occasional tropical storm are the most important rainfall generators. These storms can have significant feedbacks on soil moisture and the surface fluxes for days or even weeks. Thus, a modeling project centered over West Texas and having a duration of months must involve careful planning to ensure the accurate representation of a host of meteorological processes likely to influence air quality over the region.

2. METHODOLOGY

2.1 Model Version, Domains, Resolutions and Experiment Production

The non-hydrostatic 3-D MM5 mesoscale model (Grell et al. 1994) was used for the numerical modeling of the meteorology during the BRAVO study period. The MM5 is uses a terrain-following sigma vertical coordinate (non-dimensionalized pressure) and supports multiple grid

nesting, a full array of physical parameterizations, and four-dimensional data assimilation. Details of its design will not be reviewed here and interested readers are directed to Grell et al. (1994) for further information. The latest public-release version of the modeling system available from NCAR at the time of the BRAVO numerical modeling study (MM5v3) was used as the basis for all model runs. With very few exceptions (see Section 2.4), all codes used in the BRAVO meteorological modeling were selected from standard options of the NCAR-supported publicly available software.

Penn State adopted a triply nested domain configuration, as designed in agreement with the BRAVO science committee. The nested domains had horizontal grid resolutions of 36-km, 12-km and 4-km, and are shown in **Figure 4**. The terrain for the 12-km and 4-km domains is shown in **Figures 5 and 6**, respectively. In particular, **Figure 6** reveals that much of West Texas and northern Mexico have extremely rugged terrain.

Each domain was applied with 35 vertical layers. The middle of the first layer (first computation level) was at 18 m above ground level (AGL). Above the first level, the layer thickness was gradually increased with height, so that the greatest resolution was be in the boundary layer. The model top was placed at 50 mb, instead of the usual 100-mb top often used in air-quality applications involving the MM5. The high model top allowed more of the lower stratosphere to be included in the domains to ensure that overshooting updrafts in deep thunderstorms could not approach or reach the model's lid, which could cause numerical instability. Objective analyses for initial and lateral boundary conditions were generated by horizontally interpolating archived NCEP Eta-model fields onto the 36-km MM5 domains as the background. The finer grids of the MM5 were initialized by interpolating from the 36-km-grid fields. In addition three-hourly objective surface analyses were generated from the surface observations for use in the model's data assimilation system (Sec. 2.3).

The MM5 runs were produced as a series of segments, with most segments being 5 1/2 days in length. Re-initialization of the model at the end of every 5 1/2 days ensured that there would not be an accumulation of numerical errors that could degrade the usefulness of the model fields (also see Sec. 2.3). A 12-h overlap was provided between each segment, representing a "spin-up" period during which the model can come into dynamical balance from the somewhat unbalanced initial states. The spin-up periods at the beginning of each segment should always to discarded when using the model outputs to perform subsequent studies for air-quality applications. The 36- and 12-km domains were run simultaneously using two-way interactive nested grids for the entire four-month BRAVO period. Because of the heavy computational burden imposed by very high grid resolution, the 4-km domain was run for two limited intensive-study periods of about 10 days each and selected by the BRAVO committee. The first intensive period extended from 1200 UTC, 15 August to 1200 UTC, 26 August 1999. The second intensive period was defined from 0000 UTC, 7 October through 0000 UTC, 16 October 1999. The intensive study periods were divided into two run segments each. The 4-km domain was run with a one-way interactive nest interface, based on hourly fields saved from the 12-km model domain. Complete MM5 output fields were written and archived for all domains at 1-h intervals for the appropriated study periods.

MM5 domain locations

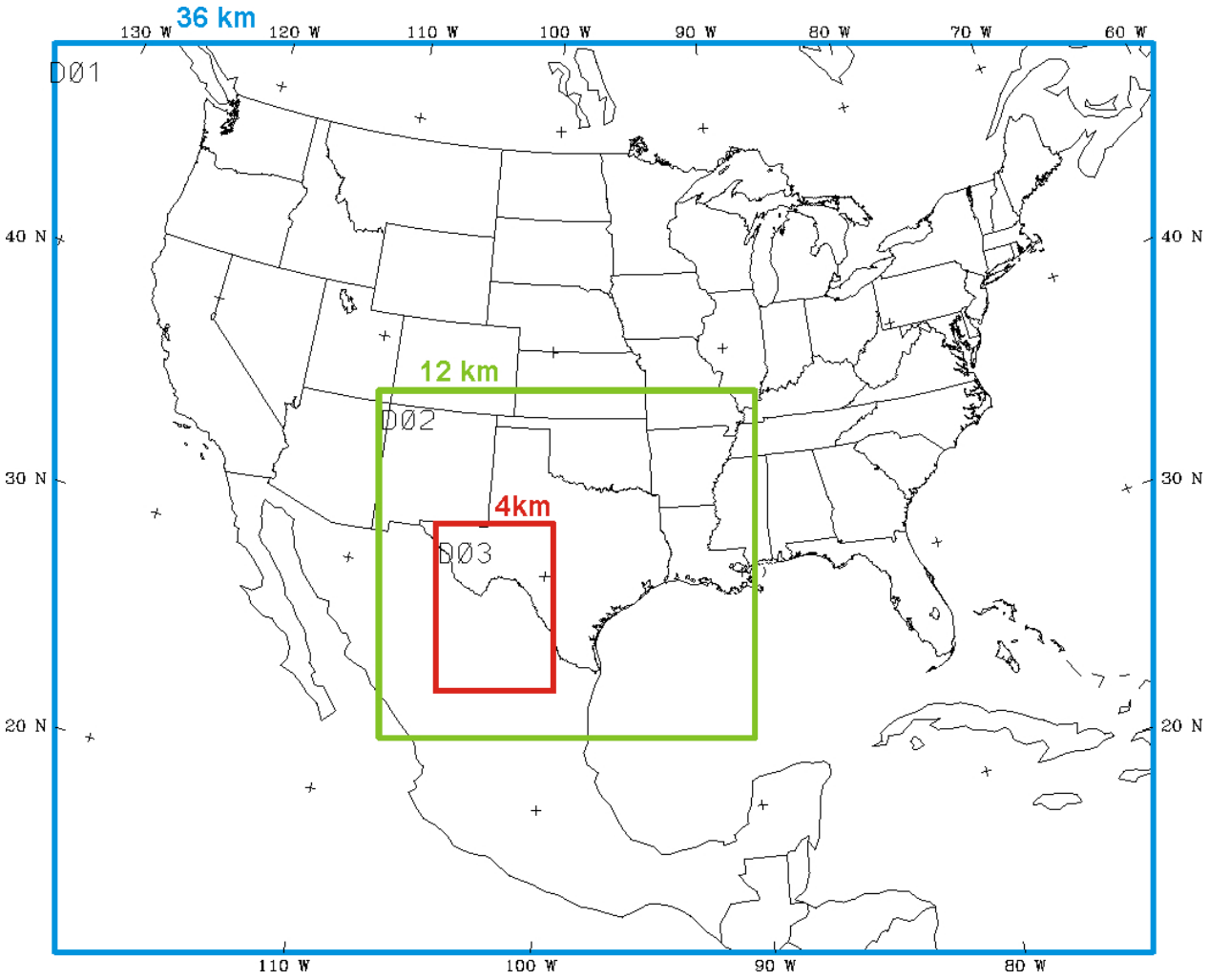

Figure 4. Location of the triply nested MM5 domains, having grid resolutions of 36-, 12- and 4-km.

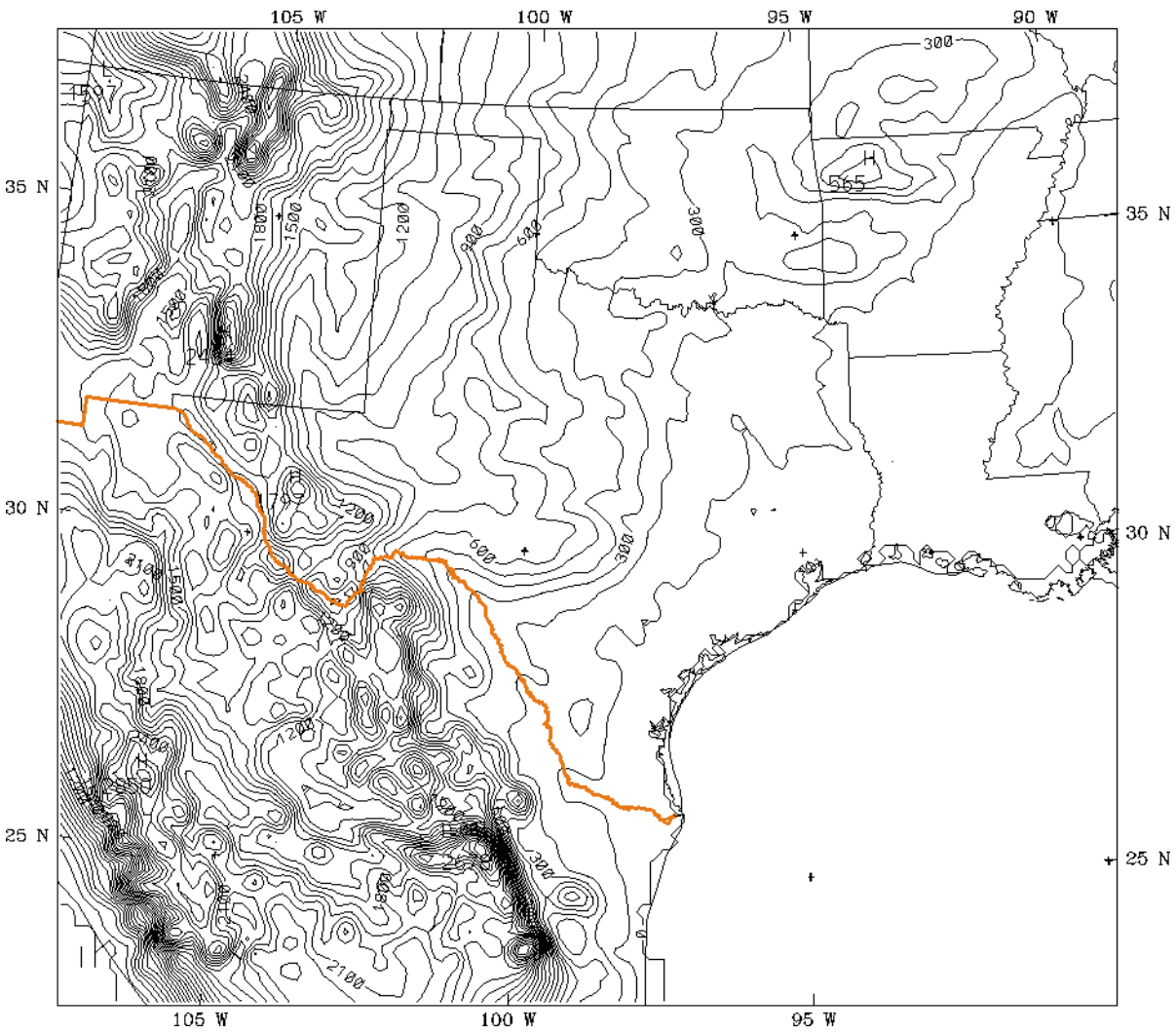

Figure 5. Terrain (m) on the 12-km MM5 domain. Contour interval is 100 m.

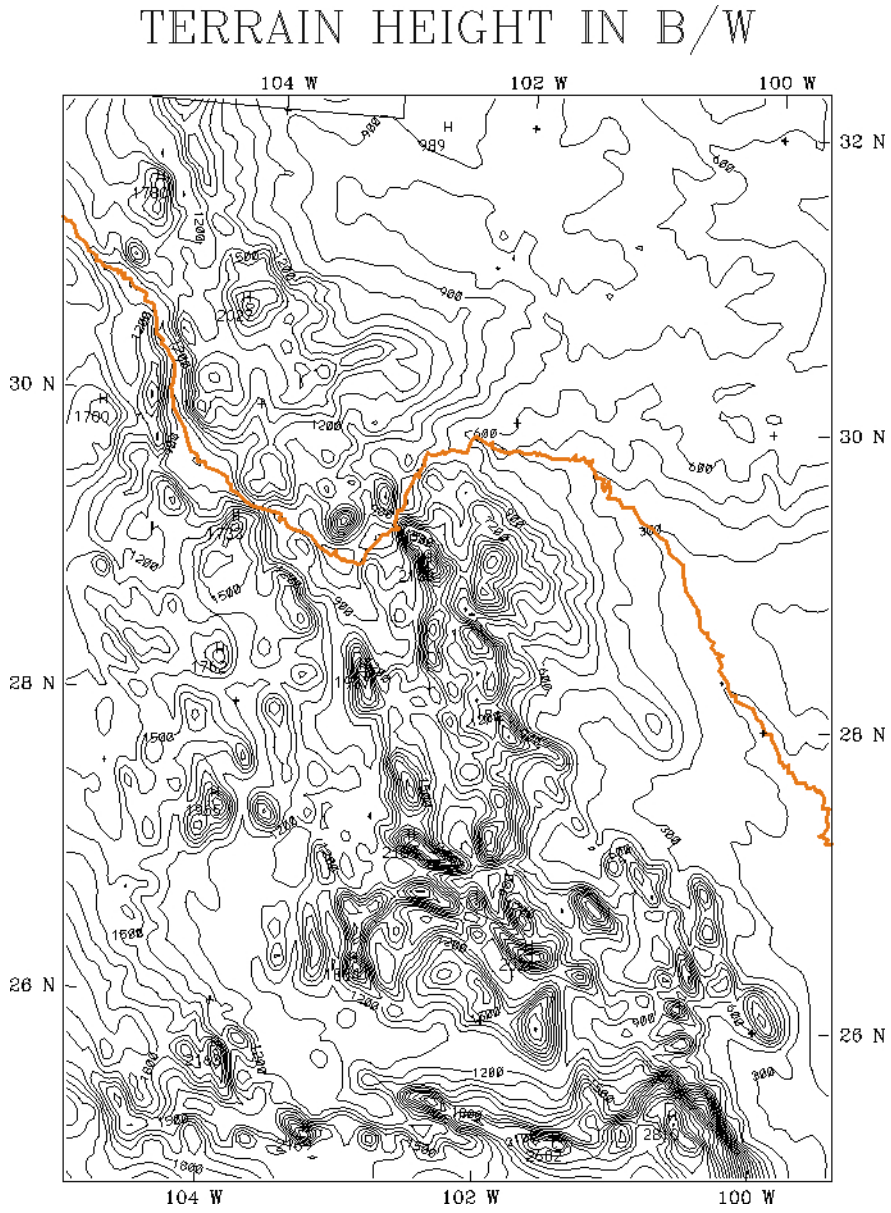

Figure 6. Terrain (m) on the 4-km MM5 domain. Contour interval is 100 m.

To enable the key products, especially the 4-km model fields, to be available as quickly as possible, the two intensive study periods were given top priority. First, the 36/12-km runs were completed for the August intensive episode. As soon as these model results were quality-checked, both segments of the first episode were run on the 4-km domain. Following a final quality-check, these fields were delivered to Dr. Christian Seigneur of AER, Inc. Next, the second BRAVO intensive episode, in October 1999, was run in a similar manner, was quality-checked and delivered to AER. After completion of the two intensive periods, the rest of the four-month BRAVO period was modeled on the 36- and 12-km domains.

2.2 Selection of Physical Parameterizations

The MM5 has the greatest range of options for physical processes of all general use mesoscale models available today. The accuracy of the model solutions often depends on selecting a combination of options for deep convection, resolved-scale precipitation, turbulence, surface fluxes and radiation that are both individually of high quality and are also compatible with each other. The proposed choice of physics options for BRAVO is made on the basis of accuracy, versatility and reliability, without consideration of the computational load.

For the BRAVO study, Penn State proposes used the Kain-Fritsch deep-convection parameterization (Kain and Fritsch 1990, 1993). This scheme has been evaluated along with several other schemes and has been found to have excellent performance characteristics (Wang and Seaman 1997), especially for the semi-arid climate of central and western North America. It also has been used successfully in previous meteorological modeling in support of air-quality studies (e.g., Shafran et al. 2000, Seaman and Michelson 2000). Parameterization of convection was required for the 12-km and 36-km domains only, where the grid resolution is much larger than the scale of individual thunderstorm updrafts.

Resolved-scale (explicit) cloud microphysics and precipitation were parameterized using the Dudhia (1989) microphysics scheme, which has prognostic equations for cloud liquid, cloud ice, liquid precipitation and frozen precipitation (no mixed phase water). Although there are other explicit-precipitation options in the MM5 system that also include one or more mixed-phase conditions (liquid and ice in the same grid cell), we have not used those options for BRAVO. In most side-by-side tests of the available explicit microphysics schemes, the addition of the mixed phase has not produced a significant change in the model solutions. Therefore, because the Dudhia microphysics has been more thoroughly tested, we believe was a more reliable choice for this application.

To simulate the planetary boundary layer and other turbulence-related phenomena, Penn State used the 1.5-order turbulence scheme developed by Shafran et al. (2000). This parameterization includes a predictive equation for the turbulent kinetic energy (TKE) and has been found to more accurately represent surface temperatures and mixed-layer depths in MM5 than alternative schemes, such as the Blackadar boundary-layer model. The TKE-predictive turbulence scheme has also been improved to account for ice processes and buoyancy changes associated with saturated conditions (Stauffer et al. 1999). Without this saturation dependency on buoyancy, the

other turbulence schemes in the MM5 (and in most other models) underestimate turbulent mixing in cloud layers, especially when they occur at the top of the planetary boundary layer.

Finally, the surface fluxes were predicted using the Zhang- Anthes (1982) surface-flux scheme, which uses two soil layers and a predictive equation for the surface ground temperature. Atmospheric radiation was modeled using the Dudhia (1989) two-stream broad-band scheme.

2.3 Four-Dimensional Data Assimilation

The four-dimensional data assimilation (FDDA) approach used by Penn State for the BRAVO meteorological modeling was based on the Newtonian relaxation (nudging) method developed by Stauffer and Seaman (1990, 1994) and Stauffer et al. (1991). The nudging approach adds an artificial term to the primitive equations, the size of which depends on a scaling constant (the nudging factor) and a flow-dependent weighting term. The magnitude of the nudging factor is set to ensure that the size of the artificial term normally remains less than the major natural terms in the equations, so that the model's solutions remain physically consistent (Ardao-Berdejo and Stauffer 1996). The weighting term is based on the difference between the data and the current model solution (i.e., the model error). It is also a function of the distance from the observation (in space and time) and the data measurement uncertainty. Thus, the influence of the nudging terms changes continuously with the size of the model errors at each time step, so that the model states are forced gradually toward the data over time. This reduces or eliminates sudden "shocks" to the model that can cause unrealistic high-frequency responses in the solutions in so-called intermittent assimilation schemes.

There are two standard types of FDDA available in the MM5. The first is called "analysis nudging", which nudges the solutions at each grid point toward objective analyses based on the data. Between the analysis times, the observed state is estimated through temporal interpolation to the model's current time step. Analysis nudging is normally used to assimilate the standard synoptic data obtained from the NWS. Research published by Shafran et al. (2000) has found that critical features related to the PBL structure (e.g., the capping inversion and low-level jets) can be represented more accurately if analysis nudging is restricted throughout the diurnal cycle to the region above the typical depth of the afternoon mixed-layer depth. This is because the synoptic upper-air data frequently fail to resolve many of the mesoscale and evolving features of the upper PBL.

The second standard FDDA approach is called "observation nudging", which is especially valuable when the data are not limited to the standard synoptic times. Thus, the special profiler data taken during BRAVO fall into this category. In this case, the "asynoptic" data are assimilated directly into the MM5 (without gridded objective analyses), using regions of influence that are dependent on the complexity of the terrain and the height above ground (Stauffer and Seaman 1994). However, observation nudging is logistically more difficult because the special data in each field program tend to be archived in different formats and the level of quality assurance on the archived data can vary widely. Thus, Penn State adapted its software to read and reformat the BRAVO observations into a standard form for entry into the assimilation system. Careful quality checking was applied to all NWS and BRAVO data used in

the FDDA, including gross error checks, buddy checks against nearby observations and background error checks against the model fields.

2.4 Special Adaptations for BRAVO

As discussed in Section 2.1, the model design used for BRAVO by Penn State was based almost exclusively on the latest standard model version, MM5v3, publicly available from NCAR. However, based on the review of the meteorological processes likely to be critical to the success of the BRAVO modeling effort (Sec. 1.3), we believed that some limited special adaptations were important to include. The primary potential problem we hoped to avoid or minimize is that *the absence of reliable soil-moisture measurements can lead to errors in the surface sensible and latent heat fluxes*, which can adversely affect the accuracy of boundary-layer depths, humidity and aerosol deliquescence. We proposed a newly developed approach to assimilate standard surface thermodynamic and moisture data that had been previously excluded from the FDDA system.

The change to the FDDA involved assimilating analyses of the standard NWS surface temperature and dew-point data at 3-h intervals using an approach described by Alapaty et al. (2000). In the past, surface temperature was not used in the nudging scheme because a direct adjustment of the surface-layer air temperatures could lead to a sudden reversal of the sign of the air-ground temperature difference. That temperature reversal would then cause a sudden erroneous stabilization of the boundary layer, which would be very detrimental to the mixing processes (Stauffer et al. 1991). However, the Alapaty et al. approach uses the same data to compare the modeled versus observed differences between the air and ground temperatures (and a similar approach for the water vapor mixing ratio). Then, based on the calculated model error, an equivalent nudging term is calculated in the form of artificial surface sensible and latent heat fluxes. These modified fluxes are then used in the calculation of the ground temperature, which in turn drives the fluxes that largely control and correct the surface air temperature and humidity.

The study by Alapaty et al. was conducted using a 1-D boundary-layer model. Therefore, because there were no high-resolution BRAVO surface data for temperature and moisture, we developed equivalent codes for assimilating thermal and moisture analyses into the 3-D MM5 system. Before beginning extensive BRAVO modeling, the new code was tested and evaluated against runs made without the surface assimilation technique. Results of these tests (not shown) indicated that the Alapaty et al. technique produced only marginal improvements in the low level fields of temperature and moisture because the NWS observation database over most of TX and Mexico is very sparse, compared to the central and eastern U.S. This is especially true at times other than 0000 UTC, 1200 UTC and 1800 UTC.

Finally, there is another potential problem that relates to the use of very fine 4-km resolution in a mesoscale model (not limited to the MM5). That is, *in light-wind cases a significant amount of spurious small-scale energy can be generated in the low-level solutions, especially in the wind field*. This occurs for at least two reasons. First, as the fine-mesh size approaches the scale of the boundary-layer depth, the model's grid begins to resolve some of the largest turbulent eddies in the boundary layer. In light-wind conditions, this turbulence can become a large fraction of

the background wind speed, leading to enhanced local variability in the solutions that is not representative of average conditions. This type of response can lead to model solutions that appear to contain boundary layer rolls, a physical phenomenon, but which are generally aliased to horizontal scales that are greater than those in the atmosphere (~3-6 km). This problem is especially evident when convective PBL depths become very large (~3 km), which is quite possible in the BRAVO study area during the summer months.

Secondly, local transient wind gusts in the low-level horizontal winds also can occur at very fine model resolutions due to rapidly evolving downdrafts from local thunderstorms. To remove similar turbulent fluctuations when taking routine wind observations, meteorologists always report the wind as the average of the fluctuating winds over a 5-minute period. Thus, output data sets from a fine-mesh meteorological model at a given time step, which may be written once per hour, can easily appear contaminated by transient turbulent components. However, since thunderstorms are not very common over most of the inner MM5 BRAVO domains during late summer and early autumn, convection induced wind gusts are not expected to be a large factor.

If the instantaneous 4-km model wind solutions output at each hour do contain significant turbulent fluctuations, such as boundary layer rolls, then an air-quality model (AQM) using those winds will have small-scale wind perturbations that vary only as the fields are interpolated between the model output times, or they may be held constant for an entire hour (depending on how the AQM uses the meteorology). This could damage air-chemistry calculations due to spurious local convergence/divergence patterns. In some instances, it even appears that smoother 12-km meteorological fields can actually produce somewhat better chemistry predictions in an AQMs than do these instantaneous 4-km fields (Ralph Morris, ENVIRON, personal communication, 2000). Therefore, the model output has been evaluated with consideration for the possibility that the 4-km fields could contain some unrealistic fine-scale components.

2.5 Data Acquisition

For the BRAVO meteorological modeling effort, data were acquired from the Desert Research Institute (DRI). DRI is the official archive of the BRAVO special data. Penn State worked with DRI personnel to review the quality assurance protocols used on the special profiler data, after which Penn State performed the additional quality checks described above in Sec. 2.3. The NCAR archives were also accessed for the Eta model fields and standard NWS surface and upper-air data.

3. Model Results

Because the length of the study period is four months, it is not feasible to examine visually the spatial details of the simulated fields in this report. Therefore, the model evaluations concentrate on statistical methods, with a few visual presentations to provide typical examples of the character of the MM5 solutions. The statistics (described below) are calculated separately for each 5 1/2 day segment and on the entire 12-km domain. The same statistics also are calculated

for the 36-km solutions, but the area of the validation is limited to the same region as the 12-km domain. There are two major reasons for this restriction: (1) the special BRAVO data sets are available only on the 12-km domain, and (2) it then becomes easy to compare directly the statistical results calculated over an identical region on the 36- and 12-km domains. To a good approximation at least, the statistical skill shown for the 36-km solutions over the region of the 12-km domain should be representative of the complete 36-km domain, as well. Finally, domain-wide statistics are calculated on the entire 4-km grid for the two intensive study periods in August and October.

The statistics for each 5 1/2 day segment are plotted graphically to show the diurnal variability and any trends in the statistics, from hourly to monthly. Samples of these plotted statistics are shown in this report. Next, the statistics are presented in tabular form, showing the individual model run segments (5 1/2 days each) and then aggregated statistics that have been averaged for longer periods: (a) the intensive periods, (b) months, and (d) the entire four-month BRAVO period.

Since upper-air data for BRAVO were obtained mostly from radar wind profilers, statistics aloft are limited to wind speed and direction. At the surface, statistics include temperature, water vapor mixing ratio, wind speed and wind direction. The surface layer statistics are calculated at the mid-level of the model's lowest layer, which for this study is located ~15 m above ground level (AGL). Aloft the processing software bundles, or aggregates, many individual model levels into several deeper layers. Thus the layer above the surface is formed by averaging the model levels from 30-1500 m AGL, which approximates the mean depth of the convective PBL for most regions across the central U.S. from July - October. (However, 1500 m almost certainly underestimates the mean convective PBL depth during summer in the 4-km BRAVO domain. This does not make the statistics for the 30-1500 m any less valid. It merely means that we are focusing on the lower and middle part of the PBL region that is typical for summer over semi-arid regions of west TX and northern MX.) The third and final layer examined in this report consists of the average of all model levels between 1500 - 5000 m. Thus, the third layer may include the upper part of very deep convective PBLs in summer, but is primarily representative of the lower half of the free atmosphere lying above most direct surface influences induced by ground based turbulence.

Although these layers are somewhat idealized, they nevertheless provide useful guidance for interpreting the otherwise overwhelming volume of model statistical information calculated for individual layers. The surface layer is, of course, important for understanding basic model accuracy and is the level at which we have the richest datasets. The 30-1500 m layer, or the nominal PBL, is very important in air-quality studies because it represents the zone in which most of the local and regional mass transport takes place for surface-based emissions and their subsequent secondary chemical and aerosol species. The 1500-5000 m layer is valuable because it represents the layer where comparatively little of the local and regional transport occurs, where surface fluxes and vertical turbulent transport are minimal, but where long-range inter-regional or intercontinental transport may be important (in addition to the lower two layers, of course.)

The statistical measures of accuracy used in this report are the root mean square error (RMSE), the mean absolute error (MAE) and the mean error (or bias error) (ME). Definitions are given in

Stauffer and Seaman (1990). Because the root mean square error gives greatest weight to the largest errors ("outliers"), it is useful for alerting the user to situations in which the model may have intermittent large errors that could otherwise be masked by longer periods of good performance. The mean absolute error gives the magnitude of the most typical error, without considering whether the errors are positive or negative. Finally, the mean or bias error allows for cancellation of positive and negative errors, which may be quite acceptable in certain situations. For example, small bias errors in the wind speed and direction may under many circumstances indicate that long-term transport is reasonably accurate, even though the instantaneous winds may have considerably larger errors. Reliance solely on any one of these statistics is apt to give a distorted view of overall model performance. While it cannot be claimed that these are the only statistics that may give insight into meteorological model accuracy for air-quality applications, when considered together they do give a fairly broad understanding of model performance.

Lastly, before examining the results of the MM5 modeling experiment, it is useful to provide a benchmark for meteorological model accuracy that is widely considered acceptable for air-quality applications. ENVIRON Corp. among others has analyzed results from over 30 modeling studies to formulate typical standards for meteorological skill. These are summarized in **Table 1**.

Table 1. Standard benchmarks of surface-layer meteorological model accuracy for air-quality applications, summarized by ENVIRON Corp.

Variable:	Temp. (C)	Mix. Ratio (g/kg)	Wind Speed (m/s)	Wind Dir. (deg.)
Benchmark	MAE< 2.0	MAE< 2.0	RMSE < 2.0	MAE< 30.0
Sfc-Layer Score	Bias < 0.5	Bias < 1.0	Bias < 0.5	Bias < 10.0

3.1 Intensive Study Periods

3.1.1 August Intensive, 15 - 26 August

We begin evaluation of the BRAVO August Intensive Period by examining **Table 2**, which summarizes the statistical accuracy calculated across the full 4-km MM5 domain. The table is organized so that the longer averaging periods appear to the right. In the case of the August Intensive Period there are two segments: the first covers 1200 Z, 15 August - 0000 Z, 21 August 1999, and the second extends from 1200 Z, 20 August - 0000 Z, 26 August 1999. Although the table contains the statistics for each segment for reference, we will concentrate on the Intensive Period's average statistics.

First, **Table 2** shows that for temperature the period-averaged RMSE = 2.55 C and the MAE = 2.30 C on the 4-km domain. The latter is moderately greater than the benchmark MAE of 2.0 C given in **Table 1**, indicating that the typical temperature errors in the August period are a bit high on the 4-km domain. The average ME for temperature during the August Intensive is shown as -1.70 C, which is considerably greater than the desirable standard of ME < 0.5 C. The large cool

bias found in the 4-km MM5 domain in August approaches the size of the MAE, which indicates that it is very likely that most of the model error is systematic and could be eliminated rather easily by resetting land-surface specifications, such as the soil moisture availability. Next, the table shows similar indications of systematic errors for the water vapor mixing ratio. The surface-layer mixing ratio bias (ME) for the August Intensive is +1.36 g kg^{-1}, while the MAE = 1.82 g kg^{-1}. Therefore, MAE for mixing ratio falls just within the benchmark of 2 g kg^{-1}, while the bias is moderately larger than preferred. Again, the large systematic error suggested by the moist bias indicates that these errors could be reduced substantially if some additional modeling runs were performed. The implications of these scores for surface temperature and water vapor mixing ratio are clear. That is, the mean soil moisture values specified for the BRAVO study, although set to one-half of the default MM5 summertime values for semi-arid land categories (see Grell et al. 1994), are still too moist for this particular 10-day period, leading to cool, moist conditions near the surface relative to the observations.

Table 2. Statistics calculated on the MM5 4-km domain for the BRAVO August Intensive Period, 15-26 August 1999.

Variable	Verif. Layer	Segment Dates	Stat. Type	Segment Score	Avg. Score for Aug. Intensive
Temp. (C)	**15 m AGL**	12Z,15Aug - 00Z,21Aug	RMSE	2.66	
		12Z,20Aug - 00Z,26Aug	RMSE	2.44	**2.55**
		12Z,15Aug - 00Z,21Aug	MAE	2.51	
		12Z,20Aug - 00Z,26Aug	MAE	2.09	**2.30**
		12Z,15Aug - 00Z,21Aug	ME	-2.29	
		12Z,20Aug - 00Z,26Aug	ME	-1.11	**-1.70**
Mixing Ratio ($g\ kg^{-1}$)	**15 m AGL**	12Z,15Aug - 00Z,21Aug	RMSE	2.20	
		12Z,20Aug - 00Z,26Aug	RMSE	1.75	**1.98**
		12Z,15Aug - 00Z,21Aug	MAE	2.03	
		12Z,20Aug - 00Z,26Aug	MAE	1.61	**1.82**
		12Z,15Aug - 00Z,21Aug	ME	+1.73	
		12Z,20Aug - 00Z,26Aug	ME	+0.99	**+1.36**
Wind Speed ($m\ s^{-1}$)	**1500 - 5000 m AGL**	12Z,15Aug - 00Z,21Aug	RMSE	1.41	
		12Z,20Aug - 00Z,26Aug	RMSE	1.52	**1.47**
		12Z,15Aug - 00Z,21Aug	MAE	1.31	
		12Z,20Aug - 00Z,26Aug	MAE	1.40	**1.36**
		12Z,15Aug - 00Z,21Aug	ME	-0.37	
		12Z,20Aug - 00Z,26Aug	ME	-0.41	**-0.39**
	30-1500 m AGL	12Z,15Aug - 00Z,21Aug	RMSE	1.42	
		12Z,20Aug - 00Z,26Aug	RMSE	1.50	**1.46**
		12Z,15Aug - 00Z,21Aug	MAE	1.32	
		12Z,20Aug - 00Z,26Aug	MAE	1.38	**1.35**
		12Z,15Aug - 00Z,21Aug	ME	-0.34	
		12Z,20Aug - 00Z,26Aug	ME	-0.29	**-0.32**
	15 m AGL	12Z,15Aug - 00Z,21Aug	RMSE	1.37	
		12Z,20Aug - 00Z,26Aug	RMSE	1.82	**1.60**
		12Z,15Aug - 00Z,21Aug	MAE	1.17	
		12Z,20Aug - 00Z,26Aug	MAE	1.51	**1.34**
		12Z,15Aug - 00Z,21Aug	ME	-0.33	
		12Z,20Aug - 00Z,26Aug	ME	+0.25	**-0.04**
Wind Direction (deg.)	**1500 - 5000 m AGL**	12Z,15Aug - 00Z,21Aug	RMSE	17.9	
		12Z,20Aug - 00Z,26Aug	RMSE	14.7	**16.3**
		12Z,15Aug - 00Z,21Aug	MAE	16.5	
		12Z,20Aug - 00Z,26Aug	MAE	13.2	**14.9**
		12Z,15Aug - 00Z,21Aug	ME	-2.4	
		12Z,20Aug - 00Z,26Aug	ME	+0.9	**-0.8**
	30-1500 m AGL	12Z,15Aug - 00Z,21Aug	RMSE	23.9	
		12Z,20Aug - 00Z,26Aug	RMSE	22.9	**23.4**
		12Z,15Aug - 00Z,21Aug	MAE	21.7	
		12Z,20Aug - 00Z,26Aug	MAE	20.6	**21.2**
		12Z,15Aug - 00Z,21Aug	ME	-7.0	
		12Z,20Aug - 00Z,26Aug	ME	-3.2	**-5.1**
	15 m AGL	12Z,15Aug - 00Z,21Aug	RMSE	42.8	
		12Z,20Aug - 00Z,26Aug	RMSE	50.4	**46.6**
		12Z,15Aug - 00Z,21Aug	MAE	34.1	
		12Z,20Aug - 00Z,26Aug	MAE	41.1	**37.6**
		12Z,15Aug - 00Z,21Aug	ME	-6.8	
		12Z,20Aug - 00Z,26Aug	ME	+4.0	**-1.4**

Returning to **Table 2**, we next examine the wind speed in the surface layer (15 m AGL). The RMSE for surface wind speed on the 4-km domain for the August Intensive is 1.60 m s^{-1}, while the ME = -0.04 m s^{-1}. This indicates that the MM5 data-assimilated model solutions have virtually no speed bias over a period of several days and that large speed errors are infrequent. Both scores fall well within the standard accuracy measures of RMSE=2.0 m s^{-1} and ME < 0.5 m s^{-1}. Moreover, further examination of the table indicates that the RMSE for speed decreases with height above ground as the influence of turbulence and the irregular terrain gradually decrease. Thus, the table shows an RMSE = 1.46 m s^{-1} in the 30-1500 m layer and 1.36 m s^{-1} in the 1500-5000 m layer. The MEs in these two layers are -0.32 m s^{-1} and -0.39 m s^{-1}, respectively. These are very small values, especially since the mean speed aloft normally increases with height in mid-latitudes. Thus, the wind speeds simulated at all three levels by the MM5 appear to be quite suitable for use in air-quality studies.

In the surface layer, the table shows that the wind direction errors have a MAE = 37.6 degrees during the August Intensive Period, while the ME = -1.4 degrees. The ME is very small and is well within the 10-degree bias standard given in **Table 1**. However, the MAE is moderately larger than the surface-layer standard. Comparison with the MAE of just 21.2 degrees and ME of -5.1 degrees for the 30-1500 m layer, on the other hand, shows that the transport is likely to be more accurate than implied by the larger surface MAE, which is affected greatly by terrain irregularities. Thus, regional scale transport simulated using the MM5 solution is still likely to be quite acceptable for the August Intensive Period.

Similar statistics for the August Intensive Period on the full 12-km domain are shown in **Table 3**. Comparison of the two tables immediately reveals that the domain-averaged errors are about the same or smaller on the 12-km domain for almost all statistics and variable types. This result is expected because the 12-km domain includes all of the available 10 profilers, while the 4-km domain encompasses only the Big Bend and Eagle Pass profilers. Many of the additional profilers in the 12-km domain are located over the Great Plains where terrain forcing should be weaker and surface-layer variability ought to be less extreme than near Big Bend National Park. For example the MAE for temperature on the 12-km domain in the August Intensive is found to be 1.40 C, versus 2.30 C on the 4-km domain. The ME for temperature on the 12-km domain is only -0.62 C, compared with -1.70 C on the 4-km domain. Moreover the bias of the 12-km mixing ratio is +0.48 g kg^{-1}, compared to +1.36 g kg^{-1} on the 4-km domain. In summary, the errors found in the 12-km temperature and mixing ratio fields for the August Intensive are well within the benchmark limits that have become standards for air-quality studies.

Comparison of **Tables 2 and 3** also shows general improvement in the statistics for wind speed and wind direction on the 12-km domain. The 12-km RMSE and ME for surface wind speed are only 1.39 m s^{-1} and +0.16 m s^{-1}, respectively. The corresponding MAE and ME for surface wind direction are 24.0 degrees and -0.4 degrees. Further comparison of speed and direction errors for the uppermost layer (1500-5000 m) reveals that at those altitudes there is very little difference between the statistics on the two domains. This result is also expected because in the upper atmosphere local terrain influences are minor so that there is no reason to expect that the errors detected at Big Bend and Eagle Pass should be greater than at the other profiler sites over the Great Plains.

Table 3. Statistics calculated on the MM5 12-km domain for the BRAVO August Intensive Period, 15-26 August 1999.

Variable	Verif. Layer	Segment Dates	Stat. Type	Segment Score	Avg. Score for Aug. Intensive
Temp. (C)	**15 m AGL**	12Z,15Aug - 00Z,21Aug	RMSE	1.70	
		12Z,20Aug - 00Z,26Aug	RMSE	1.78	**1.74**
		12Z,15Aug - 00Z,21Aug	MAE	1.37	
		12Z,20Aug - 00Z,26Aug	MAE	1.42	**1.40**
		12Z,15Aug - 00Z,21Aug	ME	-0.59	
		12Z,20Aug - 00Z,26Aug	ME	-0.65	**-0.62**
Mixing Ratio ($g\ kg^{-1}$)	**15 m AGL**	12Z,15Aug - 00Z,21Aug	RMSE	2.26	
		12Z,20Aug - 00Z,26Aug	RMSE	2.35	**2.30**
		12Z,15Aug - 00Z,21Aug	MAE	1.69	
		12Z,20Aug - 00Z,26Aug	MAE	1.66	**1.68**
		12Z,15Aug - 00Z,21Aug	ME	+0.65	
		12Z,20Aug - 00Z,26Aug	ME	+0.31	**+0.48**
Wind Speed ($m\ s^{-1}$)	**1500 - 5000 m AGL**	12Z,15Aug - 00Z,21Aug	RMSE	1.33	
		12Z,20Aug - 00Z,26Aug	RMSE	1.36	**1.35**
		12Z,15Aug - 00Z,21Aug	MAE	1.02	
		12Z,20Aug - 00Z,26Aug	MAE	1.04	**1.03**
		12Z,15Aug - 00Z,21Aug	ME	-0.57	
		12Z,20Aug - 00Z,26Aug	ME	-0.52	**-0.55**
	30-1500 m AGL	12Z,15Aug - 00Z,21Aug	RMSE	1.36	
		12Z,20Aug - 00Z,26Aug	RMSE	1.48	**1.42**
		12Z,15Aug - 00Z,21Aug	MAE	1.08	
		12Z,20Aug - 00Z,26Aug	MAE	1.20	**1.14**
		12Z,15Aug - 00Z,21Aug	ME	-0.27	
		12Z,20Aug - 00Z,26Aug	ME	-0.22	**-0.25**
	15 m AGL	12Z,15Aug - 00Z,21Aug	RMSE	1.30	
		12Z,20Aug - 00Z,26Aug	RMSE	1.47	**1.39**
		12Z,15Aug - 00Z,21Aug	MAE	1.06	
		12Z,20Aug - 00Z,26Aug	MAE	1.19	**1.13**
		12Z,15Aug - 00Z,21Aug	ME	+0.11	
		12Z,20Aug - 00Z,26Aug	ME	+0.21	**+0.16**
Wind Direction (deg.)	**1500 - 5000 m AGL**	12Z,15Aug - 00Z,21Aug	RMSE	17.6	
		12Z,20Aug - 00Z,26Aug	RMSE	18.4	**18.0**
		12Z,15Aug - 00Z,21Aug	MAE	11.9	
		12Z,20Aug - 00Z,26Aug	MAE	12.2	**12.1**
		12Z,15Aug - 00Z,21Aug	ME	-0.2	
		12Z,20Aug - 00Z,26Aug	ME	1.3	**+0.6**
	30-1500 m AGL	12Z,15Aug - 00Z,21Aug	RMSE	23.7	
		12Z,20Aug - 00Z,26Aug	RMSE	23.4	**23.6**
		12Z,15Aug - 00Z,21Aug	MAE	17.2	
		12Z,20Aug - 00Z,26Aug	MAE	17.3	**17.3**
		12Z,15Aug - 00Z,21Aug	ME	-0.9	
		12Z,20Aug - 00Z,26Aug	ME	-1.3	**-1.1**
	15 m AGL	12Z,15Aug - 00Z,21Aug	RMSE	33.0	
		12Z,20Aug - 00Z,26Aug	RMSE	34.4	**33.7**
		12Z,15Aug - 00Z,21Aug	MAE	23.5	
		12Z,20Aug - 00Z,26Aug	MAE	24.5	**24.0**
		12Z,15Aug - 00Z,21Aug	ME	-1.1	
		12Z,20Aug - 00Z,26Aug	ME	+0.3	**-0.4**

The statistics shown in **Tables 2 and 3** probably contain somewhat lower errors than would have occurred if the model solutions could be verified using an independent data set from that used in the obs-nudging data assimilation. No large independent data set is readily available in this case. However, previous studies in which independent data sets have been available (e.g., Seaman et al. 1995) have demonstrated that the effect of verifying against non-independent data (that is, data which have been assimilated) is fairly small (~10-15 % of the overall value gained through FDDA). Since the 12-km domain statistics are well within the standard limits, it is very likely that an independent dataset would show the solutions lie within those, as well limits.

Comparable statistics for the 36-km domain during the August Intensive Period are shown in **Table 4**. Comparison between results shown for **Tables 3 and 4** indicate that for most variables and levels, the statistical skill on the 12 km domain is greater than that found for the 36-km solutions. The only exceptions are for the surface layer temperature, where the RMSE and MAE are a bit smaller in the 36-km solutions, and likewise for the surface layer ME of mixing ratio. All other temperature and moisture statistics, and all those for the wind speed and direction at all levels favor the 12-km MM5 solutions. Moreover, the differences in most cases are fairly substantial. For example the surface layer wind speed RMSE = 1.66 m s^{-1} on the 36-km grid, but for the very same region, the RMSE = 1.39 m s^{-1} on the 12-km grid. The corresponding RMSEs for wind direction in the surface layer are 42.5 degrees and 33.7 degrees on the 36-km and 12-km domains, respectively. The improvement of performance on the 12-km domain, versus the 36-km domain, is explained by the use of the special BRAVO observations through obs-nudging on the inner two domains. Only analysis nudging is used on the 36-km domain. Thus, of all three domains, the 12-km solutions clearly have the lowest errors during the August Intensive Period, with very few exceptions, and are expected to have the greatest applicability for air-quality modeling.

Finally, visual inspections of the plotted horizontal model fields (not shown) indicated that the MM5 solutions on the sub-portion of the 12-km domain that coincides with the 4-km domain are somewhat smoother than the solutions on the finer grid. That is expected because fewer local terrain features are resolved by the coarser grid. However, the solutions are not dramatically different. Taken altogether, it appears that the 12-km results for the August Intensive Period should represent a very suitable dataset that meets the accuracy goals normally set for air-quality applications.

Table 4. Statistics calculated on the MM5 36-km domain for the BRAVO August Intensive Period, 15-26 August 1999.

Variable	Verif. Layer	Segment Dates	Stat. Type	Segment Score	Avg. Score for Aug. Intensive
Temp. (C)	**15 m AGL**	12Z,15Aug - 00Z,21Aug	RMSE	1.57	
		12Z,20Aug - 00Z,26Aug	RMSE	1.63	**1.60**
		12Z,15Aug - 00Z,21Aug	MAE	1.28	
		12Z,20Aug - 00Z,26Aug	MAE	1.32	**1.30**
		12Z,15Aug - 00Z,21Aug	ME	-0.67	
		12Z,20Aug - 00Z,26Aug	ME	-0.79	**-0.73**
Mixing Ratio ($g\ kg^{-1}$)	**15 m AGL**	12Z,15Aug - 00Z,21Aug	RMSE	2.41	
		12Z,20Aug - 00Z,26Aug	RMSE	2.54	**2.48**
		12Z,15Aug - 00Z,21Aug	MAE	1.83	
		12Z,20Aug - 00Z,26Aug	MAE	1.82	**1.82**
		12Z,15Aug - 00Z,21Aug	ME	+0.64	
		12Z,20Aug - 00Z,26Aug	ME	+0.24	**+0.44**
Wind Speed ($m\ s^{-1}$)	**1500 - 5000 m AGL**	12Z,15Aug - 00Z,21Aug	RMSE	2.06	
		12Z,20Aug - 00Z,26Aug	RMSE	2.24	**2.15**
		12Z,15Aug - 00Z,21Aug	MAE	1.67	
		12Z,20Aug - 00Z,26Aug	MAE	1.80	**1.74**
		12Z,15Aug - 00Z,21Aug	ME	-0.72	
		12Z,20Aug - 00Z,26Aug	ME	-0.90	**-0.81**
	30-1500 m AGL	12Z,15Aug - 00Z,21Aug	RMSE	2.39	
		12Z,20Aug - 00Z,26Aug	RMSE	2.73	**2.56**
		12Z,15Aug - 00Z,21Aug	MAE	1.99	
		12Z,20Aug - 00Z,26Aug	MAE	2.32	**2.15**
		12Z,15Aug - 00Z,21Aug	ME	+0.37	
		12Z,20Aug - 00Z,26Aug	ME	+0.18	**+0.28**
	15 m AGL	12Z,15Aug - 00Z,21Aug	RMSE	1.50	
		12Z,20Aug - 00Z,26Aug	RMSE	1.82	**1.66**
		12Z,15Aug - 00Z,21Aug	MAE	1.25	
		12Z,20Aug - 00Z,26Aug	MAE	1.51	**1.38**
		12Z,15Aug - 00Z,21Aug	ME	+0.41	
		12Z,20Aug - 00Z,26Aug	ME	+0.48	**+0.44**
Wind Direction (deg.)	**1500 - 5000 m AGL**	12Z,15Aug - 00Z,21Aug	RMSE	35.6	
		12Z,20Aug - 00Z,26Aug	RMSE	34.4	**35.0**
		12Z,15Aug - 00Z,21Aug	MAE	26.1	
		12Z,20Aug - 00Z,26Aug	MAE	24.7	**25.4**
		12Z,15Aug - 00Z,21Aug	ME	-0.5	
		12Z,20Aug - 00Z,26Aug	ME	+4.5	**+2.0**
	30-1500 m AGL	12Z,15Aug - 00Z,21Aug	RMSE	44.1	
		12Z,20Aug - 00Z,26Aug	RMSE	41.8	**43.0**
		12Z,15Aug - 00Z,21Aug	MAE	34.9	
		12Z,20Aug - 00Z,26Aug	MAE	32.4	**33.7**
		12Z,15Aug - 00Z,21Aug	ME	-7.0	
		12Z,20Aug - 00Z,26Aug	ME	-6.0	**-6.5**
	15 m AGL	12Z,15Aug - 00Z,21Aug	RMSE	42.8	
		12Z,20Aug - 00Z,26Aug	RMSE	42.1	**42.5**
		12Z,15Aug - 00Z,21Aug	MAE	31.3	
		12Z,20Aug - 00Z,26Aug	MAE	31.3	**31.3**
		12Z,15Aug - 00Z,21Aug	ME	-2.7	
		12Z,20Aug - 00Z,26Aug	ME	+0.7	**-1.0**

3.1.2 October Intensive, 7 - 16 October

Next, statistics were calculated for the two segments that make up the BRAVO October Intensive Period. The first segment is defined as 0000 Z, 7 October - 0000 Z, 11 October 1999, while the second segment covers 1200 Z, 10 October - 0000 Z, 16 October. Notice that because the first segment is shorter than the second, statistics from the two segments were weighted accordingly when calculating the average statistics for the full October Intensive Period.

Table 5 shows the results of the statistical evaluation on the 4-km domain for the October Intensive in the same format used to present results from the August Intensive. Comparison with **Table 2** indicates that the negative surface temperature bias and positive moisture bias noted in August have persisted in the October Intensive simulation [temperature ME=1.56 C and mixing ratio ME=+0.93 g kg^{-1}], but they are smaller than in August. This result suggests that the moist bias in the soil moisture detected in August for arid land-use types is probably present in October, but is smaller as well (i.e., closer to the climatological average used in the MM5 land-use tables). Reduction of these biases, compared to the August Intensive, has led to corresponding reduction in the 4-km MAE for surface temperature to 2.10 C and in the 4-km MAE for surface mixing ratio to 1.42 g kg^{-1}.

Evaluation of the wind speed and direction errors on the 4-km domain during the October Intensive Period (**Table 5**) also reveals only modest differences from those found during August. The surface-layer RMSE for wind speed in October on this fine-grid domain is 1.46 m s^{-1}, compared to 1.60 m s^{-1} in the earlier Intensive Period. The speed bias in October at the surface is -0.26 m s^{-1}, which is about the same size as in August when the ME was +0.25 m s^{-1}. This is a rather favorable result, given that the mean winds in October should be greater than in August because of the stronger dynamical forcing driven by the intensification of the meridional thermal gradient over North America during autumn. This creates the zonal height gradient (pressure gradient force) that drives the westerly (zonal) mid-latitude winds, which tend to increase with height. Surprisingly, the simulated surface-layer wind directions in this autumn regime have considerably larger surface errors (MAE=47.2 degrees, ME=+3.2 degrees), compared to the August Intensive, when MAE=37.6 degrees and ME=-1.4 degrees. The tables show that the directional errors for the October Intensive become dramatically smaller above the surface, however, as was found in the August Intensive Period. Thus, the overall impact of model errors in the 4-km domain on transport of mass in the mixed layer should be within the widely accepted standards.

Table 5. Statistics calculated on the MM5 4-km domain for the BRAVO October Intensive Period, 7-16 August 1999.

Variable	Verif. Layer	Segment Dates	Stat. Type	Segment Score	Avg. Score for Aug. Intensive
Temp. (C)	**15 m AGL**	00Z,7Oct - 00Z,11Oct	RMSE	2.66	
		12Z,10Oct - 00Z,16Oct	RMSE	2.30	**2.44**
		00Z,7Oct - 00Z,11Oct	MAE	2.28	
		12Z,10Oct - 00Z,16Oct	MAE	1.97	**2.10**
		00Z,7Oct - 00Z,11Oct	ME	-1.62	
		12Z,10Oct - 00Z,16Oct	ME	-1.52	**-1.56**
Mixing Ratio ($g\ kg^{-1}$)	**15 m AGL**	00Z,7Oct - 00Z,11Oct	RMSE	1.86	
		12Z,10Oct - 00Z,16Oct	RMSE	1.31	**1.54**
		00Z,7Oct - 00Z,11Oct	MAE	1.75	
		12Z,10Oct - 00Z,16Oct	MAE	1.18	**1.42**
		00Z,7Oct - 00Z,11Oct	ME	+1.51	
		12Z,10Oct - 00Z,16Oct	ME	+0.52	**+0.93**
Wind Speed ($m\ s^{-1}$)	**1500 - 5000 m AGL**	00Z,7Oct - 00Z,11Oct	RMSE	1.97	
		12Z,10Oct - 00Z,16Oct	RMSE	1.45	**1.67**
		00Z,7Oct - 00Z,11Oct	MAE	1.85	
		12Z,10Oct - 00Z,16Oct	MAE	1.31	**1.54**
		00Z,7Oct - 00Z,11Oct	ME	-1.19	
		12Z,10Oct - 00Z,16Oct	ME	-0.73	**-0.92**
	30-1500 m AGL	00Z,7Oct - 00Z,11Oct	RMSE	1.72	
		12Z,10Oct - 00Z,16Oct	RMSE	1.56	**1.62**
		00Z,7Oct - 00Z,11Oct	MAE	1.60	
		12Z,10Oct - 00Z,16Oct	MAE	1.43	**1.50**
		00Z,7Oct - 00Z,11Oct	ME	-0.83	
		12Z,10Oct - 00Z,16Oct	ME	-0.93	**-0.89**
	15 m AGL	00Z,7Oct - 00Z,11Oct	RMSE	1.61	
		12Z,10Oct - 00Z,16Oct	RMSE	1.34	**1.46**
		00Z,7Oct - 00Z,11Oct	MAE	1.35	
		12Z,10Oct - 00Z,16Oct	MAE	1.13	**1.23**
		00Z,7Oct - 00Z,11Oct	ME	-0.25	
		12Z,10Oct - 00Z,16Oct	ME	-0.26	**-0.26**
Wind Direction (deg.)	**1500 - 5000 m AGL**	00Z,7Oct - 00Z,11Oct	RMSE	14.2	
		12Z,10Oct - 00Z,16Oct	RMSE	20.0	**17.6**
		00Z,7Oct - 00Z,11Oct	MAE	12.9	
		12Z,10Oct - 00Z,16Oct	MAE	17.2	**15.4**
		00Z,7Oct - 00Z,11Oct	ME	+2.9	
		12Z,10Oct - 00Z,16Oct	ME	+0.9	**+1.7**
	30-1500 m AGL	00Z,7Oct - 00Z,11Oct	RMSE	17.4	
		12Z,10Oct - 00Z,16Oct	RMSE	25.4	**22.0**
		00Z,7Oct - 00Z,11Oct	MAE	15.1	
		12Z,10Oct - 00Z,16Oct	MAE	22.5	**19.4**
		00Z,7Oct - 00Z,11Oct	ME	-2.1	
		12Z,10Oct - 00Z,16Oct	ME	-0.5	**-1.2**
	15 m AGL	00Z,7Oct - 00Z,11Oct	RMSE	46.2	
		12Z,10Oct - 00Z,16Oct	RMSE	67.1	**58.3**
		00Z,7Oct - 00Z,11Oct	MAE	37.0	
		12Z,10Oct - 00Z,16Oct	MAE	54.6	**47.2**
		00Z,7Oct - 00Z,11Oct	ME	+3.4	
		12Z,10Oct - 00Z,16Oct	ME	+3.1	**+3.2**

Before continuing the statistical evaluation, it is helpful to gain a better perspective on the model errors by examining briefly some samples of the evolution of the model fields compared to observations. To begin, **Figure 7** presents the hourly evolution of the modeled and observed surface temperatures for a four-day segment during the October Intensive Period from 7-11 October 1999. **Figure 7** indicates that during this segment the model has a cool bias. **Table 5** indicated that the average surface layer bias for this segment was actually -1.62 C. The figure shows that greatest bias generally occurred during the afternoons, which is common for many models. The evolution of mixing ratio for the same period is shown in **Figure 8**. The dry bias noted earlier for the 4-km domain during the October Intensive is clearly evident. However, despite this flaw, the model reproduces daily trends in the evolution of surface-layer moisture.

Figure 9 shows an example of the hourly evolution of MM5 surface-layer wind speeds versus observed speeds on the 4-km domain for the period from 7-11 October 1999. The figure shows that the MM5 tracks the main diurnal and multi-day trends reasonably well. However, during the middle of this four-day period, the observed winds exhibit a series of rapid hourly wind fluctuations that are almost impossible for a model to capture. The model does exhibit similar rapid speed fluctuations, but their exact phases and amplitudes cannot be expected to match closely those that are observed. Naturally, this contributes to the speed errors shown in **Table 5**. At other times, such as the second half of the first day, **Figure 9** shows that the model may simply fail to capture the longer-term evolution of the winds. In this case the speed errors on the domain grow to nearly 2 ms^{-1} before the simulation adjusts to better match the data.

Much of the error shown in **Figure 9** is related to local terrain irregularities that are especially large in the region covered by the 4-km domain. **Figure 10** presents the hourly evolution of the observed and simulated winds for the same period during the October Intensive in the nominal PBL (30-1500 m AGL). This figure indicates that the winds in the PBL are considerably stronger than in the surface layer, as expected, and that the model fits the wind variations rather well. The observations show nearly continuous hour-to-hour fluctuations on the order of 1 ms^{-1}, which contributes substantially to the RMSE and MAE. It is unlikely that any mesoscale model, even with FDDA, would be able to simulate such rapid fluctuations. Closer examination of the database revealed that many surface sites reported hourly observations, while others reported only every 3 hours. The periodic loss of many sites appears to have been the primary cause of the apparent rapid wind fluctuations. However, the model also appears to have a small slow bias during this run segment, which in principle could be overcome. These characteristics found in **Figure 10** are corroborated by the statistics for the first segment presented in **Table 5**.

Meanwhile, **Figure 11** presents the evolution of the domain-averaged surface-layer wind directions for 7-11 October 1999 on the 4-km grid. While the model is successful in reproducing the major trends of wind direction, it exhibits a large bias of nearly 20 degrees on the first day. However, for the rest of the period, there appears to be little substantial bias, while the observed and modeled winds exhibit large and rapid fluctuations in direction (sometimes more than 100 degrees in an hour). Contributing to the impact of the data intermittence noted above, these large changes in direction are due in part to the fact that the 4-km domain covers a data-sparse region having few observing sites. Thus, a wind shift or data loss at just a couple of sites may cause the domain statistics to respond dramatically. As expected, the wind biases and much of the wind fluctuations evident at the surface become less severe in the PBL above the surface (**Figure 12**).

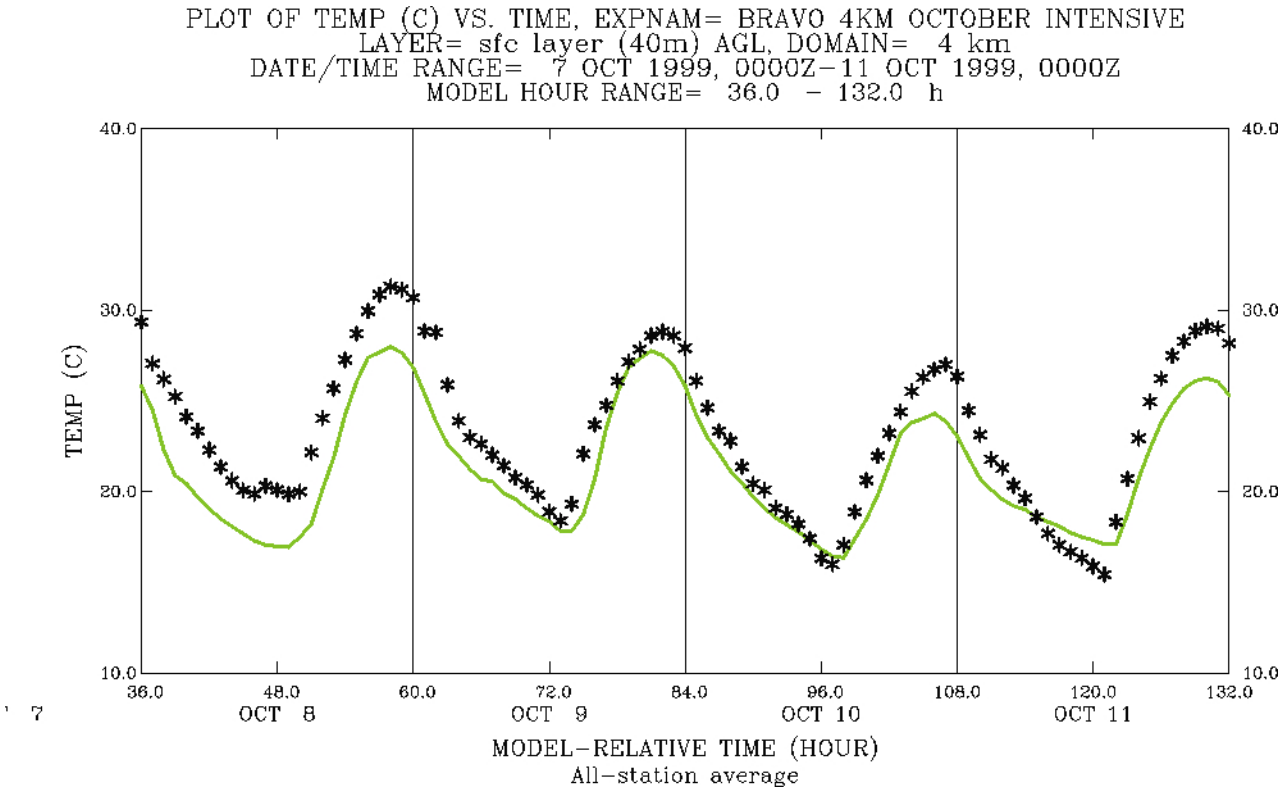

Figure 7. Domain-averaged hourly surface-layer temperature (C) on the 4-km domain for the period from 0000 UTC, 7 October to 0000 UTC, 11 October 1999. Solid line represents MM5 temperatures; asterisks represent observed temperatures.

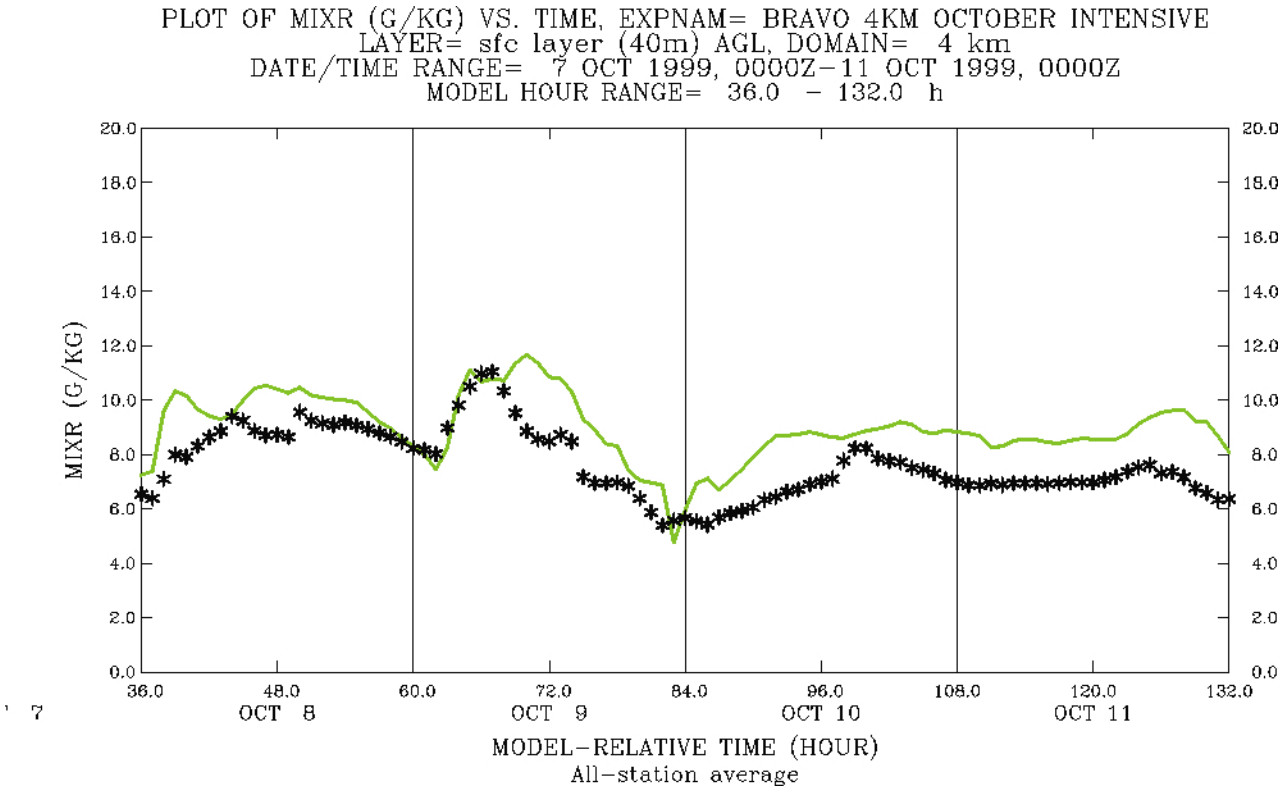

Figure 8. Domain-averaged hourly surface-layer water vapor mixing ratio (g kg^{-1}) on the 4-km domain for the period from 0000 UTC, 7 October to 0000 UTC, 11 October 1999. Solid line represents MM5 mixing ratios; asterisks represent observed mixing ratios.

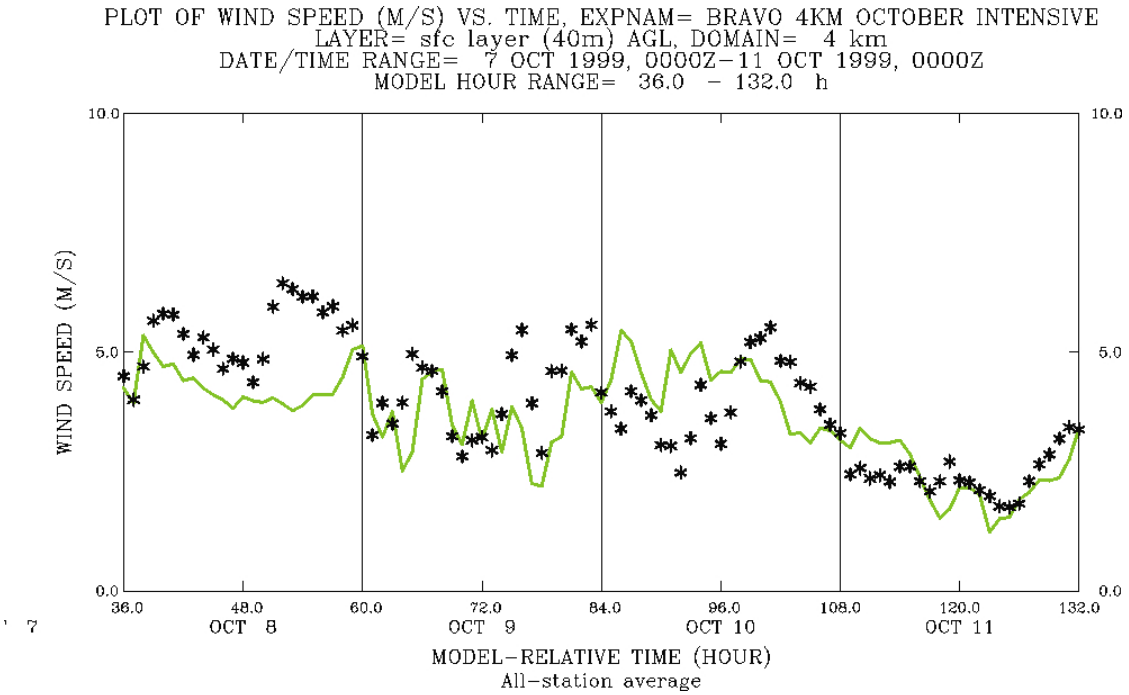

Figure 9. Domain-averaged hourly surface-layer wind speeds (m s^{-1}) on the 4-km domain for the period from 0000 UTC, 7 October to 0000 UTC, 11 October 1999. Solid line represents MM5 winds; asterisks represent observed winds.

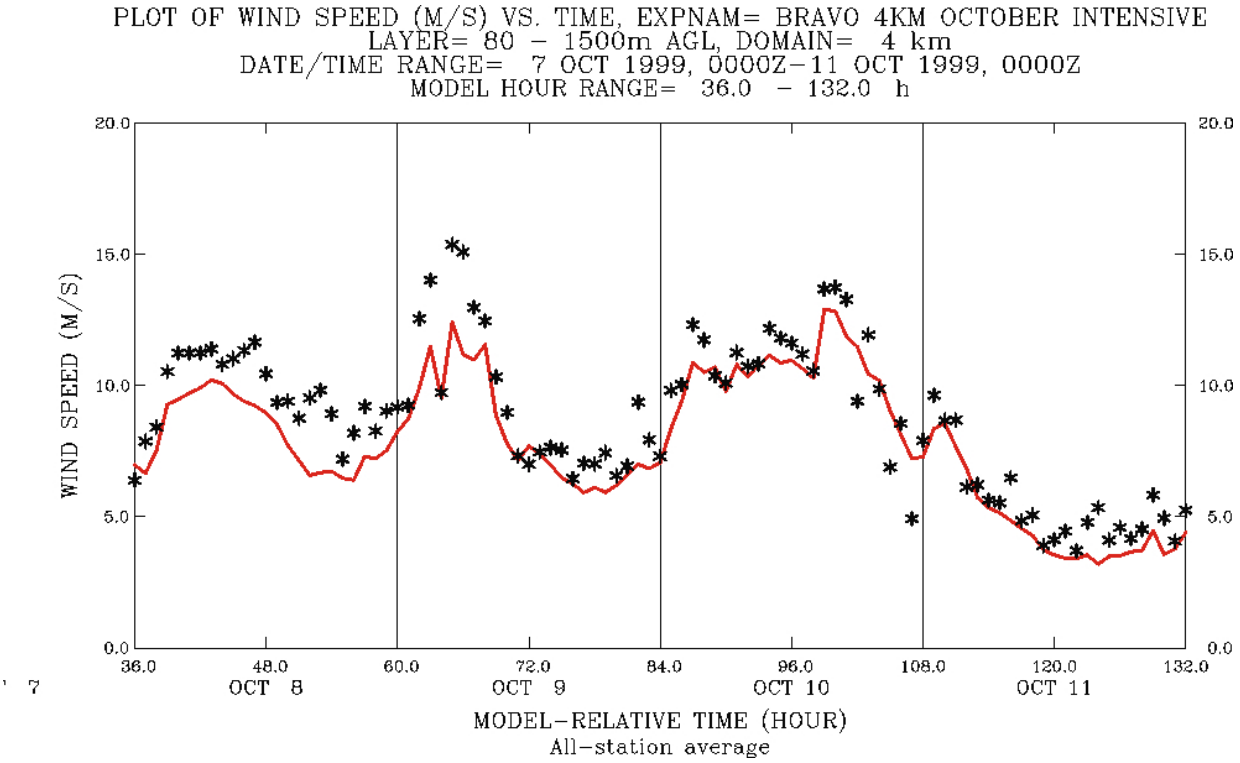

Figure 10. Domain-averaged hourly wind speeds (m s^{-1}) on the 4-km domain in the layer from 30-1500 m AGL for the period from 0000 UTC, 7 October to 0000 UTC, 11 October 1999. Solid line represents MM5 winds; asterisks represent observed winds.

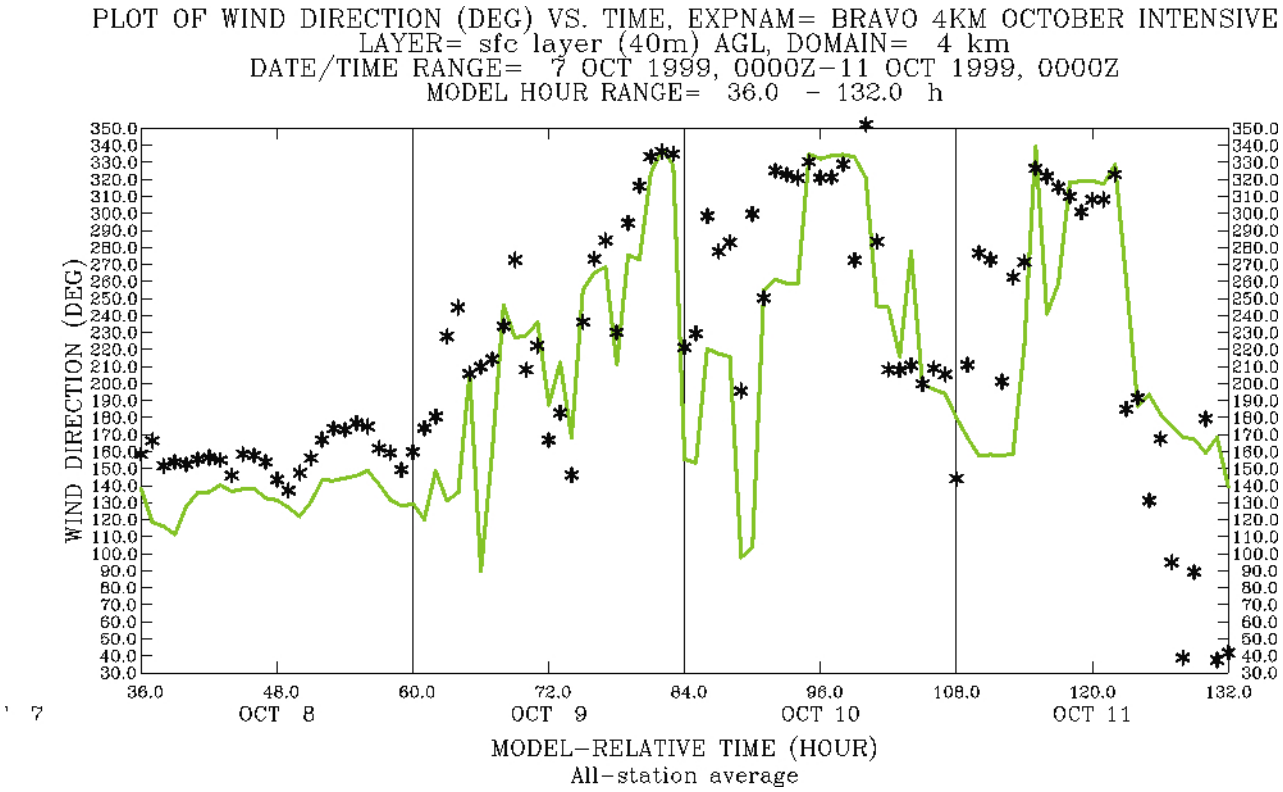

Figure 11. Domain-averaged hourly surface-layer wind direction (degrees) on the 4-km domain for the period from 0000 UTC, 7 October to 0000 UTC, 11 October 1999. Solid line represents MM5 winds; asterisks represent observed winds.

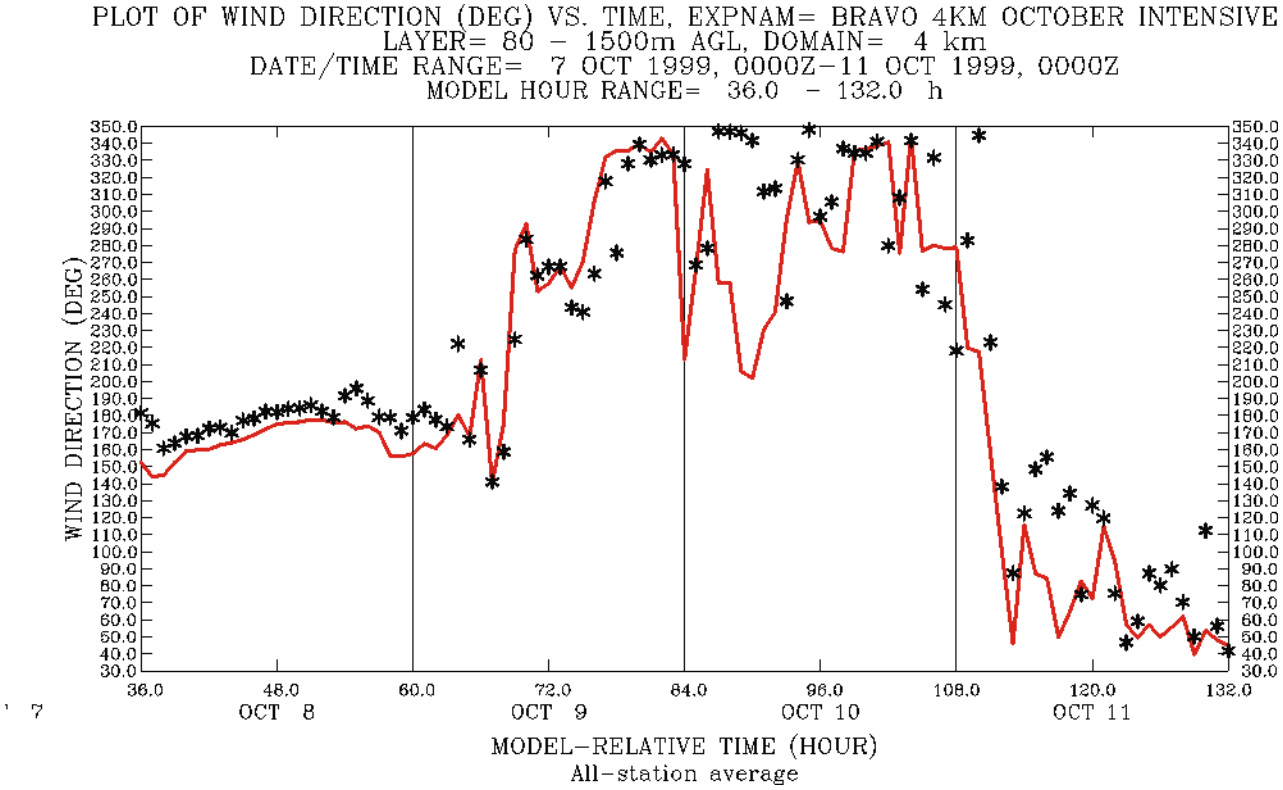

Figure 12. Domain-averaged hourly wind direction (degrees) on the 4-km domain in the 30-1500 m layer for the period from 0000 UTC, 7 October to 0000 UTC, 11 October 1999. Solid line represents MM5 winds; asterisks represent observed winds.

Table 6 presents the statistics calculated for the MM5 simulation on the 12-km domain during the October Intensive Period. Comparison with the statistics for the 4-km domain during the same period (**Table 5**) shows trends that are very similar to those found when comparing statistical accuracy for the domains during the August Intensive. The improved statistics for the 12-km domain extend to virtually all variables, statistical types and layers. For example, the surface temperature bias has dropped from -1.56 C on the 4-km domain to -0.57 C on the 12-km domain. Meanwhile the mixing ratio bias has decreased from +0.93 g kg^{-1} to only +0.18 g kg^{-1}. The smaller biases have contributed to similar drops in the MAEs to 1.65 C for temperature and 1.26 g kg^{-1} for mixing ratio. Thus, the 12-km error statistics for temperature and moisture in the simulations of the October Intensive Period are well within the targets for use in air-quality applications shown in **Table 1**, except that the temperature bias is still slightly larger than desired.

At the same time the 12-km solutions for wind speed and direction also fall within the standard range preferred for air-quality studies. The RMSE for speed in the surface layer is 1.37 m s^{-1}, while the speed bias is +0.33 m s^{-1}. Corresponding surface wind directions on the 12-km domain have MAE=23.8 degrees and ME=-0.4 degrees. These results are well within the benchmark guidelines recommended for use in air quality applications developed from past studies, leading to the conclusion that they would also have met the criteria if an independent quality-checked dataset of comparable extent and density were used for the evaluations (Seaman et al. 1995). As expected the RMSE and MAE for wind direction tend to decrease with height above the surface and are smaller for the 12-km domain than those found on the 4-km domain. As noted for the August period, the improved performance on the 12-km domain for all variables is most likely caused by the greater number of profilers in the larger area, including a number located over the relatively flat Great Plains. Overall, the evaluations for the MM5 12-km domain during the October Intensive Period indicate that the solutions are quite suitable for the study of regional transport affecting BBNP.

In **Table 7** we examine the statistics on the sub-region of the 36-km domains corresponding to the area of the 12-km domain during the October Intensive Period. Along with **Table 6**, **Table 7** shows that the wind errors are generally smaller in the 12-km model solutions at all levels. However, for the surface temperature and mixing ratio, the errors are slightly lower on the 36-km domain, but the differences are not significant. Altogether, it appears that the MM5 solutions on the 12-km domain are superior to those of the 36-km domain, as expected.

As for the 4-km domain discussed earlier, we present here a sample of the evolution of domain-wide temperature, mixing ratio and winds for the 12-km grid (**Figures 13-18**). **Figure 13** shows the surface layer temperature evolution for the model and observations during the period from 7-11 October 1999. Comparison with **Figure 7** reveals that the 12-km domain has a much better representation of the diurnal cycle. The minimums are simulated very well by the model, although the maximums remain a couple of degrees too cool. **Figure 13** confirms that the model is reproducing the temperature pattern well and that the cool bias in the 4-km domain may be confined primarily to areas with exceptionally dry soil conditions. This conclusion is corroborated by **Figure 14**, which shows that on the 12-km domain the model has reproduced nearly every trend in the evolution of the surface-layer mixing ratio.

Table 6. Statistics calculated on the MM5 12-km domain for the BRAVO October Intensive Period, 7-16 October 1999.

Variable	Verif. Layer	Segment Dates	Stat. Type	Segment Score	Avg. Score for Aug. Intensive
Temp. (C)	**15 m AGL**	00Z,7Oct - 00Z,11Oct	RMSE	1.61	
		12Z,10Oct - 00Z,16Oct	RMSE	1.67	**1.65**
		00Z,7Oct - 00Z,11Oct	MAE	1.26	
		12Z,10Oct - 00Z,16Oct	MAE	1.36	**1.32**
		00Z,7Oct - 00Z,11Oct	ME	-0.48	
		12Z,10Oct - 00Z,16Oct	ME	-0.64	**-0.57**
Mixing Ratio ($g\ kg^{-1}$)	**15 m AGL**	00Z,7Oct - 00Z,11Oct	RMSE	1.29	
		12Z,10Oct - 00Z,16Oct	RMSE	1.25	**1.26**
		00Z,7Oct - 00Z,11Oct	MAE	1.08	
		12Z,10Oct - 00Z,16Oct	MAE	1.01	**1.04**
		00Z,7Oct - 00Z,11Oct	ME	+0.24	
		12Z,10Oct - 00Z,16Oct	ME	+0.14	**+0.18**
Wind Speed ($m\ s^{-1}$)	**1500 - 5000 m AGL**	00Z,7Oct - 00Z,11Oct	RMSE	1.82	
		12Z,10Oct - 00Z,16Oct	RMSE	1.40	**1.57**
		00Z,7Oct - 00Z,11Oct	MAE	1.39	
		12Z,10Oct - 00Z,16Oct	MAE	1.09	**1.21**
		00Z,7Oct - 00Z,11Oct	ME	-0.56	
		12Z,10Oct - 00Z,16Oct	ME	-0.48	**-0.52**
	30-1500 m AGL	00Z,7Oct - 00Z,11Oct	RMSE	1.60	
		12Z,10Oct - 00Z,16Oct	RMSE	1.37	**1.46**
		00Z,7Oct - 00Z,11Oct	MAE	1.29	
		12Z,10Oct - 00Z,16Oct	MAE	1.10	**1.18**
		00Z,7Oct - 00Z,11Oct	ME	-0.16	
		12Z,10Oct - 00Z,16Oct	ME	-0.33	**-0.26**
	15 m AGL	00Z,7Oct - 00Z,11Oct	RMSE	1.52	
		12Z,10Oct - 00Z,16Oct	RMSE	1.25	**1.37**
		00Z,7Oct - 00Z,11Oct	MAE	1.22	
		12Z,10Oct - 00Z,16Oct	MAE	1.02	**1.10**
		00Z,7Oct - 00Z,11Oct	ME	+0.42	
		12Z,10Oct - 00Z,16Oct	ME	+0.26	**+0.33**
Wind Direction (deg.)	**1500 - 5000 m AGL**	00Z,7Oct - 00Z,11Oct	RMSE	14.9	
		12Z,10Oct - 00Z,16Oct	RMSE	15.0	**15.0**
		00Z,7Oct - 00Z,11Oct	MAE	10.0	
		12Z,10Oct - 00Z,16Oct	MAE	10.2	**10.1**
		00Z,7Oct - 00Z,11Oct	ME	-0.5	
		12Z,10Oct - 00Z,16Oct	ME	+0.6	**+0.1**
	30-1500 m AGL	00Z,7Oct - 00Z,11Oct	RMSE	18.3	
		12Z,10Oct - 00Z,16Oct	RMSE	20.2	**19.4**
		00Z,7Oct - 00Z,11Oct	MAE	13.3	
		12Z,10Oct - 00Z,16Oct	MAE	14.8	**14.2**
		00Z,7Oct - 00Z,11Oct	ME	-1.5	
		12Z,10Oct - 00Z,16Oct	ME	-0.9	**-1.1**
	15 m AGL	00Z,7Oct - 00Z,11Oct	RMSE	38.2	
		12Z,10Oct - 00Z,16Oct	RMSE	30.7	**33.8**
		00Z,7Oct - 00Z,11Oct	MAE	27.1	
		12Z,10Oct - 00Z,16Oct	MAE	21.3	**23.8**
		00Z,7Oct - 00Z,11Oct	ME	+0.4	
		12Z,10Oct - 00Z,16Oct	ME	-1.1	**-0.4**

Table 7. Statistics calculated on the MM5 36-km domain for the BRAVO October Intensive Period, 7-16 October 1999.

Variable	Verif. Layer	Segment Dates	Stat. Type	Segment Score	Avg. Score for Aug. Intensive
Temp. (C)	**15 m AGL**	00Z,7Oct - 00Z,11Oct	RMSE	1.53	
		12Z,10Oct - 00Z,16Oct	RMSE	1.53	**1.53**
		00Z,7Oct - 00Z,11Oct	MAE	1.21	
		12Z,10Oct - 00Z,16Oct	MAE	1.24	**1.22**
		00Z,7Oct - 00Z,11Oct	ME	-0.48	
		12Z,10Oct - 00Z,16Oct	ME	-0.59	**-0.54**
Mixing Ratio ($g\ kg^{-1}$)	**15 m AGL**	00Z,7Oct - 00Z,11Oct	RMSE	1.21	
		12Z,10Oct - 00Z,16Oct	RMSE	1.21	**1.21**
		00Z,7Oct - 00Z,11Oct	MAE	1.01	
		12Z,10Oct - 00Z,16Oct	MAE	0.99	**1.00**
		00Z,7Oct - 00Z,11Oct	ME	+0.26	
		12Z,10Oct - 00Z,16Oct	ME	+0.21	**+0.23**
Wind Speed ($m\ s^{-1}$)	**1500 - 5000 m AGL**	00Z,7Oct - 00Z,11Oct	RMSE	2.86	
		12Z,10Oct - 00Z,16Oct	RMSE	2.41	**2.60**
		00Z,7Oct - 00Z,11Oct	MAE	2.31	
		12Z,10Oct - 00Z,16Oct	MAE	1.95	**2.10**
		00Z,7Oct - 00Z,11Oct	ME	-0.85	
		12Z,10Oct - 00Z,16Oct	ME	-1.07	**-0.98**
	30-1500 m AGL	00Z,7Oct - 00Z,11Oct	RMSE	2.79	
		12Z,10Oct - 00Z,16Oct	RMSE	2.69	**2.73**
		00Z,7Oct - 00Z,11Oct	MAE	2.32	
		12Z,10Oct - 00Z,16Oct	MAE	2.20	**2.25**
		00Z,7Oct - 00Z,11Oct	ME	-0.34	
		12Z,10Oct - 00Z,16Oct	ME	+0.02	**-0.15**
	15 m AGL	00Z,7Oct - 00Z,11Oct	RMSE	1.77	
		12Z,10Oct - 00Z,16Oct	RMSE	1.56	**1.64**
		00Z,7Oct - 00Z,11Oct	MAE	1.45	
		12Z,10Oct - 00Z,16Oct	MAE	1.31	**1.37**
		00Z,7Oct - 00Z,11Oct	ME	+0.77	
		12Z,10Oct - 00Z,16Oct	ME	+0.61	**+0.67**
Wind Direction (deg.)	**1500 - 5000 m AGL**	00Z,7Oct - 00Z,11Oct	RMSE	23.9	
		12Z,10Oct - 00Z,16Oct	RMSE	31.9	**28.5**
		00Z,7Oct - 00Z,11Oct	MAE	17.7	
		12Z,10Oct - 00Z,16Oct	MAE	24.1	**21.4**
		00Z,7Oct - 00Z,11Oct	ME	-0.5	
		12Z,10Oct - 00Z,16Oct	ME	-1.5	**-1.1**
	30-1500 m AGL	00Z,7Oct - 00Z,11Oct	RMSE	31.8	
		12Z,10Oct - 00Z,16Oct	RMSE	38.9	**36.0**
		00Z,7Oct - 00Z,11Oct	MAE	24.1	
		12Z,10Oct - 00Z,16Oct	MAE	30.2	**27.6**
		00Z,7Oct - 00Z,11Oct	ME	-1.5	
		12Z,10Oct - 00Z,16Oct	ME	-4.2	**-3.0**
	15 m AGL	00Z,7Oct - 00Z,11Oct	RMSE	44.0	
		12Z,10Oct - 00Z,16Oct	RMSE	40.4	**41.9**
		00Z,7Oct - 00Z,11Oct	MAE	32.1	
		12Z,10Oct - 00Z,16Oct	MAE	28.4	**30.0**
		00Z,7Oct - 00Z,11Oct	ME	+2.8	
		12Z,10Oct - 00Z,16Oct	ME	-2.21	**+0.0**

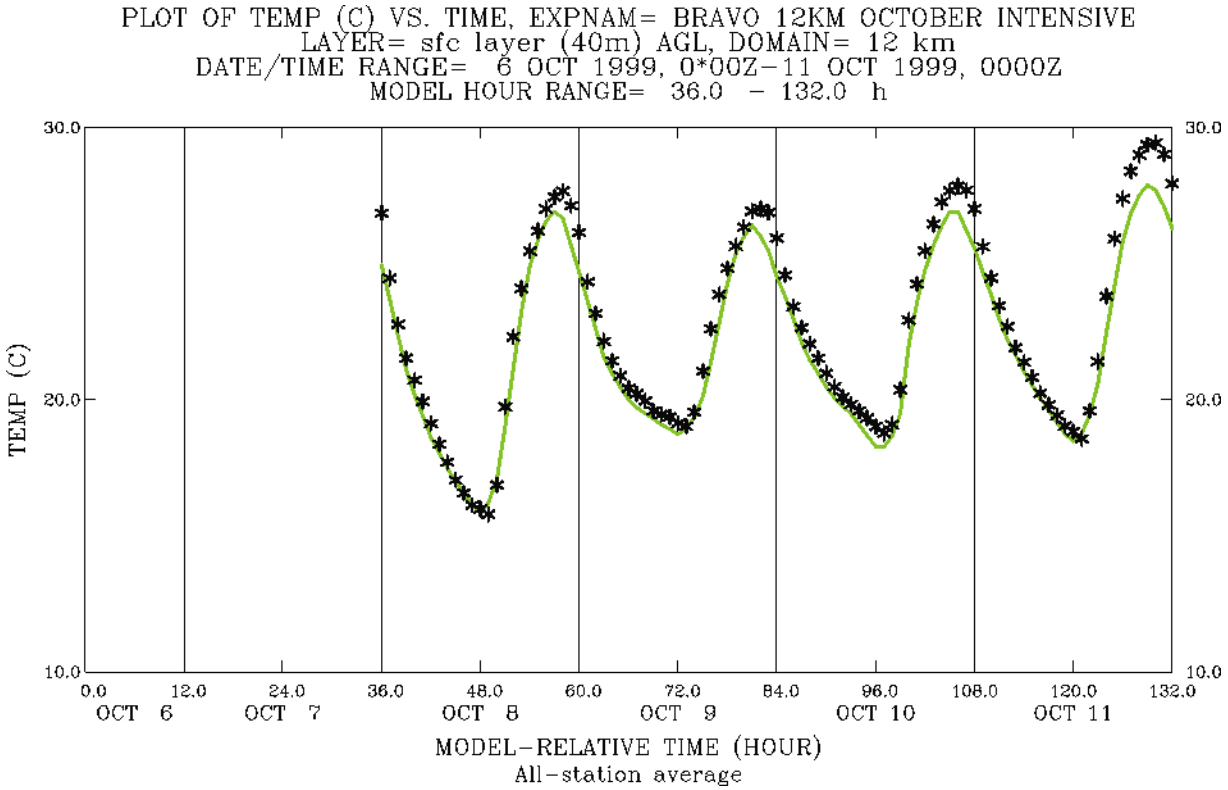

Figure 13. Domain-averaged hourly surface-layer temperature (C) on the 12-km domain for the period from 0000 UTC, 7 October to 0000 UTC, 11 October 1999. Solid line represents MM5 temperatures; asterisks represent observed temperatures.

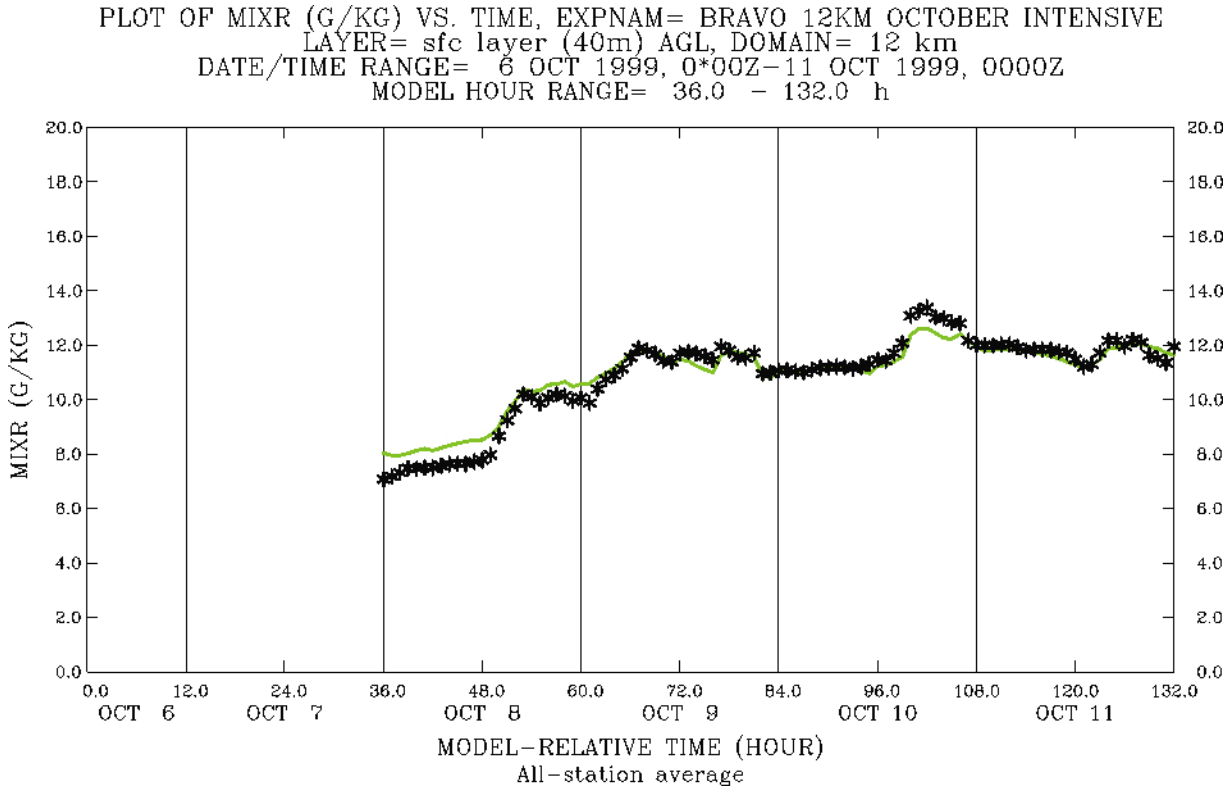

Figure 14. Domain-averaged hourly surface-layer water vapor mixing ratio (g kg^{-1}) on the 12-km domain for the period from 0000 UTC, 7 October to 0000 UTC, 11 October 1999. Solid line represents MM5 mixing ratios; asterisks represent observed mixing ratios.

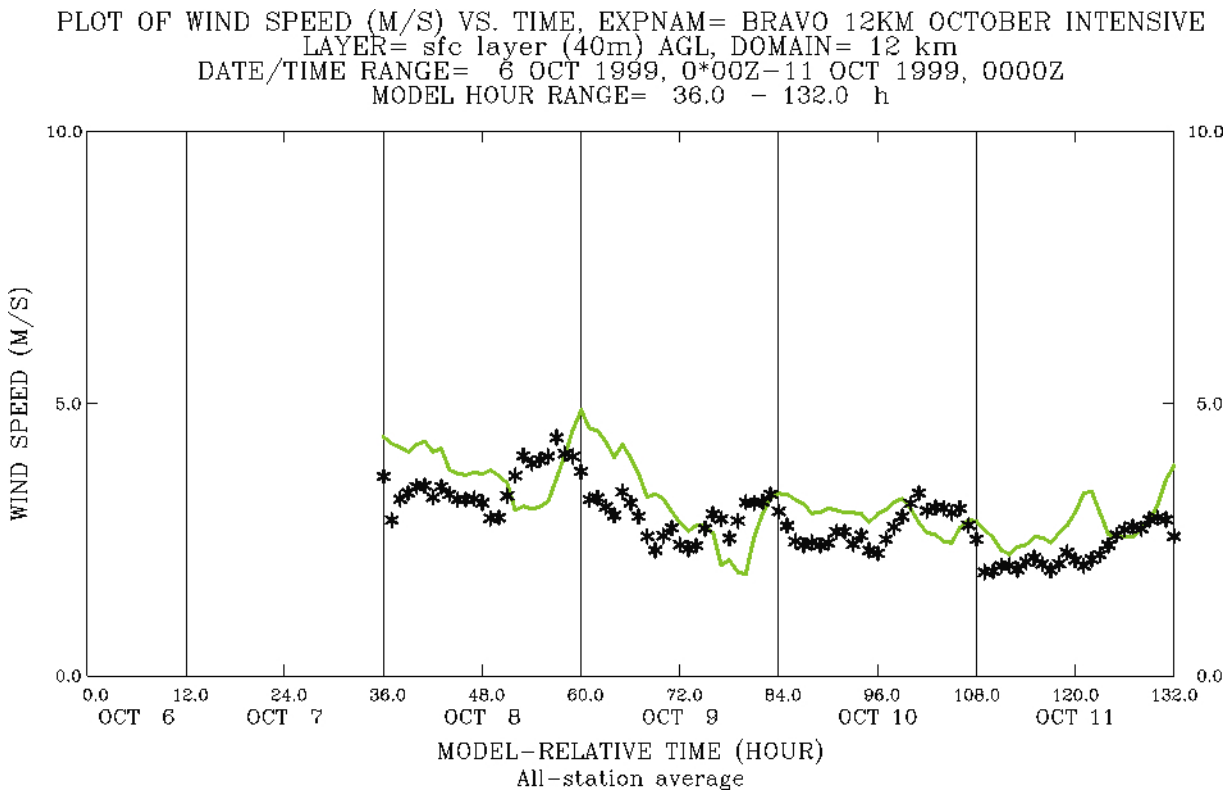

Figure 15. Domain-averaged hourly surface-layer wind speeds (m s^{-1}) on the 12-km domain for the period from 0000 UTC, 7 October to 0000 UTC, 11 October 1999. Solid line represents MM5 winds; asterisks represent observed winds.

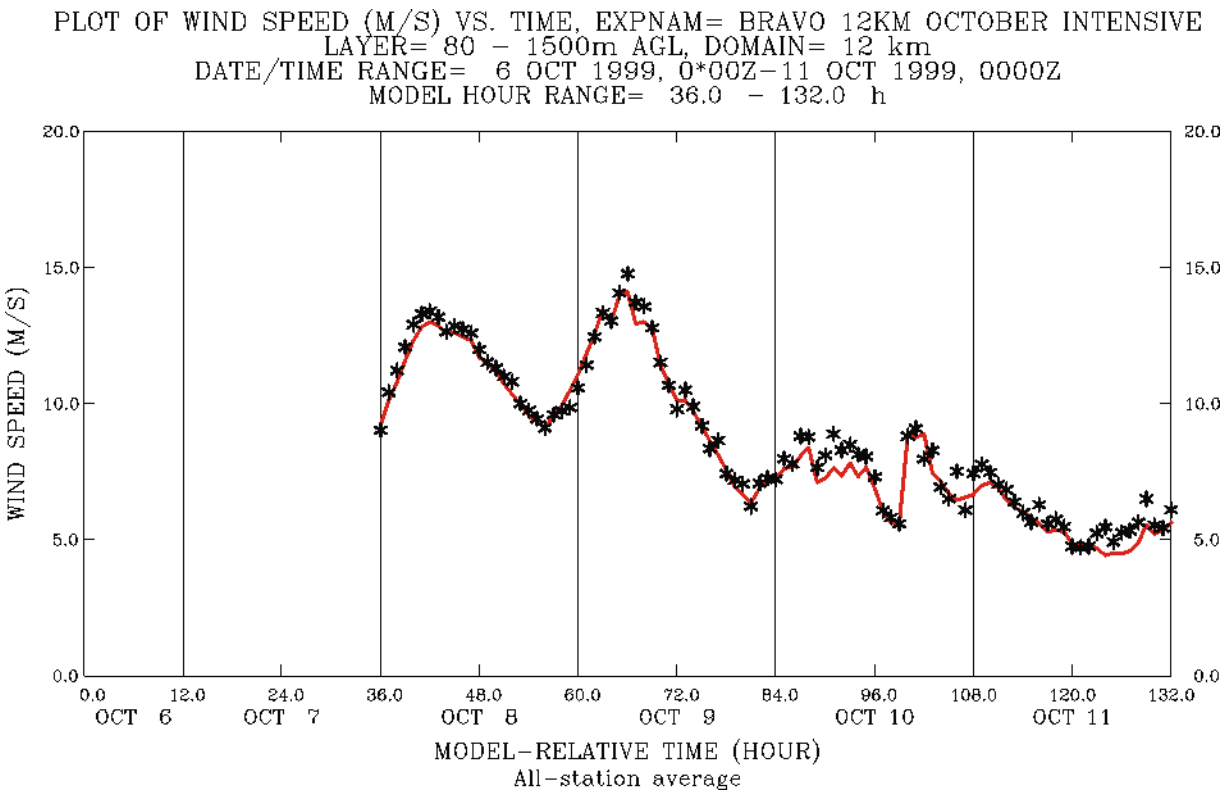

Figure 16. Domain-averaged hourly wind speeds (m s^{-1}) on the 12-km domain in the layer from 30-1500 m AGL for the period from 0000 UTC, 7 October to 0000 UTC, 11 October 1999. Solid line represents MM5 winds; asterisks represent observed winds.

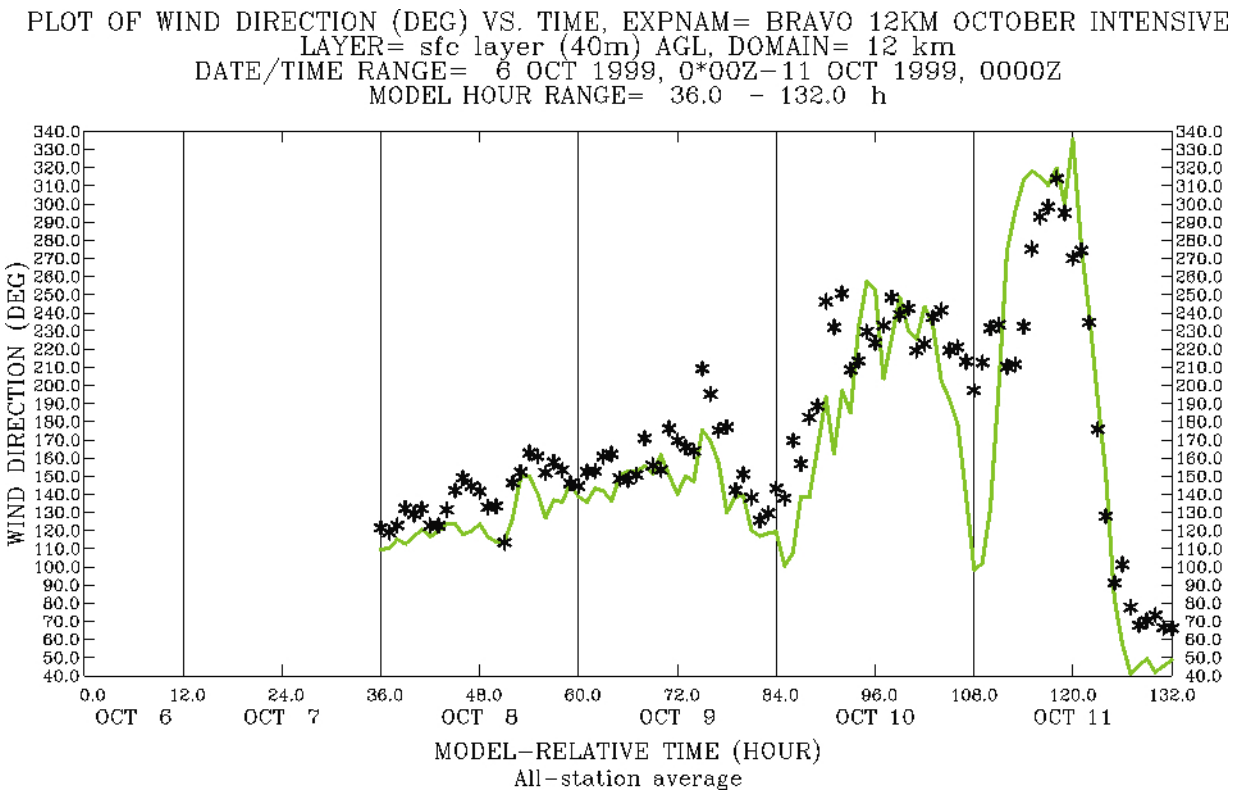

Figure 17. Domain-averaged hourly surface-layer wind direction (degrees) on the 12-km domain for the period from 0000 UTC, 7 October to 0000 UTC, 11 October 1999. Solid line represents MM5 winds; asterisks represent observed winds.

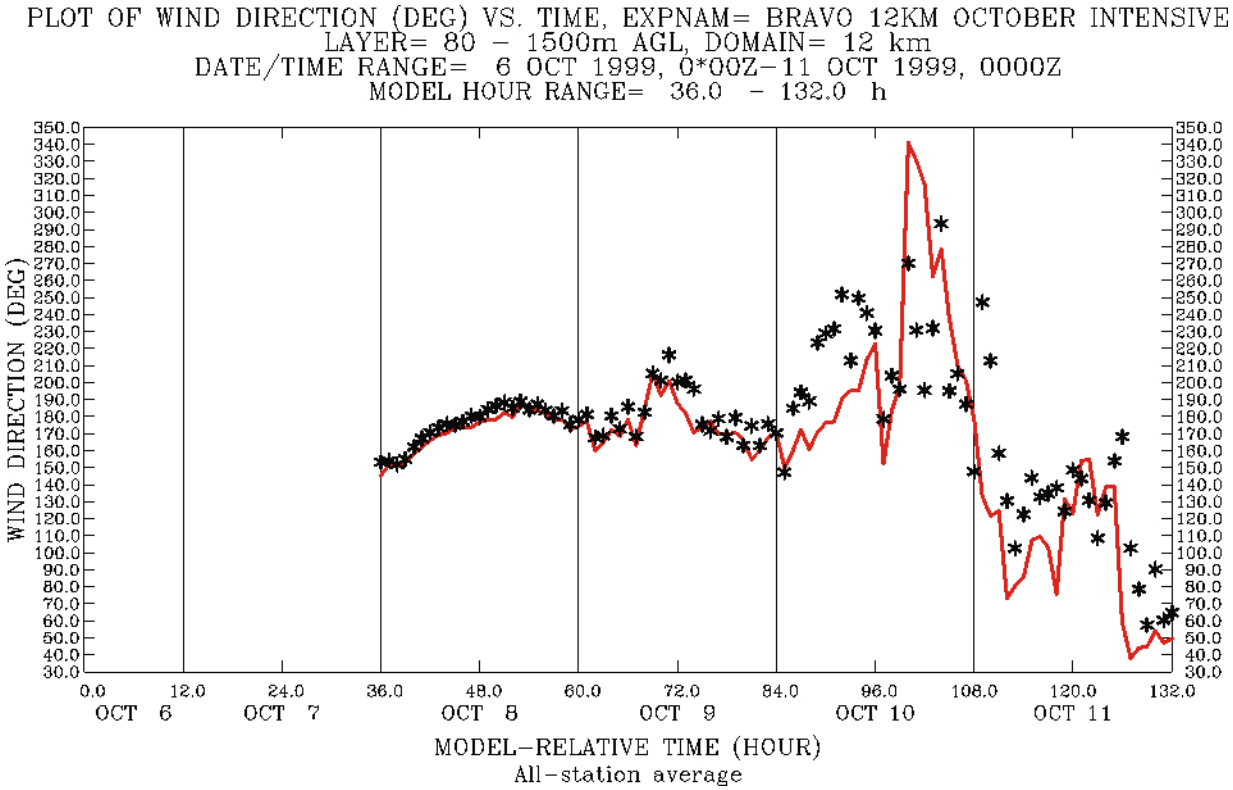

Figure 18. Domain-averaged hourly wind direction (degrees) on the 12-km domain in the 30-1500 m layer for the period from 0000 UTC, 7 October to 0000 UTC, 11 October 1999. Solid line represents MM5 winds; asterisks represent observed winds.

Figure 15 shows the evolution of the surface-layer winds, simulated and observed, on the 12-km domain for the same period during the October Intensive. The figure reveals that the 12-km domain exhibits no persistent speed bias, with errors on the order of 1 ms^{-1} fluctuating over periods of roughly 6-12 hours. The rapid hour-to-hour fluctuations noted in the surface layer on the 4-km domain (**Figure 7**) are not as evident on the 12-km domain, confirming that these were partly due to the scarcity of data in the model's fine grid region. **Figure 16** reveals the wind speed evolution for the nominal PBL on the 12-km for the same days, 7-11 October 1999. The model has captured the significant changes of wind speed that occur over periods ranging from 3 - 24 h with remarkable accuracy. There is little bias in the solution and the hourly errors contributing to the MAE are small at most times. The surface and PBL changes in the wind direction on the 12-km domain largely reflect what has been noted for the speed. **Figure 17** indicates that the observed winds on the 12-km domain have modest hourly fluctuations of direction, much like those found on the 4-km domain (**Figure 11**). However, the fluctuations are much smaller on this coarser domain and the model generally fits the observations much more closely than in the 4-km simulation. Above the surface in the 30-1500 m layer of the 12-km domain, **Figure 18** shows that the model reproduces the swings in wind direction quite well, as expected for this larger domain, except when large sudden changes of direction occur.

In addition to the statistical evaluations, visual comparisons were made between analyzed fields and variable fields simulated by the model. It is unnecessary to present extensive comparisons of spatial fields, but a single example is shown here to indicate the typical level of detail found in the wind fields generated by the MM5. **Figure 19** shows the model-simulated surface wind field at 2100 UTC (15:00 LST) on the 12-km domain for 7 October, during the October Intensive Period. This case exhibits the common situation over TX in which the Rio Grande Valley is experiencing southeasterly flow, while westerly flow is found to the west of a cold front from El Paso to northeastern NM. **Figure 20** shows a NCEP surface analysis 3 h earlier from 1800 UTC (12:00 LST). The analysis confirms the surface flow pattern simulated by the MM5.

It is noted that the very similar characteristics in the statistics for the model simulations during the August and October Intensive Periods suggests that the model should perform reasonably well during the entire four-month BRAVO period. Comparisons of the 4-km and 12-km results have indicated that the 12-km results capture considerable detail (not shown) and the statistics for the 12-km domain compare very favorably to those calculated on the 4-km and 36-km domains.

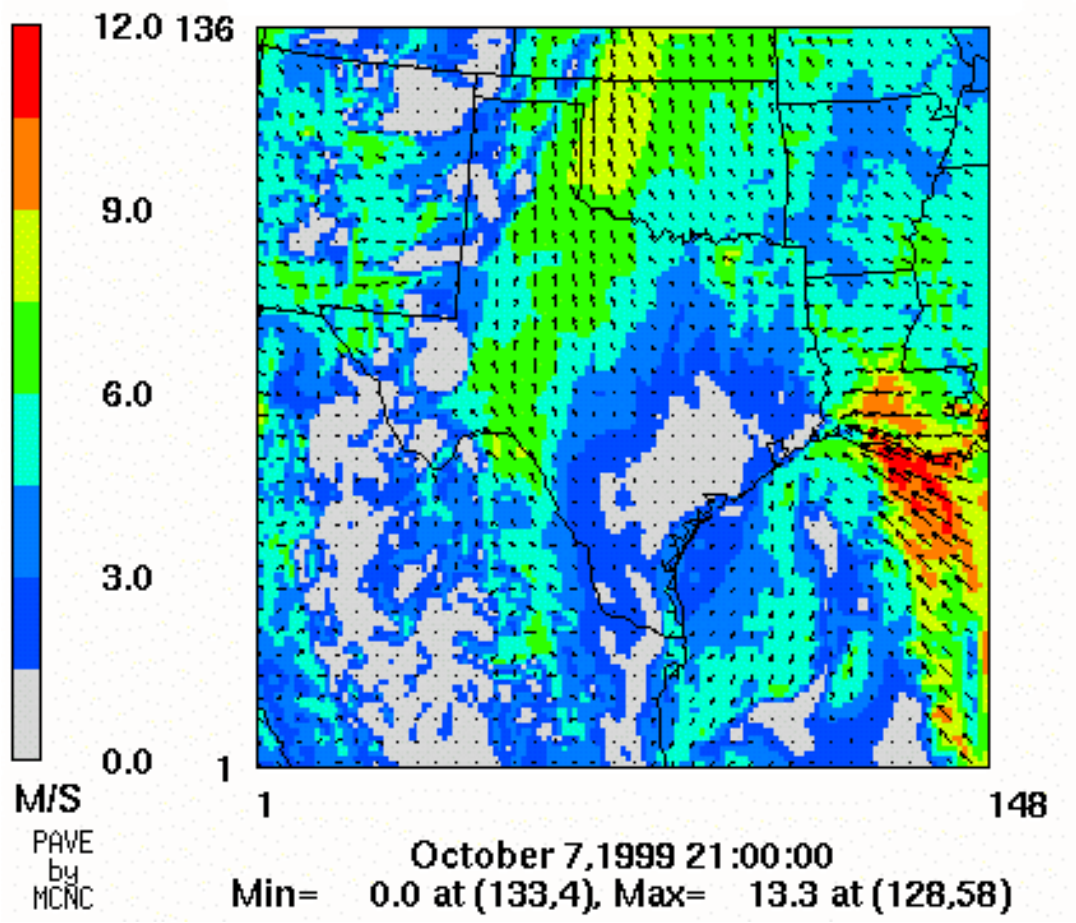

Figure 19. Surface-layer wind field (m s^{-1}) simulated by the MM5 on the 12-km domain at 2100 UTC (15:00 CST), 7 October 1999. Speed (m s^{-1}) is represented by the color fill.

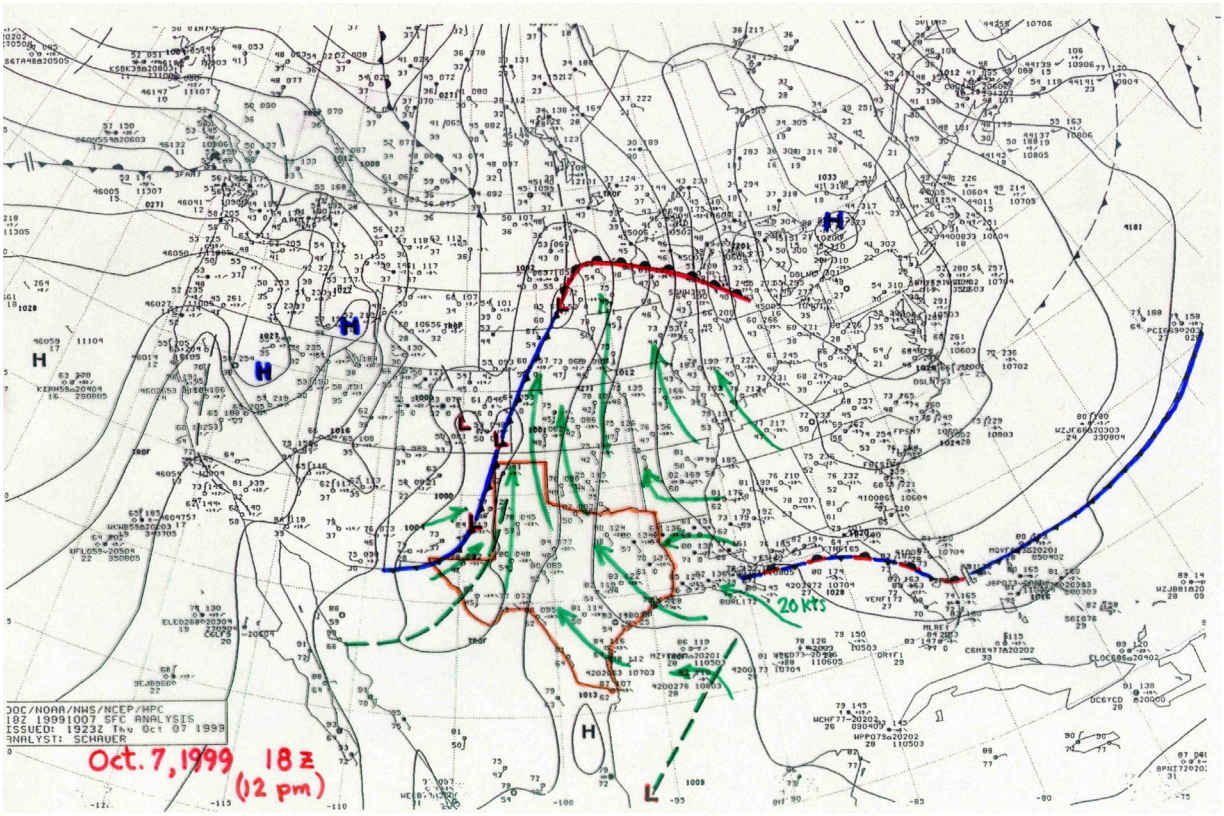

Figure 20. NCEP surface analysis for 1800 UTC (12:00 CST) showing regional flow over TX and the surrounding area (green arrows). Isobar interval is 4 mb.

3.2 Four-Month BRAVO Period

Having examined the two BRAVO Intensive Periods at length, we are now ready to turn to the full four-month BRAVO period for which only the 12-km and 36-km MM5 solutions are available. The statistics for surface temperature and mixing ratio are summarized in **Tables 8-13**, while the wind speed and direction statistics from the surface to 5000 m are given in **Tables 14-25**. They provide the most complete evaluation for the MM5 BRAVO simulations. In particular, these tables are useful for spotting trends, such as seasonality and in the case of the winds other factors that may be related to the vertical structure of the atmosphere. While examining the statistics, it should be remembered that for this study the MM5's FDDA system primarily assimilates wind data at the surface and aloft. These are by far the most abundant data in the BRAVO database. Temperature is not assimilated between the surface and 1500 m AGL, but it is assimilated in the free troposphere above 1500 m. Mixing ratio is assimilated above the PBL, but with a nudging coefficient that is more than an order of magnitude smaller than used for wind and temperature. At the surface winds are assimilated in a manner similar to the upper levels, except that the radius of influence given to the observations is smaller than it is aloft. In this study surface temperature and mixing ratio data are assimilated at the surface, using an indirect approach that estimates the error in the surface sensible and latent heat fluxes from the surface atmospheric observations (Alapaty et al. 2001). No temperature or moisture nudging is applied within the PBL.

One additional factor of interest in the interpretation of **Tables 8-25** is that NCEP experienced a serious fire in its computer facility on 27 September 1999 that effectively destroyed much of its computational capacity. Backup procedures were invoked whereby the other two operational centers in the U.S. (the Air Force Weather Agency in Omaha and the Navy's Fleet Numerical Meteorological and Oceanographical Center in Monterey) rapidly came to NCEP's assistance. In an impressive display of dedication and technical expertise, these centers rapidly converted non-critical portions of their model run schedules to install and run the most essential NCEP products on their own computer systems, including the NCEP global modeling system used for the background states of the MM5 analyses. Thus, PSU was able to return to NCEP model products for the BRAVO study almost immediately, with only a brief switch to ECMWF global model fields for a couple of days (primarily, the segment from 24-30 September would be affected). However, the effect on MM5 solutions should be minimal because MM5 continues to assimilate the BRAVO observations and analyses through its data assimilation scheme. In addition the operational centers carefully track and compare the accuracy of their global models and it is well established that on average there is little difference in the accuracy between the NCEP and ECMWF solutions. (In fact ECMWF's global products typically score slightly better for some common measures of skill.) Consequently, the impact of this change was not found to be discernible in the MM5 statistical results.

Tables 8-10 present the statistical evaluations for the 12-km RMSE, MAE, and ME, respectively, for the surface temperature and water-vapor mixing ratio over the entire period, bundled by run segment, month, and the full four-month study period. First, we note that the ME of mixing ratio (**Table 10**) indicates that the model simulations begin with a small dry bias in July of -0.19 g kg^{-1}, but they then develop a modest moist bias for the remaining three months

(+0.32-0.42 g kg^{-1}). These biases are small, with only a few 5 1/2 day segments exceeding the standard target for mixing ratio bias of <0.5 g kg^{-1}, so that the average moisture bias for the four-month BRAVO period is only +0.24 g kg^{-1}. The model-simulated surface-layer moisture, of course, is strongly related to the model's surface evaporative flux, which in turn is influenced strongly by the model's specification of the soil moisture availability. The consistency of the comparatively small biases shows that the soil moisture availability on the 12-km domain is, on average, slightly too large, but not by very much except in a few particularly dry segments. One of these dry spells appears to have coincided roughly with the August Intensive Period, which had a ME=+0.48 g kg^{-1} (**Table 3**), but the results shown here in **Table 10** indicate that the model error for that Intensive Period was not typical of the full four-month study. The only other segments with notably positive surface-layer moist biases occurred at the end of October, when the bias jumped to +0.81 g kg^{-1} in the final segment. Even so, the monthly surface moisture bias in October was not very severe (ME_{OCT}=+0.42 g kg^{-1}).

The biases expected in the surface temperature simulations for any predictive model are expected to be closely linked to mixing ratio errors and in turn to soil moisture uncertainty. **Table 10** indicates that the 12-km ME for surface-layer temperature had a consistent cool bias that extended through all four months. The bias was smallest during July (ME_{JUL}=-0.31 C), but then became larger during August-October, ranging between -0.51 and -0.60 C, coinciding with the time when the simulated surface mixing ratio developed a moderate moist bias. This is consistent with the trend in the bias diagnosed for soil moisture availability, as inferred from the mixing ratio errors discussed in the preceding paragraph. Overall, the four-month 12-km temperature bias is -0.49 C, which is about equal to the standard target established in **Table 1**. The segments having the largest cool bias occur at the end of October (up to -0.9 C), when the moisture bias is also greatest.

The fairly small biases for temperature and moisture found in the surface layer of the 12-km domain mean that there should be only small systematic errors contributing to RMSE and MAE for these two variable fields (**Tables 8 and 9**). Thus, **Table 9** indicates that the MAE for 12-km surface temperature over the BRAVO period is only 1.37 C, with monthly average MAEs ranging from 1.24 C in July to 1.48 C in October. The same table reveals that the four-month MAE for 12-km mixing ratio was only 1.22 g kg^{-1}, while the monthly average MAEs range from 1.56 g kg^{-1} in August to 0.95 g kg^{-1} in October. Therefore, the standard targets for MAE of surface layer temperature and mixing ratio have been met quite easily in the 12-km MM5 BRAVO simulation and these fields should be very suitable for air-quality applications.

Examination of the 36-km domain statistics for surface-layer temperature and mixing ratio during the four-month BRAVO period reveals that the biases on the two domains are virtually the same, with no evidence of statistically significant differences (**Table 13**). **Tables 11 and 12** show that there are no important differences in surface layer mixing ratio RMSE and MAE on the 36-km domain, as well (compare to **Tables 8 and 9**). However, the same figures indicate that there does appear to be a small but significant reduction of RMSE and MAE in the 36-km surface temperatures versus those on the 12-km domain. Specifically, the 36-km temperature MAE = 1.26 C, while on the 12-km domain the MAE = 1.37 C for the four-month period.

Table 8. Root Mean Square Error statistics for surface layer temperature and mixing ratio calculated on the MM5 12-km domain for the entire BRAVO study period from 1 July -31 October 1999.

Variable	Verif. Layer	Segment Dates	Stat. Type	Segment Score	Monthly Score	Avg. Score for full BRAVO study
Temp. (C)	**15 m AGL**	12Z,1Jul-00,7Jul		1.60	**July**	
		12Z,6Jul-00Z,12Jul		1.62		
		12Z,11Jul-00Z,17Jul		1.52		
		12Z,16Jul-00Z,22Jul		1.47	**1.57**	
		12Z,21Jul-00Z,27Jul		1.57		
		12Z,26Jul-00Z,1Aug		1.66		
		12Z,31Jul-00Z,6Aug		1.59	**August**	
		12Z,5Aug-00Z,11Aug		1.71		
		12Z,10Aug-00Z,16Aug		1.69		
		12Z,15Aug-00Z,21Aug		1.70	**1.71**	
		12Z,20Aug-00Z,26Aug		1.78		
		12Z,25Aug-00Z31Aug		1.80		
		12Z,30Aug-00Z,5Sep	**RMSE**	1.69	**September**	**1.71**
		12Z,4Sep-00Z,10Sep		Missing		
		12Z,9Sep-00Z,15Sep		Missing		
		12Z,14Sep-00Z,20Sep		Missing	**1.72**	
		12Z,19Sep-00Z,25Sep		1.67		
		12Z,24Sep-00Z30Sep		1.81		
		12Z,30Sep-00Z,6Oct		1.82	**October**	
		00Z,7Oct-00Z,11Oct		1.61		
		12Z,10Oct-00Z,16Oct		1.67		
		12Z,15Oct-00Z,21Oct		1.63	**1.84**	
		12Z,20Oct-00Z26Oct		2.22		
		12Z,25Oct-00Z,31Oct		2.08		
Mixing Ratio ($g\ kg^{-1}$)	**15 m AGL**	12Z,1Jul-00,7Jul		1.95	**July**	
		12Z,6Jul-00Z,12Jul		1.62		
		12Z,11Jul-00Z,17Jul		1.48		
		12Z,16Jul-00Z,22Jul		1.51	**1.75**	
		12Z,21Jul-00Z,27Jul		1.70		
		12Z,26Jul-00Z,1Aug		2.23		
		12Z,31Jul-00Z,6Aug		1.99	**August**	
		12Z,5Aug-00Z,11Aug		2.03		
		12Z,10Aug-00Z,16Aug		2.23		
		12Z,15Aug-00Z,21Aug		2.26	**2.18**	
		12Z,20Aug-00Z,26Aug		2.35		
		12Z,25Aug-00Z31Aug		2.20		
		12Z,30Aug-00Z,5Sep	**RMSE**	1.81	**September**	**1.62**
		12Z,4Sep-00Z,10Sep		Missing		
		12Z,9Sep-00Z,15Sep		Missing		
		12Z,14Sep-00Z,20Sep		Missing	**1.39**	
		12Z,19Sep-00Z,25Sep		1.12		
		12Z,24Sep-00Z30Sep		1.23		
		12Z,30Sep-00Z,6Oct		1.22	**October**	
		00Z,7Oct-00Z,11Oct		1.29		
		12Z,10Oct-00Z,16Oct		1.25		
		12Z,15Oct-00Z,21Oct		0.85	**1.17**	
		12Z,20Oct-00Z26Oct		1.09		
		12Z,25Oct-00Z,31Oct		1.29		

Table 9. Mean Absolute Error statistics for surface layer temperature and mixing ratio calculated on the MM5 12-km domain for the entire BRAVO study period from 1 July -31 October 1999.

Variable	Verif. Layer	Segment Dates	Stat. Type	Segment Score	Monthly Score	Avg. Score for full BRAVO study
Temp. (C)	**15 m AGL**	12Z,1Jul-00,7Jul		1.25	**July**	
		12Z,6Jul-00Z,12Jul		1.28		
		12Z,11Jul-00Z,17Jul		1.20		
		12Z,16Jul-00Z,22Jul		1.12	**1.24**	
		12Z,21Jul-00Z,27Jul		1.23		
		12Z,26Jul-00Z,1Aug		1.34		
		12Z,31Jul-00Z,6Aug		1.27	**August**	
		12Z,5Aug-00Z,11Aug		1.40		
		12Z,10Aug-00Z,16Aug		1.34		
		12Z,15Aug-00Z,21Aug		1.37	**1.38**	
		12Z,20Aug-00Z,26Aug		1.43		
		12Z,25Aug-00Z31Aug		1.46		
		12Z,30Aug-00Z,5Sep	**MAE**	1.34	**September**	**1.37**
		12Z,4Sep-00Z,10Sep		Missing		
		12Z,9Sep-00Z,15Sep		Missing		
		12Z,14Sep-00Z,20Sep		Missing	**1.38**	
		12Z,19Sep-00Z,25Sep		1.32		
		12Z,24Sep-00Z30Sep		1.48		
		12Z,30Sep-00Z,6Oct		1.44	**October**	
		00Z,7Oct-00Z,11Oct		1.26		
		12Z,10Oct-00Z,16Oct		1.36		
		12Z,15Oct-00Z,21Oct		1.30	**1.48**	
		12Z,20Oct-00Z26Oct		1.83		
		12Z,25Oct-00Z,31Oct		1.68		
Mixing Ratio ($g\ kg^{-1}$)	**15 m AGL**	12Z,1Jul-00,7Jul		1.39	**July**	
		12Z,6Jul-00Z,12Jul		1.20		
		12Z,11Jul-00Z,17Jul		1.12		
		12Z,16Jul-00Z,22Jul		1.11	**1.28**	
		12Z,21Jul-00Z,27Jul		1.24		
		12Z,26Jul-00Z,1Aug		1.62		
		12Z,31Jul-00Z,6Aug		1.34	**August**	
		12Z,5Aug-00Z,11Aug		1.42		
		12Z,10Aug-00Z,16Aug		1.65		
		12Z,15Aug-00Z,21Aug		1.69	**1.56**	
		12Z,20Aug-00Z,26Aug		1.66		
		12Z,25Aug-00Z31Aug		1.62		
		12Z,30Aug-00Z,5Sep	**MAE**	1.37	**September**	**1.22**
		12Z,4Sep-00Z,10Sep		Missing		
		12Z,9Sep-00Z,15Sep		Missing		
		12Z,14Sep-00Z,20Sep		Missing	**1.10**	
		12Z,19Sep-00Z,25Sep		0.94		
		12Z,24Sep-00Z30Sep		0.99		
		12Z,30Sep-00Z,6Oct		0.96	**October**	
		00Z,7Oct-00Z,11Oct		1.08		
		12Z,10Oct-00Z,16Oct		1.01		
		12Z,15Oct-00Z,21Oct		0.65	**0.95**	
		12Z,20Oct-00Z26Oct		0.93		
		12Z,25Oct-00Z,31Oct		1.09		

Table 10. Mean Error statistics for surface layer temperature and mixing ratio calculated on the MM5 12-km domain for the entire BRAVO study period from 1 July -31 October 1999.

Variable	Verif. Layer	Segment Dates	Stat. Type	Segment Score	Monthly Score	Avg. Score for full BRAVO study
Temp. (C)	**15 m AGL**	12Z,1Jul-00,7Jul		-0.39	**July**	
		12Z,6Jul-00Z,12Jul		-0.14		
		12Z,11Jul-00Z,17Jul		-0.21		
		12Z,16Jul-00Z,22Jul		-0.13	**-0.31**	
		12Z,21Jul-00Z,27Jul		-0.33		
		12Z,26Jul-00Z,1Aug		-0.68		
		12Z,31Jul-00Z,6Aug		-0.38	**August**	
		12Z,5Aug-00Z,11Aug		-0.60		
		12Z,10Aug-00Z,16Aug		-0.43		
		12Z,15Aug-00Z,21Aug		-0.59	**-0.53**	
		12Z,20Aug-00Z,26Aug		-0.65		
		12Z,25Aug-00Z31Aug		-0.54		
		12Z,30Aug-00Z,5Sep	**ME**	-0.48	**September**	**-0.49**
		12Z,4Sep-00Z,10Sep		Missing		
		12Z,9Sep-00Z,15Sep		Missing		
		12Z,14Sep-00Z,20Sep		Missing	**-0.51**	
		12Z,19Sep-00Z,25Sep		-0.52		
		12Z,24Sep-00Z30Sep		-0.54		
		12Z,30Sep-00Z,6Oct		-0.42	**October**	
		00Z,7Oct-00Z,11Oct		-0.48		
		12Z,10Oct-00Z,16Oct		-0.64		
		12Z,15Oct-00Z,21Oct		-0.34	**-0.60**	
		12Z,20Oct-00Z26Oct		-0.90		
		12Z,25Oct-00Z,31Oct		-0.79		
Mixing Ratio ($g\ kg^{-1}$)	**15 m AGL**	12Z,1Jul-00,7Jul		-0.37	**July**	
		12Z,6Jul-00Z,12Jul		-0.37		
		12Z,11Jul-00Z,17Jul		-0.26		
		12Z,16Jul-00Z,22Jul		-0.31	**-0.19**	
		12Z,21Jul-00Z,27Jul		-0.03		
		12Z,26Jul-00Z,1Aug		+0.22		
		12Z,31Jul-00Z,6Aug		-0.13	**August**	
		12Z,5Aug-00Z,11Aug		-0.02		
		12Z,10Aug-00Z,16Aug		+0.55		
		12Z,15Aug-00Z,21Aug		+0.65	**+0.32**	
		12Z,20Aug-00Z,26Aug		+0.31		
		12Z,25Aug-00Z31Aug		+0.55		
		12Z,30Aug-00Z,5Sep	**ME**	+0.45	**September**	**+0.24**
		12Z,4Sep-00Z,10Sep		Missing		
		12Z,9Sep-00Z,15Sep		Missing		
		12Z,14Sep-00Z,20Sep		Missing	**+0.40**	
		12Z,19Sep-00Z,25Sep		+0.35		
		12Z,24Sep-00Z30Sep		+0.40		
		12Z,30Sep-00Z,6Oct		+0.47	**October**	
		00Z,7Oct-00Z,11Oct		+0.24		
		12Z,10Oct-00Z,16Oct		+0.14		
		12Z,15Oct-00Z,21Oct		+0.08	**+0.42**	
		12Z,20Oct-00Z26Oct		+0.75		
		12Z,25Oct-00Z,31Oct		+0.81		

Table 11. Root Mean Square Error statistics for surface layer temperature and mixing ratio calculated on the MM5 36-km domain for the entire BRAVO study period from 1 July -31 October 1999.

Variable	Verif. Layer	Segment Dates	Stat. Type	Segment Score	Monthly Score	Avg. Score for full BRAVO study
Temp. (C)	**15 m AGL**	12Z,1Jul-00,7Jul		1.49	**July**	
		12Z,6Jul-00Z,12Jul		1.50		
		12Z,11Jul-00Z,17Jul		1.39		
		12Z,16Jul-00Z,22Jul		1.31	**1.23**	
		12Z,21Jul-00Z,27Jul		1.41		
		12Z,26Jul-00Z,1Aug		1.53		
		12Z,31Jul-00Z,6Aug		1.49	**August**	
		12Z,5Aug-00Z,11Aug		1.56		
		12Z,10Aug-00Z,16Aug		1.52		
		12Z,15Aug-00Z,21Aug		1.57	**1.56**	
		12Z,20Aug-00Z,26Aug		1.63		
		12Z,25Aug-00Z31Aug		1.61		
		12Z,30Aug-00Z,5Sep	**RMSE**	1.53	**September**	**1.50**
		12Z,4Sep-00Z,10Sep		1.56		
		12Z,9Sep-00Z,15Sep		Missing		
		12Z,14Sep-00Z,20Sep		Missing	**1.56**	
		12Z,19Sep-00Z,25Sep		Missing		
		12Z,24Sep-00Z30Sep		1.60		
		12Z,30Sep-00Z,6Oct		1.62	**October**	
		00Z,7Oct-00Z,11Oct		1.53		
		12Z,10Oct-00Z,16Oct		1.53		
		12Z,15Oct-00Z,21Oct		1.48	**1.66**	
		12Z,20Oct-00Z26Oct		1.97		
		12Z,25Oct-00Z,31Oct		1.82		
Mixing Ratio ($g\ kg^{-1}$)	**15 m AGL**	12Z,1Jul-00,7Jul		1.93	**July**	
		12Z,6Jul-00Z,12Jul		1.54		
		12Z,11Jul-00Z,17Jul		1.47		
		12Z,16Jul-00Z,22Jul		1.49	**1.75**	
		12Z,21Jul-00Z,27Jul		1.78		
		12Z,26Jul-00Z,1Aug		2.30		
		12Z,31Jul-00Z,6Aug		2.11	**August**	
		12Z,5Aug-00Z,11Aug		2.12		
		12Z,10Aug-00Z,16Aug		2.38		
		12Z,15Aug-00Z,21Aug		2.41	**2.29**	
		12Z,20Aug-00Z,26Aug		2.54		
		12Z,25Aug-00Z31Aug		2.20		
		12Z,30Aug-00Z,5Sep	**RMSE**	1.76	**September**	**1.69**
		12Z,4Sep-00Z,10Sep		1.77		
		12Z,9Sep-00Z,15Sep		Missing		
		12Z,14Sep-00Z,20Sep		Missing	**1.60**	
		12Z,19Sep-00Z,25Sep		Missing		
		12Z,24Sep-00Z30Sep		1.26		
		12Z,30Sep-00Z,6Oct		1.24	**October**	
		00Z,7Oct-00Z,11Oct		1.21		
		12Z,10Oct-00Z,16Oct		1.21		
		12Z,15Oct-00Z,21Oct		0.87	**1.12**	
		12Z,20Oct-00Z26Oct		1.03		
		12Z,25Oct-00Z,31Oct		1.14		

Table 12. Mean Absolute Error statistics for surface layer temperature and mixing ratio calculated on the MM5 36-km domain for the entire BRAVO study period from 1 July -31 October 1999.

Variable	Verif. Layer	Segment Dates	Stat. Type	Segment Score	Monthly Score	Avg. Score for full BRAVO study
Temp. (C)	**15 m AGL**	12Z,1Jul-00,7Jul		1.19	**July**	
		12Z,6Jul-00Z,12Jul		1.21		
		12Z,11Jul-00Z,17Jul		1.11		
		12Z,16Jul-00Z,22Jul		1.03	**1.16**	
		12Z,21Jul-00Z,27Jul		1.15		
		12Z,26Jul-00Z,1Aug		1.27		
		12Z,31Jul-00Z,6Aug		1.21	**August**	
		12Z,5Aug-00Z,11Aug		1.30		
		12Z,10Aug-00Z,16Aug		1.24		
		12Z,15Aug-00Z,21Aug		1.28	**1.28**	
		12Z,20Aug-00Z,26Aug		1.32		
		12Z,25Aug-00Z31Aug		1.33		
		12Z,30Aug-00Z,5Sep	**MAE**	1.22	**September**	**1.26**
		12Z,4Sep-00Z,10Sep		1.25		
		12Z,9Sep-00Z,15Sep		Missing		
		12Z,14Sep-00Z,20Sep		Missing	**1.26**	
		12Z,19Sep-00Z,25Sep		Missing		
		12Z,24Sep-00Z30Sep		1.31		
		12Z,30Sep-00Z,6Oct		1.30	**October**	
		00Z,7Oct-00Z,11Oct		1.21		
		12Z,10Oct-00Z,16Oct		1.24		
		12Z,15Oct-00Z,21Oct		1.18	**1.34**	
		12Z,20Oct-00Z26Oct		1.62		
		12Z,25Oct-00Z,31Oct		1.48		
Mixing Ratio ($g\ kg^{-1}$)	**15 m AGL**	12Z,1Jul-00,7Jul		1.34	**July**	
		12Z,6Jul-00Z,12Jul		1.12		
		12Z,11Jul-00Z,17Jul		1.10		
		12Z,16Jul-00Z,22Jul		1.09	**1.27**	
		12Z,21Jul-00Z,27Jul		1.27		
		12Z,26Jul-00Z,1Aug		1.68		
		12Z,31Jul-00Z,6Aug		1.46	**August**	
		12Z,5Aug-00Z,11Aug		1.49		
		12Z,10Aug-00Z,16Aug		1.81		
		12Z,15Aug-00Z,21Aug		1.83	**1.67**	
		12Z,20Aug-00Z,26Aug		1.82		
		12Z,25Aug-00Z31Aug		1.61		
		12Z,30Aug-00Z,5Sep	**MAE**	1.30	**September**	**1.26**
		12Z,4Sep-00Z,10Sep		1.26		
		12Z,9Sep-00Z,15Sep		Missing		
		12Z,14Sep-00Z,20Sep		Missing	**1.19**	
		12Z,19Sep-00Z,25Sep		Missing		
		12Z,24Sep-00Z30Sep		1.01		
		12Z,30Sep-00Z,6Oct		0.99	**October**	
		00Z,7Oct-00Z,11Oct		1.01		
		12Z,10Oct-00Z,16Oct		0.99		
		12Z,15Oct-00Z,21Oct		0.68	**0.92**	
		12Z,20Oct-00Z26Oct		0.87		
		12Z,25Oct-00Z,31Oct		0.96		

Table 13. Mean Error statistics for surface layer temperature and mixing ratio calculated on the MM5 36-km domain for the entire BRAVO study period from 1 July -31 October 1999.

Variable	Verif. Layer	Segment Dates	Stat. Type	Segment Score	Monthly Score	Avg. Score for full BRAVO study
Temp. (C)	**15 m AGL**	12Z,1Jul-00,7Jul		-0.56	**July**	
		12Z,6Jul-00Z,12Jul		-0.32		
		12Z,11Jul-00Z,17Jul		-0.35		
		12Z,16Jul-00Z,22Jul		-0.25	**-0.47**	
		12Z,21Jul-00Z,27Jul		-0.51		
		12Z,26Jul-00Z,1Aug		-0.81		
		12Z,31Jul-00Z,6Aug		-0.50	**August**	
		12Z,5Aug-00Z,11Aug		-0.73		
		12Z,10Aug-00Z,16Aug		-0.56		
		12Z,15Aug-00Z,21Aug		-0.67	**-0.65**	
		12Z,20Aug-00Z,26Aug		-0.79		
		12Z,25Aug-00Z31Aug		-0.65		
		12Z,30Aug-00Z,5Sep	**ME**	-0.50	**September**	**-0.53**
		12Z,4Sep-00Z,10Sep		-0.33		
		12Z,9Sep-00Z,15Sep		Missing		
		12Z,14Sep-00Z,20Sep		Missing	**-0.46**	
		12Z,19Sep-00Z,25Sep		Missing		
		12Z,24Sep-00Z30Sep		-0.54		
		12Z,30Sep-00Z,6Oct		-0.41	**October**	
		00Z,7Oct-00Z,11Oct		-0.48		
		12Z,10Oct-00Z,16Oct		-0.59		
		12Z,15Oct-00Z,21Oct		-0.33	**-0.54**	
		12Z,20Oct-00Z26Oct		-0.76		
		12Z,25Oct-00Z,31Oct		-0.69		
Mixing Ratio ($g\ kg^{-1}$)	**15 m AGL**	12Z,1Jul-00,7Jul		-0.33	**July**	
		12Z,6Jul-00Z,12Jul		-0.21		
		12Z,11Jul-00Z,17Jul		-0.26		
		12Z,16Jul-00Z,22Jul		-0.22	**-0.14**	
		12Z,21Jul-00Z,27Jul		-0.01		
		12Z,26Jul-00Z,1Aug		+0.19		
		12Z,31Jul-00Z,6Aug		+0.00	**August**	
		12Z,5Aug-00Z,11Aug		-0.02		
		12Z,10Aug-00Z,16Aug		+0.56		
		12Z,15Aug-00Z,21Aug		+0.64	**+0.31**	
		12Z,20Aug-00Z,26Aug		+0.24		
		12Z,25Aug-00Z31Aug		+0.42		
		12Z,30Aug-00Z,5Sep	**ME**	+0.29	**September**	**+0.22**
		12Z,4Sep-00Z,10Sep		+0.21		
		12Z,9Sep-00Z,15Sep		Missing		
		12Z,14Sep-00Z,20Sep		Missing	**+0.31**	
		12Z,19Sep-00Z,25Sep		Missing		
		12Z,24Sep-00Z30Sep		+0.44		
		12Z,30Sep-00Z,6Oct		+0.51	**October**	
		00Z,7Oct-00Z,11Oct		+0.26		
		12Z,10Oct-00Z,16Oct		+0.21		
		12Z,15Oct-00Z,21Oct		+0.08	**+0.40**	
		12Z,20Oct-00Z26Oct		+0.67		
		12Z,25Oct-00Z,31Oct		+0.66		

Turning to the wind fields, **Tables 14-16** present the errors calculated for the model's wind speeds on the 12-km domain in the surface layer, the nominal PBL, and the free lower troposphere. First, **Table 16** indicates that the 12-km ME is consistently small at all three levels and for each month of the four-month study. The model simulations tend to have a small slow biases of about -0.4 to 0.5 m s^{-1} in the free troposphere (1500 - 5000 m AGL) and a smaller fast bias in the model's surface layer of ~ +0.2-0.5 m s^{-1}. These mean errors are within the standard target of <0.5 m s^{-1} for speed bias given in **Table 1**. This assessment is true for nearly all individual segments, as well. The corresponding RMS errors for speed appear in **Table 14**, which shows the four-month averaged RMSE ranging from 1.33 m s^{-1} in the free troposphere to 1.48 m s^{-1} in the surface layer. Further examination of this table shows that the RMSE aloft in the free troposphere is smallest in July (1.19 m s^{-1}) and grows gradually with time, reaching 1.44 m s^{-1} in October. This small but steadily upward trend in the RMSE aloft is a consequence of the steady growth in the mean zonal wind as the atmosphere shifts from a summertime barotropic environment toward a high-wind autumn baroclinic environment. No such seasonal trend is evident at the surface in **Table 14** because the errors there are dominated by the complexities of terrain variability. The RMSEs for wind speed fall well within the standard target generally used for air-quality applications (<2.0 m s^{-1}). In fact, not a single 5 1/2-day segment at any level failed to have an RMSE within the target. The largest wind speed RMSE = 1.82 m s^{-1} which occurred in a segment during October in the 1500-5000 m layer. Thus, the model's simulation of 12-km wind speeds appears to have been quite successful.

When the wind speed errors on the 12-km domain are compared to those found in the 36-km solutions (**Tables 17-19**), it immediately becomes evident that the 36-km domain has generally larger errors. Comparison of **Tables 16 and 19** shows that the wind speed biases have the same trends on the 36-km domain (negative bias in the free troposphere changing to a positive speed bias at the surface). However, the biases are about 50% larger than on the 12-km domain, so that the objective of having the bias < 0.5 m s^{-1} is violated in every month for the surface and free troposphere, including almost every 5 1/2 day segment. In the nominal boundary layer between 30-1500 m, which represents something of a transition layer, the biases remain small for each month, and also for the four-month average (ME=+0.17 m s^{-1}).

The larger errors in the 36-km solutions are continued in the RMSEs and MAEs shown in **Tables 17 and 18**, respectively. **Table 17** does reveal that the RMSE in the surface layer wind speed remains below the benchmark target of 2.0 m s^{-1} in all but two 5 1/2-day segments, so that the monthly and four-monthly averages are satisfactory. However, the four-month BRAVO $RMSE_{36}$ = 1.80 m s^{-1}, while on the 12-km domain, $RMSE_{12}$ = 1.48 m s^{-1}. This degradation of the RMSE in the 36-km solutions is partly due to the reduced horizontal resolution, of course, but is also influenced by the absence of observation nudging which is applied only to the 12-km and 4-km BRAVO domains. The error reduction in the 12-km solutions is about 22%, which is somewhat greater than the ~15% error reduction that can be expected due to the fact that the 12-km solutions cannot be evaluated with an independent data set. Despite this apparent difficulty in interpretation, it must be noted that on the 36-km domain the surface wind errors remain within the benchmark target even without obs-nudging and with independent verification of the solutions.

Table 14. Root Mean Square Error statistics for wind speed calculated on the MM5 12-km domain for the entire BRAVO study period from 1 July -31 October 1999.

Variable	Verif. Layer	Segment Dates	Stat. Type	Segment Score	Monthly Score	Avg. Score for full BRAVO study
Wind Speed ($m\ s^{-1}$)	**1500-5000 m AGL**	12Z,1Jul-00,7Jul		1.22	**July**	
		12Z,6Jul-00Z,12Jul		1.22		
		12Z,11Jul-00Z,17Jul		1.21		
		12Z,16Jul-00Z,22Jul		1.14	**1.19**	
		12Z,21Jul-00Z,27Jul		1.14		
		12Z,26Jul-00Z,1Aug		1.23		
		12Z,31Jul-00Z,6Aug		1.29	**August**	
		12Z,5Aug-00Z,11Aug		1.27		
		12Z,10Aug-00Z,16Aug		1.29		
		12Z,15Aug-00Z,21Aug		1.33	**1.31**	
		12Z,20Aug-00Z,26Aug		1.36		
		12Z,25Aug-00Z31Aug		1.32		
		12Z,30Aug-00Z,5Sep	**RMSE**	1.27	**September**	**1.33**
		12Z,4Sep-00Z,10Sep		Missing		
		12Z,9Sep-00Z,15Sep		Missing		
		12Z,14Sep-00Z,20Sep		Missing	**1.37**	
		12Z,19Sep-00Z,25Sep		1.27		
		12Z,24Sep-00Z30Sep		1.56		
		12Z,30Sep-00Z,6Oct		1.35	**October**	
		00Z,7Oct-00Z,11Oct		1.82		
		12Z,10Oct-00Z,16Oct		1.40		
		12Z,15Oct-00Z,21Oct		1.44	**1.44**	
		12Z,20Oct-00Z26Oct		1.20		
		12Z,25Oct-00Z,31Oct		1.40		
	30-1500 m AGL	12Z,1Jul-00,7Jul		1.53	**July**	
		12Z,6Jul-00Z,12Jul		1.37		
		12Z,11Jul-00Z,17Jul		1.38		
		12Z,16Jul-00Z,22Jul		1.31	**1.39**	
		12Z,21Jul-00Z,27Jul		1.33		
		12Z,26Jul-00Z,1Aug		1.39		
		12Z,31Jul-00Z,6Aug		1.44	**August**	
		12Z,5Aug-00Z,11Aug		1.43		
		12Z,10Aug-00Z,16Aug		1.50		
		12Z,15Aug-00Z,21Aug		1.36	**1.39**	
		12Z,20Aug-00Z,26Aug		1.48		
		12Z,25Aug-00Z31Aug		1.13		
		12Z,30Aug-00Z,5Sep	**RMSE**	1.33	**September**	**1.36**
		12Z,4Sep-00Z,10Sep		Missing		
		12Z,9Sep-00Z,15Sep		Missing		
		12Z,14Sep-00Z,20Sep		Missing	**1.44**	
		12Z,19Sep-00Z,25Sep		1.41		
		12Z,24Sep-00Z30Sep		1.59		
		12Z,30Sep-00Z,6Oct		1.45	**October**	
		00Z,7Oct-00Z,11Oct		1.60		
		12Z,10Oct-00Z,16Oct		1.37		
		12Z,15Oct-00Z,21Oct		1.48	**1.21**	
		12Z,20Oct-00Z26Oct		1.35		
		12Z,25Oct-00Z,31Oct		1.50		

Table 14., Cont'd. Root Mean Square Error statistics for wind speed calculated on the MM5 12-km domain for the entire BRAVO study period from 1 July -31 October 1999.

Variable	Verif. Layer	Segment Dates	Stat. Type	Segment Score	Monthly Score	Avg. Score for full BRAVO study
Wind Speed ($m\ s^{-1}$)	**15 m AGL**	12Z,1Jul-00,7Jul	**RMSE**	1.74	**July**	**1.48**
		12Z,6Jul-00Z,12Jul		1.44		
		12Z,11Jul-00Z,17Jul		1.52		
		12Z,16Jul-00Z,22Jul		1.53	**1.53**	
		12Z,21Jul-00Z,27Jul		1.42		
		12Z,26Jul-00Z,1Aug		1.54		
		12Z,31Jul-00Z,6Aug		1.34	**August**	
		12Z,5Aug-00Z,11Aug		1.52		
		12Z,10Aug-00Z,16Aug		1.58		
		12Z,15Aug-00Z,21Aug		1.30	**1.43**	
		12Z,20Aug-00Z,26Aug		1.47		
		12Z,25Aug-00Z31Aug		1.38		
		12Z,30Aug-00Z,5Sep		1.44	**September**	
		12Z,4Sep-00Z,10Sep		Missing		
		12Z,9Sep-00Z,15Sep		Missing		
		12Z,14Sep-00Z,20Sep		Missing	**1.50**	
		12Z,19Sep-00Z,25Sep		1.40		
		12Z,24Sep-00Z30Sep		1.67		
		12Z,30Sep-00Z,6Oct		1.56	**October**	
		00Z,7Oct-00Z,11Oct		1.52		
		12Z,10Oct-00Z,16Oct		1.25		
		12Z,15Oct-00Z,21Oct		1.53	**1.45**	
		12Z,20Oct-00Z26Oct		1.29		
		12Z,25Oct-00Z,31Oct		1.53		

Table 15. Mean Absolute Error statistics for wind speed calculated on the MM5 12-km domain for the entire BRAVO study period from 1 July -31 October 1999.

Variable	Verif. Layer	Segment Dates	Stat. Type	Segment Score	Monthly Score	Avg. Score for full BRAVO study
Wind Speed (ms^{-1})	**1500-5000 m AGL**	12Z,1Jul-00,7Jul		0.93	**July**	
		12Z,6Jul-00Z,12Jul		0.93		
		12Z,11Jul-00Z,17Jul		0.91		
		12Z,16Jul-00Z,22Jul		0.86	**0.90**	
		12Z,21Jul-00Z,27Jul		0.86		
		12Z,26Jul-00Z,1Aug		0.93		
		12Z,31Jul-00Z,6Aug		0.98	**August**	
		12Z,5Aug-00Z,11Aug		0.95		
		12Z,10Aug-00Z,16Aug		0.99		
		12Z,15Aug-00Z,21Aug		1.02	**1.00**	
		12Z,20Aug-00Z,26Aug		1.04		
		12Z,25Aug-00Z31Aug		1.01		
		12Z,30Aug-00Z,5Sep	**MAE**	0.97	**September**	**1.04**
		12Z,4Sep-00Z,10Sep		Missing		
		12Z,9Sep-00Z,15Sep		Missing		
		12Z,14Sep-00Z,20Sep		Missing	**1.17**	
		12Z,19Sep-00Z,25Sep		0.98		
		12Z,24Sep-00Z30Sep		1.56		
		12Z,30Sep-00Z,6Oct		1.05	**October**	
		00Z,7Oct-00Z,11Oct		1.39		
		12Z,10Oct-00Z,16Oct		1.09		
		12Z,15Oct-00Z,21Oct		1.10	**1.10**	
		12Z,20Oct-00Z26Oct		0.92		
		12Z,25Oct-00Z,31Oct		1.07		
	30-1500 m AGL	12Z,1Jul-00,7Jul		1.21	**July**	
		12Z,6Jul-00Z,12Jul		1.09		
		12Z,11Jul-00Z,17Jul		1.10		
		12Z,16Jul-00Z,22Jul		1.04	**1.10**	
		12Z,21Jul-00Z,27Jul		1.06		
		12Z,26Jul-00Z,1Aug		1.10		
		12Z,31Jul-00Z,6Aug		1.14	**August**	
		12Z,5Aug-00Z,11Aug		1.13		
		12Z,10Aug-00Z,16Aug		1.20		
		12Z,15Aug-00Z,21Aug		1.08	**1.15**	
		12Z,20Aug-00Z,26Aug		1.20		
		12Z,25Aug-00Z31Aug		1.13		
		12Z,30Aug-00Z,5Sep	**MAE**	1.05	**September**	**1.14**
		12Z,4Sep-00Z,10Sep		Missing		
		12Z,9Sep-00Z,15Sep		Missing		
		12Z,14Sep-00Z,20Sep		Missing	**1.15**	
		12Z,19Sep-00Z,25Sep		1.12		
		12Z,24Sep-00Z30Sep		1.27		
		12Z,30Sep-00Z,6Oct		1.17	**October**	
		00Z,7Oct-00Z,11Oct		1.29		
		12Z,10Oct-00Z,16Oct		1.10		
		12Z,15Oct-00Z,21Oct		1.19	**1.17**	
		12Z,20Oct-00Z26Oct		1.07		
		12Z,25Oct-00Z,31Oct		1.20		

Table 15., Cont'd. Mean Absolute Error statistics for wind speed calculated on the MM5 12-km domain for the entire BRAVO study period from 1 July -31 October 1999.

Variable	Verif. Layer	Segment Dates	Stat. Type	Segment Score	Monthly Score	Avg. Score for full BRAVO study
Wind Speed ($m\ s^{-1}$)	**15 m AGL**	12Z,1Jul-00,7Jul	**MAE**	1.45	**July**	**1.22**
		12Z,6Jul-00Z,12Jul		1.15		
		12Z,11Jul-00Z,17Jul		1.26		
		12Z,16Jul-00Z,22Jul		1.25	**1.27**	
		12Z,21Jul-00Z,27Jul		1.18		
		12Z,26Jul-00Z,1Aug		1.30		
		12Z,31Jul-00Z,6Aug		1.10	**August**	
		12Z,5Aug-00Z,11Aug		1.26		
		12Z,10Aug-00Z,16Aug		1.32		
		12Z,15Aug-00Z,21Aug		1.06	**1.18**	
		12Z,20Aug-00Z,26Aug		1.19		
		12Z,25Aug-00Z31Aug		1.13		
		12Z,30Aug-00Z,5Sep		1.19	**September**	
		12Z,4Sep-00Z,10Sep		Missing		
		12Z,9Sep-00Z,15Sep		Missing		
		12Z,14Sep-00Z,20Sep		Missing	**1.24**	
		12Z,19Sep-00Z,25Sep		1.15		
		12Z,24Sep-00Z30Sep		1.38		
		12Z,30Sep-00Z,6Oct		1.29	**October**	
		00Z,7Oct-00Z,11Oct		1.22		
		12Z,10Oct-00Z,16Oct		1.02		
		12Z,15Oct-00Z,21Oct		1.26	**1.18**	
		12Z,20Oct-00Z26Oct		1.06		
		12Z,25Oct-00Z,31Oct		1.25		

Table 16. Mean Error statistics for wind speed calculated on the MM5 12-km domain for the entire BRAVO study period from 1 July -31 October 1999.

Variable	Verif. Layer	Segment Dates	Stat. Type	Segment Score	Monthly Score	Avg. Score for full BRAVO study
Wind Speed ($m\ s^{-1}$)	**1500-5000 m AGL**	12Z,1Jul-00,7Jul	**ME**	-0.41	**July**	**-0.46**
		12Z,6Jul-00Z,12Jul		-0.50		
		12Z,11Jul-00Z,17Jul		-0.41		
		12Z,16Jul-00Z,22Jul		-0.43	**-0.46**	
		12Z,21Jul-00Z,27Jul		-0.48		
		12Z,26Jul-00Z,1Aug		-0.55		
		12Z,31Jul-00Z,6Aug		-0.53	**August**	
		12Z,5Aug-00Z,11Aug		-0.53		
		12Z,10Aug-00Z,16Aug		-0.44		
		12Z,15Aug-00Z,21Aug		-0.57	**-0.51**	
		12Z,20Aug-00Z,26Aug		-0.52		
		12Z,25Aug-00Z31Aug		-0.48		
		12Z,30Aug-00Z,5Sep		-0.53	**September**	
		12Z,4Sep-00Z,10Sep		Missing		
		12Z,9Sep-00Z,15Sep		Missing		
		12Z,14Sep-00Z,20Sep		Missing	**-0.45**	
		12Z,19Sep-00Z,25Sep		-0.37		
		12Z,24Sep-00Z30Sep		-0.45		
		12Z,30Sep-00Z,6Oct		-0.41	**October**	
		00Z,7Oct-00Z,11Oct		-0.56		
		12Z,10Oct-00Z,16Oct		-0.48		
		12Z,15Oct-00Z,21Oct		-0.36	**-0.43**	
		12Z,20Oct-00Z26Oct		-0.33		
		12Z,25Oct-00Z,31Oct		-0.46		
	30-1500 m AGL	12Z,1Jul-00,7Jul	**ME**	+0.04	**July**	**-0.20**
		12Z,6Jul-00Z,12Jul		-0.17		
		12Z,11Jul-00Z,17Jul		-0.15		
		12Z,16Jul-00Z,22Jul		-0.08	**-0.12**	
		12Z,21Jul-00Z,27Jul		-0.19		
		12Z,26Jul-00Z,1Aug		-0.16		
		12Z,31Jul-00Z,6Aug		-0.08	**August**	
		12Z,5Aug-00Z,11Aug		-0.24		
		12Z,10Aug-00Z,16Aug		-0.27		
		12Z,15Aug-00Z,21Aug		-0.27	**-0.21**	
		12Z,20Aug-00Z,26Aug		-0.22		
		12Z,25Aug-00Z31Aug		-0.18		
		12Z,30Aug-00Z,5Sep		-0.16	**September**	
		12Z,4Sep-00Z,10Sep		Missing		
		12Z,9Sep-00Z,15Sep		Missing		
		12Z,14Sep-00Z,20Sep		Missing	**-0.18**	
		12Z,19Sep-00Z,25Sep		-0.24		
		12Z,24Sep-00Z30Sep		-0.13		
		12Z,30Sep-00Z,6Oct		-0.27	**October**	
		00Z,7Oct-00Z,11Oct		-0.16		
		12Z,10Oct-00Z,16Oct		-0.33		
		12Z,15Oct-00Z,21Oct		-0.24	**-0.28**	
		12Z,20Oct-00Z26Oct		-0.29		
		12Z,25Oct-00Z,31Oct		-0.41		

Table 16., Cont'd. Mean Error statistics for wind speed calculated on the MM5 12-km domain for the entire BRAVO study period from 1 July -31 October 1999.

Variable	Verif. Layer	Segment Dates	Stat. Type	Segment Score	Monthly Score	Avg. Score for full BRAVO study
Wind Speed ($m\ s^{-1}$)	**15 m AGL**	12Z,1Jul-00,7Jul	**ME**	+0.74	**July**	**+0.38**
		12Z,6Jul-00Z,12Jul		+0.15		
		12Z,11Jul-00Z,17Jul		+0.38		
		12Z,16Jul-00Z,22Jul		+0.48	**+0.41**	
		12Z,21Jul-00Z,27Jul		+0.24		
		12Z,26Jul-00Z,1Aug		+0.44		
		12Z,31Jul-00Z,6Aug		+0.12	**August**	
		12Z,5Aug-00Z,11Aug		+0.23		
		12Z,10Aug-00Z,16Aug		+0.46		
		12Z,15Aug-00Z,21Aug		+0.11	**+0.20**	
		12Z,20Aug-00Z,26Aug		+0.21		
		12Z,25Aug-00Z31Aug		+0.08		
		12Z,30Aug-00Z,5Sep		+0.35	**September**	
		12Z,4Sep-00Z,10Sep		Missing		
		12Z,9Sep-00Z,15Sep		Missing		
		12Z,14Sep-00Z,20Sep		Missing	**+0.49**	
		12Z,19Sep-00Z,25Sep		+0.37		
		12Z,24Sep-00Z30Sep		+0.75		
		12Z,30Sep-00Z,6Oct		+0.62	**October**	
		00Z,7Oct-00Z,11Oct		+0.42		
		12Z,10Oct-00Z,16Oct		+0.26		
		12Z,15Oct-00Z,21Oct		+0.57	**+0.40**	
		12Z,20Oct-00Z26Oct		+0.28		
		12Z,25Oct-00Z,31Oct		+0.24		

Table 17. Root Mean Square Error statistics for wind speed calculated on the MM5 36-km domain for the entire BRAVO study period from 1 July -31 October 1999.

Variable	Verif. Layer	Segment Dates	Stat. Type	Segment Score	Monthly Score	Avg. Score for full BRAVO study
Wind Speed ($m\ s^{-1}$)	**1500-5000 m AGL**	12Z,1Jul-00,7Jul		1.97	**July**	
		12Z,6Jul-00Z,12Jul		1.90		
		12Z,11Jul-00Z,17Jul		1.98		
		12Z,16Jul-00Z,22Jul		1.78	**1.89**	
		12Z,21Jul-00Z,27Jul		1.83		
		12Z,26Jul-00Z,1Aug		1.85		
		12Z,31Jul-00Z,6Aug		1.94	**August**	
		12Z,5Aug-00Z,11Aug		1.98		
		12Z,10Aug-00Z,16Aug		2.12		
		12Z,15Aug-00Z,21Aug		2.06	**2.08**	
		12Z,20Aug-00Z,26Aug		2.24		
		12Z,25Aug-00Z31Aug		2.15		
		12Z,30Aug-00Z,5Sep	**RMSE**	1.92	**September**	**2.16**
		12Z,4Sep-00Z,10Sep		2.54		
		12Z,9Sep-00Z,15Sep		Missing		
		12Z,14Sep-00Z,20Sep		Missing	**2.29**	
		12Z,19Sep-00Z,25Sep		Missing		
		12Z,24Sep-00Z30Sep		2.42		
		12Z,30Sep-00Z,6Oct		2.22	**October**	
		00Z,7Oct-00Z,11Oct		2.86		
		12Z,10Oct-00Z,16Oct		2.41		
		12Z,15Oct-00Z,21Oct		2.30	**2.37**	
		12Z,20Oct-00Z26Oct		2.03		
		12Z,25Oct-00Z,31Oct		2.37		
	30-1500 m AGL	12Z,1Jul-00,7Jul		2.90	**July**	
		12Z,6Jul-00Z,12Jul		2.68		
		12Z,11Jul-00Z,17Jul		2.55		
		12Z,16Jul-00Z,22Jul		2.58	**2.60**	
		12Z,21Jul-00Z,27Jul		2.38		
		12Z,26Jul-00Z,1Aug		2.50		
		12Z,31Jul-00Z,6Aug		2.54	**August**	
		12Z,5Aug-00Z,11Aug		2.60		
		12Z,10Aug-00Z,16Aug		2.73		
		12Z,15Aug-00Z,21Aug		2.39	**2.58**	
		12Z,20Aug-00Z,26Aug		2.73		
		12Z,25Aug-00Z31Aug		2.47		
		12Z,30Aug-00Z,5Sep	**RMSE**	2.32	**September**	**2.64**
		12Z,4Sep-00Z,10Sep		2.78		
		12Z,9Sep-00Z,15Sep		Missing		
		12Z,14Sep-00Z,20Sep		Missing	**2.66**	
		12Z,19Sep-00Z,25Sep		Missing		
		12Z,24Sep-00Z30Sep		2.87		
		12Z,30Sep-00Z,6Oct		2.83	**October**	
		00Z,7Oct-00Z,11Oct		2.79		
		12Z,10Oct-00Z,16Oct		2.69		
		12Z,15Oct-00Z,21Oct		2.64	**2.71**	
		12Z,20Oct-00Z26Oct		2.59		
		12Z,25Oct-00Z,31Oct		2.71		

Table 17., Cont'd. Root Mean Square Error statistics for wind speed calculated on the MM5 36-km domain for the entire BRAVO study period from 1 July -31 October 1999.

Variable	Verif. Layer	Segment Dates	Stat. Type	Segment Score	Monthly Score	Avg. Score for full BRAVO study
Wind Speed ($m\ s^{-1}$)	**15 m AGL**	12Z,1Jul-00,7Jul	**RMSE**	2.10	**July**	**1.80**
		12Z,6Jul-00Z,12Jul		1.73		
		12Z,11Jul-00Z,17Jul		1.80		
		12Z,16Jul-00Z,22Jul		1.82	**1.82**	
		12Z,21Jul-00Z,27Jul		1.65		
		12Z,26Jul-00Z,1Aug		1.80		
		12Z,31Jul-00Z,6Aug		1.64	**August**	
		12Z,5Aug-00Z,11Aug		1.80		
		12Z,10Aug-00Z,16Aug		1.96		
		12Z,15Aug-00Z,21Aug		1.50	**1.77**	
		12Z,20Aug-00Z,26Aug		1.82		
		12Z,25Aug-00Z31Aug		1.61		
		12Z,30Aug-00Z,5Sep		1.69	**September**	
		12Z,4Sep-00Z,10Sep		1.74		
		12Z,9Sep-00Z,15Sep		Missing		
		12Z,14Sep-00Z,20Sep		Missing	**1.82**	
		12Z,19Sep-00Z,25Sep		Missing		
		12Z,24Sep-00Z30Sep		2.02		
		12Z,30Sep-00Z,6Oct		1.95	**October**	
		00Z,7Oct-00Z,11Oct		1.77		
		12Z,10Oct-00Z,16Oct		1.56		
		12Z,15Oct-00Z,21Oct		1.89	**1.77**	
		12Z,20Oct-00Z26Oct		1.66		
		12Z,25Oct-00Z,31Oct		1.77		

Table 18. Mean Absolute Error statistics for wind speed calculated on the MM5 36-km domain for the entire BRAVO study period from 1 July -31 October 1999.

Variable	Verif. Layer	Segment Dates	Stat. Type	Segment Score	Monthly Score	Avg. Score for full BRAVO study
Wind Speed (ms^{-1})	**1500-5000 m AGL**	12Z,1Jul-00,7Jul		1.58	**July**	
		12Z,6Jul-00Z,12Jul		1.53		
		12Z,11Jul-00Z,17Jul		1.59		
		12Z,16Jul-00Z,22Jul		1.44	**1.52**	
		12Z,21Jul-00Z,27Jul		1.47		
		12Z,26Jul-00Z,1Aug		1.49		
		12Z,31Jul-00Z,6Aug		1.56	**August**	
		12Z,5Aug-00Z,11Aug		1.58		
		12Z,10Aug-00Z,16Aug		1.68		
		12Z,15Aug-00Z,21Aug		1.67	**1.67**	
		12Z,20Aug-00Z,26Aug		1.80		
		12Z,25Aug-00Z31Aug		1.72		
		12Z,30Aug-00Z,5Sep	**MAE**	1.55	**September**	**1.74**
		12Z,4Sep-00Z,10Sep		2.02		
		12Z,9Sep-00Z,15Sep		Missing		
		12Z,14Sep-00Z,20Sep		Missing	**1.84**	
		12Z,19Sep-00Z,25Sep		Missing		
		12Z,24Sep-00Z30Sep		1.96		
		12Z,30Sep-00Z,6Oct		1.80	**October**	
		00Z,7Oct-00Z,11Oct		2.31		
		12Z,10Oct-00Z,16Oct		1.95		
		12Z,15Oct-00Z,21Oct		1.85	**1.91**	
		12Z,20Oct-00Z26Oct		1.64		
		12Z,25Oct-00Z,31Oct		1.91		
	30-1500 m AGL	12Z,1Jul-00,7Jul		2.40	**July**	
		12Z,6Jul-00Z,12Jul		2.23		
		12Z,11Jul-00Z,17Jul		2.11		
		12Z,16Jul-00Z,22Jul		2.12	**2.15**	
		12Z,21Jul-00Z,27Jul		1.94		
		12Z,26Jul-00Z,1Aug		2.07		
		12Z,31Jul-00Z,6Aug		2.09	**August**	
		12Z,5Aug-00Z,11Aug		2.12		
		12Z,10Aug-00Z,16Aug		2.29		
		12Z,15Aug-00Z,21Aug		1.99	**2.14**	
		12Z,20Aug-00Z,26Aug		2.32		
		12Z,25Aug-00Z31Aug		2.03		
		12Z,30Aug-00Z,5Sep	**MAE**	1.91	**September**	**2.18**
		12Z,4Sep-00Z,10Sep		2.30		
		12Z,9Sep-00Z,15Sep		Missing		
		12Z,14Sep-00Z,20Sep		Missing	**2.19**	
		12Z,19Sep-00Z,25Sep		Missing		
		12Z,24Sep-00Z30Sep		2.37		
		12Z,30Sep-00Z,6Oct		2.39	**October**	
		00Z,7Oct-00Z,11Oct		2.32		
		12Z,10Oct-00Z,16Oct		2.20		
		12Z,15Oct-00Z,21Oct		2.19	**2.25**	
		12Z,20Oct-00Z26Oct		2.14		
		12Z,25Oct-00Z,31Oct		2.25		

Table 18., Cont'd. Mean Absolute Error statistics for wind speed calculated on the MM5 36-km domain for the entire BRAVO study period from 1 July -31 October 1999.

Variable	Verif. Layer	Segment Dates	Stat. Type	Segment Score	Monthly Score	Avg. Score for full BRAVO study
Wind Speed ($m\ s^{-1}$)	**15 m AGL**	12Z,1Jul-00,7Jul		1.80	**July**	
		12Z,6Jul-00Z,12Jul		1.43		
		12Z,11Jul-00Z,17Jul		1.53		
		12Z,16Jul-00Z,22Jul		1.54	**1.54**	
		12Z,21Jul-00Z,27Jul		1.41		
		12Z,26Jul-00Z,1Aug		1.54		
		12Z,31Jul-00Z,6Aug		1.38	**August**	
		12Z,5Aug-00Z,11Aug		1.55		
		12Z,10Aug-00Z,16Aug		1.66		
		12Z,15Aug-00Z,21Aug		1.25	**1.45**	
		12Z,20Aug-00Z,26Aug		1.51		
		12Z,25Aug-00Z31Aug		1.36		
		12Z,30Aug-00Z,5Sep	**MAE**	1.44	**September**	**1.51**
		12Z,4Sep-00Z,10Sep		1.48		
		12Z,9Sep-00Z,15Sep		Missing		
		12Z,14Sep-00Z,20Sep		Missing	**1.55**	
		12Z,19Sep-00Z,25Sep		Missing		
		12Z,24Sep-00Z30Sep		1.73		
		12Z,30Sep-00Z,6Oct		1.66	**October**	
		00Z,7Oct-00Z,11Oct		1.45		
		12Z,10Oct-00Z,16Oct		1.31		
		12Z,15Oct-00Z,21Oct		1.59	**1.48**	
		12Z,20Oct-00Z26Oct		1.39		
		12Z,25Oct-00Z,31Oct		1.47		

Table 19. Mean Error statistics for wind speed calculated on the MM5 36-km domain for the entire BRAVO study period from 1 July -31 October 1999.

Variable	Verif. Layer	Segment Dates	Stat. Type	Segment Score	Monthly Score	Avg. Score for full BRAVO study
Wind Speed ($m\ s^{-1}$)	**1500-5000 m AGL**	12Z,1Jul-00,7Jul	**ME**	-0.70	**July**	**-0.77**
		12Z,6Jul-00Z,12Jul		-0.71		
		12Z,11Jul-00Z,17Jul		-0.51		
		12Z,16Jul-00Z,22Jul		-0.58	**-0.67**	
		12Z,21Jul-00Z,27Jul		-0.70		
		12Z,26Jul-00Z,1Aug		-0.80		
		12Z,31Jul-00Z,6Aug		-0.74	**August**	
		12Z,5Aug-00Z,11Aug		-0.74		
		12Z,10Aug-00Z,16Aug		-0.85		
		12Z,15Aug-00Z,21Aug		-0.72	**-0.79**	
		12Z,20Aug-00Z,26Aug		-0.90		
		12Z,25Aug-00Z31Aug		-0.78		
		12Z,30Aug-00Z,5Sep		-0.74	**September**	
		12Z,4Sep-00Z,10Sep		-1.14		
		12Z,9Sep-00Z,15Sep		Missing		
		12Z,14Sep-00Z,20Sep		Missing	**-0.91**	
		12Z,19Sep-00Z,25Sep		Missing		
		12Z,24Sep-00Z30Sep		-0.86		
		12Z,30Sep-00Z,6Oct		-0.65	**October**	
		00Z,7Oct-00Z,11Oct		-0.85		
		12Z,10Oct-00Z,16Oct		-1.07		
		12Z,15Oct-00Z,21Oct		-0.48	**-0.70**	
		12Z,20Oct-00Z26Oct		-0.30		
		12Z,25Oct-00Z,31Oct		-0.86		
	30-1500 m AGL	12Z,1Jul-00,7Jul	**ME**	+0.81	**July**	**+0.17**
		12Z,6Jul-00Z,12Jul		+0.41		
		12Z,11Jul-00Z,17Jul		-0.01		
		12Z,16Jul-00Z,22Jul		+0.51	**+0.37**	
		12Z,21Jul-00Z,27Jul		+0.25		
		12Z,26Jul-00Z,1Aug		+0.26		
		12Z,31Jul-00Z,6Aug		+0.49	**August**	
		12Z,5Aug-00Z,11Aug		-0.04		
		12Z,10Aug-00Z,16Aug		-0.08		
		12Z,15Aug-00Z,21Aug		+0.37	**+0.18**	
		12Z,20Aug-00Z,26Aug		+0.18		
		12Z,25Aug-00Z31Aug		+0.13		
		12Z,30Aug-00Z,5Sep		+0.18	**September**	
		12Z,4Sep-00Z,10Sep		+0.47		
		12Z,9Sep-00Z,15Sep		Missing		
		12Z,14Sep-00Z,20Sep		Missing	**+0.34**	
		12Z,19Sep-00Z,25Sep		Missing		
		12Z,24Sep-00Z30Sep		+0.38		
		12Z,30Sep-00Z,6Oct		+0.10	**October**	
		00Z,7Oct-00Z,11Oct		-0.34		
		12Z,10Oct-00Z,16Oct		+0.02		
		12Z,15Oct-00Z,21Oct		+0.11	**-0.22**	
		12Z,20Oct-00Z26Oct		-0.43		
		12Z,25Oct-00Z,31Oct		-0.77		

Table 19., Cont'd. Mean Error statistics for wind speed calculated on the MM5 36-km domain for the entire BRAVO study period from 1 July -31 October 1999.

Variable	Verif. Layer	Segment Dates	Stat. Type	Segment Score	Monthly Score	Avg. Score for full BRAVO study
Wind Speed ($m\ s^{-1}$)	**15 m AGL**	12Z,1Jul-00,7Jul	**ME**	+1.35	**July**	**+0.73**
		12Z,6Jul-00Z,12Jul		+0.60		
		12Z,11Jul-00Z,17Jul		+0.69		
		12Z,16Jul-00Z,22Jul		+0.85	**+0.81**	
		12Z,21Jul-00Z,27Jul		+0.55		
		12Z,26Jul-00Z,1Aug		+0.80		
		12Z,31Jul-00Z,6Aug		+0.53	**August**	
		12Z,5Aug-00Z,11Aug		+0.59		
		12Z,10Aug-00Z,16Aug		+0.84		
		12Z,15Aug-00Z,21Aug		+0.41	**+0.53**	
		12Z,20Aug-00Z,26Aug		+0.48		
		12Z,25Aug-00Z31Aug		+0.35		
		12Z,30Aug-00Z,5Sep		+0.67	**September**	
		12Z,4Sep-00Z,10Sep		+0.62		
		12Z,9Sep-00Z,15Sep		Missing		
		12Z,14Sep-00Z,20Sep		Missing	**+0.82**	
		12Z,19Sep-00Z,25Sep		Missing		
		12Z,24Sep-00Z30Sep		+1.16		
		12Z,30Sep-00Z,6Oct		+1.03	**October**	
		00Z,7Oct-00Z,11Oct		+0.77		
		12Z,10Oct-00Z,16Oct		+0.61		
		12Z,15Oct-00Z,21Oct		+1.01	**+0.75**	
		12Z,20Oct-00Z26Oct		+0.60		
		12Z,25Oct-00Z,31Oct		+0.50		

Table 20. Root Mean Square Error statistics for wind direction calculated on the MM5 12-km domain for the entire BRAVO study period from 1 July -31 October 1999.

Variable	Verif. Layer	Segment Dates	Stat. Type	Segment Score	Monthly Score	Avg. Score for full BRAVO study
Wind Direction ($m\ s^{-1}$)	**1500-5000 m AGL**	12Z,1Jul-00,7Jul		15.0	**July**	
		12Z,6Jul-00Z,12Jul		19.2		
		12Z,11Jul-00Z,17Jul		19.3		
		12Z,16Jul-00Z,22Jul		19.6	**19.3**	
		12Z,21Jul-00Z,27Jul		22.1		
		12Z,26Jul-00Z,1Aug		20.5		
		12Z,31Jul-00Z,6Aug		20.2	**August**	
		12Z,5Aug-00Z,11Aug		16.9		
		12Z,10Aug-00Z,16Aug		14.3		
		12Z,15Aug-00Z,21Aug		17.6	**17.2**	
		12Z,20Aug-00Z,26Aug		18.4		
		12Z,25Aug-00Z31Aug		15.9		
		12Z,30Aug-00Z,5Sep	**RMSE**	16.9	**September**	**16.2**
		12Z,4Sep-00Z,10Sep		Missing		
		12Z,9Sep-00Z,15Sep		Missing		
		12Z,14Sep-00Z,20Sep		Missing	**15.2**	
		12Z,19Sep-00Z,25Sep		14.9		
		12Z,24Sep-00Z30Sep		13.8		
		12Z,30Sep-00Z,6Oct		12.4	**October**	
		00Z,7Oct-00Z,11Oct		14.9		
		12Z,10Oct-00Z,16Oct		15.0		
		12Z,15Oct-00Z,21Oct		12.1	**13.2**	
		12Z,20Oct-00Z26Oct		11.4		
		12Z,25Oct-00Z,31Oct		13.4		
	30-1500 m AGL	12Z,1Jul-00,7Jul		17.1	**July**	
		12Z,6Jul-00Z,12Jul		24.6		
		12Z,11Jul-00Z,17Jul		19.5		
		12Z,16Jul-00Z,22Jul		16.5	**19.7**	
		12Z,21Jul-00Z,27Jul		20.6		
		12Z,26Jul-00Z,1Aug		19.9		
		12Z,31Jul-00Z,6Aug		24.9	**August**	
		12Z,5Aug-00Z,11Aug		24.6		
		12Z,10Aug-00Z,16Aug		20.9		
		12Z,15Aug-00Z,21Aug		23.7	**23.7**	
		12Z,20Aug-00Z,26Aug		23.4		
		12Z,25Aug-00Z31Aug		24.8		
		12Z,30Aug-00Z,5Sep	**RMSE**	21.3	**September**	**21.0**
		12Z,4Sep-00Z,10Sep		Missing		
		12Z,9Sep-00Z,15Sep		Missing		
		12Z,14Sep-00Z,20Sep		Missing	**21.4**	
		12Z,19Sep-00Z,25Sep		25.1		
		12Z,24Sep-00Z30Sep		17.7		
		12Z,30Sep-00Z,6Oct		19.7	**October**	
		00Z,7Oct-00Z,11Oct		18.3		
		12Z,10Oct-00Z,16Oct		20.2		
		12Z,15Oct-00Z,21Oct		20.4	**19.0**	
		12Z,20Oct-00Z26Oct		20.0		
		12Z,25Oct-00Z,31Oct		15.5		

Table 20., Cont'd. Root Mean Square Error statistics for wind direction calculated on the MM5 12-km domain for the entire BRAVO study period from 1 July -31 October 1999.

Variable	Verif. Layer	Segment Dates	Stat. Type	Segment Score	Monthly Score	Avg. Score for full BRAVO study
Wind Direction ($m\ s^{-1}$)	**15 m AGL**	12Z,1Jul-00,7Jul		30.5	**July**	
		12Z,6Jul-00Z,12Jul		41.3		
		12Z,11Jul-00Z,17Jul		33.2		
		12Z,16Jul-00Z,22Jul		30.4	**31.7**	
		12Z,21Jul-00Z,27Jul		28.9		
		12Z,26Jul-00Z,1Aug		25.9		
		12Z,31Jul-00Z,6Aug		43.1	**August**	
		12Z,5Aug-00Z,11Aug		35.3		
		12Z,10Aug-00Z,16Aug		28.1		
		12Z,15Aug-00Z,21Aug		33.0	**35.6**	
		12Z,20Aug-00Z,26Aug		34.4		
		12Z,25Aug-00Z31Aug		39.9		
		12Z,30Aug-00Z,5Sep	**RMSE**	32.8	**September**	**32.3**
		12Z,4Sep-00Z,10Sep		Missing		
		12Z,9Sep-00Z,15Sep		Missing		
		12Z,14Sep-00Z,20Sep		Missing	**30.2**	
		12Z,19Sep-00Z,25Sep		32.0		
		12Z,24Sep-00Z30Sep		25.8		
		12Z,30Sep-00Z,6Oct		29.9	**October**	
		00Z,7Oct-00Z,11Oct		38.2		
		12Z,10Oct-00Z,16Oct		30.7		
		12Z,15Oct-00Z,21Oct		26.8	**31.5**	
		12Z,20Oct-00Z26Oct		31.7		
		12Z,25Oct-00Z,31Oct		31.8		

Table 21. Mean Absolute Error statistics for wind direction calculated on the MM5 12-km domain for the entire BRAVO study period from 1 July -31 October 1999.

Variable	Verif. Layer	Segment Dates	Stat. Type	Segment Score	Monthly Score	Avg. Score for full BRAVO study
Wind Direction (degrees)	**1500-5000 m AGL**	12Z,1Jul-00,7Jul	**MAE**	10.1	**July**	**11.1**
		12Z,6Jul-00Z,12Jul		13.0		
		12Z,11Jul-00Z,17Jul		12.7		
		12Z,16Jul-00Z,22Jul		13.3	**13.0**	
		12Z,21Jul-00Z,27Jul		14.9		
		12Z,26Jul-00Z,1Aug		14.0		
		12Z,31Jul-00Z,6Aug		13.7	**August**	
		12Z,5Aug-00Z,11Aug		11.5		
		12Z,10Aug-00Z,16Aug		9.6		
		12Z,15Aug-00Z,21Aug		11.9	**11.7**	
		12Z,20Aug-00Z,26Aug		12.2		
		12Z,25Aug-00Z31Aug		11.1		
		12Z,30Aug-00Z,5Sep		11.2	**September**	
		12Z,4Sep-00Z,10Sep		Missing		
		12Z,9Sep-00Z,15Sep		Missing		
		12Z,14Sep-00Z,20Sep		Missing	**10.2**	
		12Z,19Sep-00Z,25Sep		10.0		
		12Z,24Sep-00Z30Sep		9.5		
		12Z,30Sep-00Z,6Oct		8.6	**October**	
		00Z,7Oct-00Z,11Oct		10.0		
		12Z,10Oct-00Z,16Oct		10.2		
		12Z,15Oct-00Z,21Oct		8.3	**9.3**	
		12Z,20Oct-00Z26Oct		7.8		
		12Z,25Oct-00Z,31Oct		10.7		
	30-1500 m AGL	12Z,1Jul-00,7Jul	**MAE**	11.8	**July**	**14.9**
		12Z,6Jul-00Z,12Jul		17.8		
		12Z,11Jul-00Z,17Jul		13.3		
		12Z,16Jul-00Z,22Jul		11.8	**13.7**	
		12Z,21Jul-00Z,27Jul		14.0		
		12Z,26Jul-00Z,1Aug		13.5		
		12Z,31Jul-00Z,6Aug		17.7	**August**	
		12Z,5Aug-00Z,11Aug		17.1		
		12Z,10Aug-00Z,16Aug		14.8		
		12Z,15Aug-00Z,21Aug		17.2	**17.1**	
		12Z,20Aug-00Z,26Aug		17.3		
		12Z,25Aug-00Z31Aug		18.2		
		12Z,30Aug-00Z,5Sep		15.0	**September**	
		12Z,4Sep-00Z,10Sep		Missing		
		12Z,9Sep-00Z,15Sep		Missing		
		12Z,14Sep-00Z,20Sep		Missing	**15.1**	
		12Z,19Sep-00Z,25Sep		17.8		
		12Z,24Sep-00Z30Sep		12.6		
		12Z,30Sep-00Z,6Oct		14.2	**October**	
		00Z,7Oct-00Z,11Oct		13.3		
		12Z,10Oct-00Z,16Oct		14.8		
		12Z,15Oct-00Z,21Oct		14.7	**13.7**	
		12Z,20Oct-00Z26Oct		14.3		
		12Z,25Oct-00Z,31Oct		10.7		

Table 21., Cont'd. Mean Absolute Error statistics for wind direction calculated on the MM5 12-km domain for the entire BRAVO study period from 1 July -31 October 1999.

Variable	Verif. Layer	Segment Dates	Stat. Type	Segment Score	Monthly Score	Avg. Score for full BRAVO study
Wind Direction (degrees)	**15 m AGL**	12Z,1Jul-00,7Jul	**MAE**	20.3	**July**	**22.1**
		12Z,6Jul-00Z,12Jul		29.3		
		12Z,11Jul-00Z,17Jul		22.5		
		12Z,16Jul-00Z,22Jul		21.0	**21.5**	
		12Z,21Jul-00Z,27Jul		19.1		
		12Z,26Jul-00Z,1Aug		16.9		
		12Z,31Jul-00Z,6Aug		30.4	**August**	
		12Z,5Aug-00Z,11Aug		24.2		
		12Z,10Aug-00Z,16Aug		17.6		
		12Z,15Aug-00Z,21Aug		23.5	**24.8**	
		12Z,20Aug-00Z,26Aug		24.5		
		12Z,25Aug-00Z31Aug		28.3		
		12Z,30Aug-00Z,5Sep		22.5	**September**	
		12Z,4Sep-00Z,10Sep		Missing		
		12Z,9Sep-00Z,15Sep		Missing		
		12Z,14Sep-00Z,20Sep		Missing	**20.5**	
		12Z,19Sep-00Z,25Sep		21.5		
		12Z,24Sep-00Z30Sep		17.6		
		12Z,30Sep-00Z,6Oct		20.4	**October**	
		00Z,7Oct-00Z,11Oct		27.1		
		12Z,10Oct-00Z,16Oct		21.3		
		12Z,15Oct-00Z,21Oct		18.4	**21.7**	
		12Z,20Oct-00Z26Oct		21.9		
		12Z,25Oct-00Z,31Oct		20.8		

Table 22. Mean Error statistics for wind direction calculated on the MM5 12-km domain for the entire BRAVO study period from 1 July -31 October 1999.

Variable	Verif. Layer	Segment Dates	Stat. Type	Segment Score	Monthly Score	Avg. Score for full BRAVO study
Wind Direction (degrees)	**1500-5000 m AGL**	12Z,1Jul-00,7Jul	**ME**	-0.1	**July**	**+0.2**
		12Z,6Jul-00Z,12Jul		+0.1		
		12Z,11Jul-00Z,17Jul		+0.7		
		12Z,16Jul-00Z,22Jul		-0.6	**+0.1**	
		12Z,21Jul-00Z,27Jul		+0.2		
		12Z,26Jul-00Z,1Aug		+0.1		
		12Z,31Jul-00Z,6Aug		+0.7	**August**	
		12Z,5Aug-00Z,11Aug		-0.6		
		12Z,10Aug-00Z,16Aug		-0.4		
		12Z,15Aug-00Z,21Aug		-0.2	**+0.1**	
		12Z,20Aug-00Z,26Aug		+1.3		
		12Z,25Aug-00Z31Aug		-0.0		
		12Z,30Aug-00Z,5Sep		-0.1	**September**	
		12Z,4Sep-00Z,10Sep		Missing		
		12Z,9Sep-00Z,15Sep		Missing		
		12Z,14Sep-00Z,20Sep		Missing	**+0.5**	
		12Z,19Sep-00Z,25Sep		+0.3		
		12Z,24Sep-00Z30Sep		+1.2		
		12Z,30Sep-00Z,6Oct		+0.4	**October**	
		00Z,7Oct-00Z,11Oct		-0.5		
		12Z,10Oct-00Z,16Oct		+0.6		
		12Z,15Oct-00Z,21Oct		-0.2	**+0.1**	
		12Z,20Oct-00Z26Oct		+0.1		
		12Z,25Oct-00Z,31Oct		-0.2		
	30-1500 m AGL	12Z,1Jul-00,7Jul	**ME**	-3.2	**July**	**0.0**
		12Z,6Jul-00Z,12Jul		+0.3		
		12Z,11Jul-00Z,17Jul		-0.3		
		12Z,16Jul-00Z,22Jul		-2.6	**-0.9**	
		12Z,21Jul-00Z,27Jul		+0.6		
		12Z,26Jul-00Z,1Aug		+0.1		
		12Z,31Jul-00Z,6Aug		+2.8	**August**	
		12Z,5Aug-00Z,11Aug		-0.3		
		12Z,10Aug-00Z,16Aug		+1.4		
		12Z,15Aug-00Z,21Aug		-0.9	**-0.3**	
		12Z,20Aug-00Z,26Aug		-1.3		
		12Z,25Aug-00Z31Aug		-3.5		
		12Z,30Aug-00Z,5Sep		-3.0	**September**	
		12Z,4Sep-00Z,10Sep		Missing		
		12Z,9Sep-00Z,15Sep		Missing		
		12Z,14Sep-00Z,20Sep		Missing	**+0.5**	
		12Z,19Sep-00Z,25Sep		+1.9		
		12Z,24Sep-00Z30Sep		+2.7		
		12Z,30Sep-00Z,6Oct		-1.1	**October**	
		00Z,7Oct-00Z,11Oct		-1.5		
		12Z,10Oct-00Z,16Oct		+0.9		
		12Z,15Oct-00Z,21Oct		+3.8	**+0.8**	
		12Z,20Oct-00Z26Oct		+0.8		
		12Z,25Oct-00Z,31Oct		+1.8		

Table 22., Cont'd. Mean Error statistics for wind direction calculated on the MM5 12-km domain for the entire BRAVO study period from 1 July -31 October 1999.

Variable	Verif. Layer	Segment Dates	Stat. Type	Segment Score	Monthly Score	Avg. Score for full BRAVO study
Wind Direction (degrees)	**15 m AGL**	12Z,1Jul-00,7Jul		-2.3	**July**	
		12Z,6Jul-00Z,12Jul		-0.3		
		12Z,11Jul-00Z,17Jul		-4.1		
		12Z,16Jul-00Z,22Jul		-3.0	**-2.2**	
		12Z,21Jul-00Z,27Jul		-0.6		
		12Z,26Jul-00Z,1Aug		-2.9		
		12Z,31Jul-00Z,6Aug		+6.1	**August**	
		12Z,5Aug-00Z,11Aug		+0.1		
		12Z,10Aug-00Z,16Aug		+0.5		
		12Z,15Aug-00Z,21Aug		-1.1	**+0.9**	
		12Z,20Aug-00Z,26Aug		+0.3		
		12Z,25Aug-00Z31Aug		-0.8		
		12Z,30Aug-00Z,5Sep	**ME**	-2.6	**September**	**-0.2**
		12Z,4Sep-00Z,10Sep		Missing		
		12Z,9Sep-00Z,15Sep		Missing		
		12Z,14Sep-00Z,20Sep		Missing	**+0.7**	
		12Z,19Sep-00Z,25Sep		+2.7		
		12Z,24Sep-00Z30Sep		+1.9		
		12Z,30Sep-00Z,6Oct		-4.1	**October**	
		00Z,7Oct-00Z,11Oct		+0.4		
		12Z,10Oct-00Z,16Oct		-1.1		
		12Z,15Oct-00Z,21Oct		+4.2	**-0.2**	
		12Z,20Oct-00Z26Oct		+1.1		
		12Z,25Oct-00Z,31Oct		-1.5		

Table 23. Root Mean Square Error statistics for wind direction calculated on the MM5 36-km domain for the entire BRAVO study period from 1 July -31 October 1999.

Variable	Verif. Layer	Segment Dates	Stat. Type	Segment Score	Monthly Score	Avg. Score for full BRAVO study
Wind Direction ($m\ s^{-1}$)	**1500-5000 m AGL**	12Z,1Jul-00,7Jul		26.8	**July**	
		12Z,6Jul-00Z,12Jul		35.4		
		12Z,11Jul-00Z,17Jul		33.9		
		12Z,16Jul-00Z,22Jul		34.2	**35.8**	
		12Z,21Jul-00Z,27Jul		41.7		
		12Z,26Jul-00Z,1Aug		42.5		
		12Z,31Jul-00Z,6Aug		38.6	**August**	
		12Z,5Aug-00Z,11Aug		37.2		
		12Z,10Aug-00Z,16Aug		32.8		
		12Z,15Aug-00Z,21Aug		35.6	**34.9**	
		12Z,20Aug-00Z,26Aug		34.4		
		12Z,25Aug-00Z31Aug		30.6		
		12Z,30Aug-00Z,5Sep	**RMSE**	33.6	**September**	**32.2**
		12Z,4Sep-00Z,10Sep		37.8		
		12Z,9Sep-00Z,15Sep		Missing		
		12Z,14Sep-00Z,20Sep		Missing	**32.4**	
		12Z,19Sep-00Z,25Sep		Missing		
		12Z,24Sep-00Z30Sep		25.9		
		12Z,30Sep-00Z,6Oct		25.7	**October**	
		00Z,7Oct-00Z,11Oct		23.9		
		12Z,10Oct-00Z,16Oct		31.9		
		12Z,15Oct-00Z,21Oct		23.4	**25.5**	
		12Z,20Oct-00Z26Oct		21.1		
		12Z,25Oct-00Z,31Oct		26.7		
	30-1500 m AGL	12Z,1Jul-00,7Jul		26.0	**July**	
		12Z,6Jul-00Z,12Jul		45.3		
		12Z,11Jul-00Z,17Jul		30.0		
		12Z,16Jul-00Z,22Jul		27.9	**32.0**	
		12Z,21Jul-00Z,27Jul		30.9		
		12Z,26Jul-00Z,1Aug		32.1		
		12Z,31Jul-00Z,6Aug		45.2	**August**	
		12Z,5Aug-00Z,11Aug		43.6		
		12Z,10Aug-00Z,16Aug		36.6		
		12Z,15Aug-00Z,21Aug		44.1	**42.6**	
		12Z,20Aug-00Z,26Aug		41.8		
		12Z,25Aug-00Z31Aug		44.2		
		12Z,30Aug-00Z,5Sep	**RMSE**	40.8	**September**	**37.1**
		12Z,4Sep-00Z,10Sep		40.9		
		12Z,9Sep-00Z,15Sep		Missing		
		12Z,14Sep-00Z,20Sep		Missing	**37.2**	
		12Z,19Sep-00Z,25Sep		Missing		
		12Z,24Sep-00Z30Sep		29.8		
		12Z,30Sep-00Z,6Oct		41.2	**October**	
		00Z,7Oct-00Z,11Oct		31.8		
		12Z,10Oct-00Z,16Oct		38.9		
		12Z,15Oct-00Z,21Oct		40.2	**36.7**	
		12Z,20Oct-00Z26Oct		41.1		
		12Z,25Oct-00Z,31Oct		27.2		

Table 23., Cont'd. Root Mean Square Error statistics for wind direction calculated on the MM5 36-km domain for the entire BRAVO study period from 1 July -31 October 1999.

Variable	Verif. Layer	Segment Dates	Stat. Type	Segment Score	Monthly Score	Avg. Score for full BRAVO study
Wind Direction ($m\ s^{-1}$)	**15 m AGL**	12Z,1Jul-00,7Jul	**RMSE**	35.1	**July**	**41.5**
		12Z,6Jul-00Z,12Jul		54.6		
		12Z,11Jul-00Z,17Jul		41.5		
		12Z,16Jul-00Z,22Jul		36.3	**39.9**	
		12Z,21Jul-00Z,27Jul		37.8		
		12Z,26Jul-00Z,1Aug		34.0		
		12Z,31Jul-00Z,6Aug		54.7	**August**	
		12Z,5Aug-00Z,11Aug		41.9		
		12Z,10Aug-00Z,16Aug		32.1		
		12Z,15Aug-00Z,21Aug		42.8	**43.9**	
		12Z,20Aug-00Z,26Aug		42.1		
		12Z,25Aug-00Z31Aug		50.0		
		12Z,30Aug-00Z,5Sep		43.3	**September**	
		12Z,4Sep-00Z,10Sep		52.8		
		12Z,9Sep-00Z,15Sep		Missing		
		12Z,14Sep-00Z,20Sep		Missing	**42.5**	
		12Z,19Sep-00Z,25Sep		Missing		
		12Z,24Sep-00Z30Sep		31.4		
		12Z,30Sep-00Z,6Oct		37.3	**October**	
		00Z,7Oct-00Z,11Oct		44.0		
		12Z,10Oct-00Z,16Oct		40.4		
		12Z,15Oct-00Z,21Oct		34.3	**39.5**	
		12Z,20Oct-00Z26Oct		41.7		
		12Z,25Oct-00Z,31Oct		39.3		

Table 24. Mean Absolute Error statistics for wind direction calculated on the MM5 36-km domain for the entire BRAVO study period from 1 July -31 October 1999.

Variable	Verif. Layer	Segment Dates	Stat. Type	Segment Score	Monthly Score	Avg. Score for full BRAVO study
Wind Direction (degrees)	**1500-5000 m AGL**	12Z,1Jul-00,7Jul	**MAE**	19.6	**July**	**23.6**
		12Z,6Jul-00Z,12Jul		25.9		
		12Z,11Jul-00Z,17Jul		24.7		
		12Z,16Jul-00Z,22Jul		25.2	**26.4**	
		12Z,21Jul-00Z,27Jul		30.8		
		12Z,26Jul-00Z,1Aug		32.3		
		12Z,31Jul-00Z,6Aug		28.8	**August**	
		12Z,5Aug-00Z,11Aug		27.4		
		12Z,10Aug-00Z,16Aug		23.5		
		12Z,15Aug-00Z,21Aug		26.1	**25.5**	
		12Z,20Aug-00Z,26Aug		24.7		
		12Z,25Aug-00Z31Aug		22.6		
		12Z,30Aug-00Z,5Sep		24.3	**September**	
		12Z,4Sep-00Z,10Sep		28.7		
		12Z,9Sep-00Z,15Sep		Missing		
		12Z,14Sep-00Z,20Sep		Missing	**24.1**	
		12Z,19Sep-00Z,25Sep		Missing		
		12Z,24Sep-00Z30Sep		19.2		
		12Z,30Sep-00Z,6Oct		19.2	**October**	
		00Z,7Oct-00Z,11Oct		17.7		
		12Z,10Oct-00Z,16Oct		24.1		
		12Z,15Oct-00Z,21Oct		17.3	**18.2**	
		12Z,20Oct-00Z26Oct		15.4		
		12Z,25Oct-00Z,31Oct		19.8		
	30-1500 m AGL	12Z,1Jul-00,7Jul	**MAE**	18.9	**July**	**28.1**
		12Z,6Jul-00Z,12Jul		34.4		
		12Z,11Jul-00Z,17Jul		22.1		
		12Z,16Jul-00Z,22Jul		20.7	**23.8**	
		12Z,21Jul-00Z,27Jul		23.2		
		12Z,26Jul-00Z,1Aug		23.6		
		12Z,31Jul-00Z,6Aug		34.5	**August**	
		12Z,5Aug-00Z,11Aug		32.2		
		12Z,10Aug-00Z,16Aug		27.5		
		12Z,15Aug-00Z,21Aug		34.9	**32.8**	
		12Z,20Aug-00Z,26Aug		32.4		
		12Z,25Aug-00Z31Aug		35.0		
		12Z,30Aug-00Z,5Sep		30.7	**September**	
		12Z,4Sep-00Z,10Sep		31.3		
		12Z,9Sep-00Z,15Sep		Missing		
		12Z,14Sep-00Z,20Sep		Missing	**27.9**	
		12Z,19Sep-00Z,25Sep		Missing		
		12Z,24Sep-00Z30Sep		21.8		
		12Z,30Sep-00Z,6Oct		31.6	**October**	
		00Z,7Oct-00Z,11Oct		24.1		
		12Z,10Oct-00Z,16Oct		30.2		
		12Z,15Oct-00Z,21Oct		30.4	**27.8**	
		12Z,20Oct-00Z26Oct		31.1		
		12Z,25Oct-00Z,31Oct		19.6		

Table 24., Cont'd. Mean Absolute Error statistics for wind direction calculated on the MM5 36-km domain for the entire BRAVO study period from 1 July -31 October 1999.

Variable	Verif. Layer	Segment Dates	Stat. Type	Segment Score	Monthly Score	Avg. Score for full BRAVO study
Wind Direction (degrees)	**15 m AGL**	12Z,1Jul-00,7Jul	**MAE**	24.9	**July**	**29.5**
		12Z,6Jul-00Z,12Jul		40.6		
		12Z,11Jul-00Z,17Jul		29.0		
		12Z,16Jul-00Z,22Jul		26.0	**28.0**	
		12Z,21Jul-00Z,27Jul		25.0		
		12Z,26Jul-00Z,1Aug		22.7		
		12Z,31Jul-00Z,6Aug		39.8	**August**	
		12Z,5Aug-00Z,11Aug		29.3		
		12Z,10Aug-00Z,16Aug		21.5		
		12Z,15Aug-00Z,21Aug		31.3	**31.6**	
		12Z,20Aug-00Z,26Aug		31.3		
		12Z,25Aug-00Z31Aug		36.3		
		12Z,30Aug-00Z,5Sep		31.1	**September**	
		12Z,4Sep-00Z,10Sep		38.9		
		12Z,9Sep-00Z,15Sep		Missing		
		12Z,14Sep-00Z,20Sep		Missing	**30.4**	
		12Z,19Sep-00Z,25Sep		Missing		
		12Z,24Sep-00Z30Sep		21.3		
		12Z,30Sep-00Z,6Oct		26.2	**October**	
		00Z,7Oct-00Z,11Oct		32.1		
		12Z,10Oct-00Z,16Oct		28.4		
		12Z,15Oct-00Z,21Oct		23.8	**27.8**	
		12Z,20Oct-00Z26Oct		29.9		
		12Z,25Oct-00Z,31Oct		26.6		

Table 25. Mean Error statistics for wind direction calculated on the MM5 36-km domain for the entire BRAVO study period from 1 July -31 October 1999.

Variable	Verif. Layer	Segment Dates	Stat. Type	Segment Score	Monthly Score	Avg. Score for full BRAVO study
Wind Direction (degrees)	**1500-5000 m AGL**	12Z,1Jul-00,7Jul	**ME**	-0.9	**July**	**-0.7**
		12Z,6Jul-00Z,12Jul		+0.2		
		12Z,11Jul-00Z,17Jul		+0.6		
		12Z,16Jul-00Z,22Jul		-0.6	**-0.2**	
		12Z,21Jul-00Z,27Jul		+0.3		
		12Z,26Jul-00Z,1Aug		-0.8		
		12Z,31Jul-00Z,6Aug		+3.2	**August**	
		12Z,5Aug-00Z,11Aug		-3.1		
		12Z,10Aug-00Z,16Aug		-2.4		
		12Z,15Aug-00Z,21Aug		-0.5	**+0.5**	
		12Z,20Aug-00Z,26Aug		+4.5		
		12Z,25Aug-00Z31Aug		+1.1		
		12Z,30Aug-00Z,5Sep		-0.5	**September**	
		12Z,4Sep-00Z,10Sep		-4.6		
		12Z,9Sep-00Z,15Sep		Missing		
		12Z,14Sep-00Z,20Sep		Missing	**-1.6**	
		12Z,19Sep-00Z,25Sep		Missing		
		12Z,24Sep-00Z30Sep		+0.3		
		12Z,30Sep-00Z,6Oct		-1.8	**October**	
		00Z,7Oct-00Z,11Oct		-0.5		
		12Z,10Oct-00Z,16Oct		-1.5		
		12Z,15Oct-00Z,21Oct		-1.3	**-1.4**	
		12Z,20Oct-00Z26Oct		-1.8		
		12Z,25Oct-00Z,31Oct		-1.5		
	30-1500 m AGL	12Z,1Jul-00,7Jul	**ME**	-3.8	**July**	**-3.1**
		12Z,6Jul-00Z,12Jul		-2.7		
		12Z,11Jul-00Z,17Jul		-0.2		
		12Z,16Jul-00Z,22Jul		-2.5	**-2.7**	
		12Z,21Jul-00Z,27Jul		-2.3		
		12Z,26Jul-00Z,1Aug		-4.5		
		12Z,31Jul-00Z,6Aug		+1.5	**August**	
		12Z,5Aug-00Z,11Aug		-2.5		
		12Z,10Aug-00Z,16Aug		-6.8		
		12Z,15Aug-00Z,21Aug		-7.0	**-4.9**	
		12Z,20Aug-00Z,26Aug		-6.0		
		12Z,25Aug-00Z31Aug		-8.7		
		12Z,30Aug-00Z,5Sep		-11.3	**September**	
		12Z,4Sep-00Z,10Sep		-8.7		
		12Z,9Sep-00Z,15Sep		Missing		
		12Z,14Sep-00Z,20Sep		Missing	**-4.4**	
		12Z,19Sep-00Z,25Sep		Missing		
		12Z,24Sep-00Z30Sep		+6.7		
		12Z,30Sep-00Z,6Oct		-5.1	**October**	
		00Z,7Oct-00Z,11Oct		-1.5		
		12Z,10Oct-00Z,16Oct		-4.2		
		12Z,15Oct-00Z,21Oct		+6.0	**-0.3**	
		12Z,20Oct-00Z26Oct		+2.2		
		12Z,25Oct-00Z,31Oct		+0.8		

Table 25., Cont'd. Mean Error statistics for wind direction calculated on the MM5 36-km domain for the entire BRAVO study period from 1 July -31 October 1999.

Variable	Verif. Layer	Segment Dates	Stat. Type	Segment Score	Monthly Score	Avg. Score for full BRAVO study
Wind Direction (degrees)	**15 m AGL**	12Z,1Jul-00,7Jul		-2.2	**July**	
		12Z,6Jul-00Z,12Jul		+1.4		
		12Z,11Jul-00Z,17Jul		-3.7		
		12Z,16Jul-00Z,22Jul		-3.5	**-4.0**	
		12Z,21Jul-00Z,27Jul		-6.5		
		12Z,26Jul-00Z,1Aug		-9.4		
		12Z,31Jul-00Z,6Aug		+3.6	**August**	
		12Z,5Aug-00Z,11Aug		-3.2		
		12Z,10Aug-00Z,16Aug		-3.9		
		12Z,15Aug-00Z,21Aug		-2.7	**-1.6**	
		12Z,20Aug-00Z,26Aug		+0.7		
		12Z,25Aug-00Z31Aug		-3.9		
		12Z,30Aug-00Z,5Sep	**ME**	-4.9	**September**	**-2.4**
		12Z,4Sep-00Z,10Sep		-6.5		
		12Z,9Sep-00Z,15Sep		Missing		
		12Z,14Sep-00Z,20Sep		Missing	**-2.9**	
		12Z,19Sep-00Z,25Sep		Missing		
		12Z,24Sep-00Z30Sep		+2.6		
		12Z,30Sep-00Z,6Oct		-5.5	**October**	
		00Z,7Oct-00Z,11Oct		-2.8		
		12Z,10Oct-00Z,16Oct		-2.1		
		12Z,15Oct-00Z,21Oct		+5.9	**-1.2**	
		12Z,20Oct-00Z26Oct		+2.0		
		12Z,25Oct-00Z,31Oct		-4.9		

Moving aloft, comparison of **Tables 14 and 17** shows that the 36-km solutions have RMSEs that generally are greater than 2.0 m s^{-1}. The errors in these layers are larger than at the surface because the wind speed increases with height in the mid-latitudes. The errors are greatest in the nominal boundary layer (30-1500 m), where the four-month average speed RMSE = 2.64 m s^{-1} on the 36-km domain and every 5 1/2-day segment has an error > 2.0 m s^{-1}. This error is 94% higher than on the 12-km domain, making it very clear that the absence of an independent data set to use for model evaluation definitely is not the dominant influence. Rather, the 36-km solutions above the surface layer are truly less accurate for the wind speed.

The last variable field examined here is the wind direction, which is summarized in **Tables 20-25**. The MEs for wind direction on the 12-km domain in each layer are given in **Table 22**. The table indicates that the MM5's 12-km solutions have virtually no directional bias at any level or for any month. The biases of the individual segments are almost entirely within the target accuracy limit of <5 degrees defined in **Table 1**, with the exception of one segment for the surface layer in early August (ME=+6.1 degrees). This favorable result is especially important for establishing the validity of the 12-km MM5 simulations for use in estimating regional-scale and inter-regional scale transport of atmospheric trace constituents. For transport on these spatial scales (hundreds to thousands of kilometers), instantaneous and local errors in wind direction are not especially important, while daily and multi-day errors showing up as biases will tend to dominate. The results shown in **Table 22** are indicative of these longer time periods, as are the low 12-km speed biases shown earlier in **Table 16**.

The approximate size of the instantaneous local errors in wind direction can be evaluated by examining the MAEs compiled in **Table 21**. Recall that the MAE reveals the average (most typical) difference between observed winds and model-generated winds (interpolated to the observing sites), without an opportunity for positive and negative directional errors to cancel one another. The table shows that on the 12-km domain the four-month average surface-layer MAE = 22.1 degrees, with monthly averages ranging from 20.5 to 24.8 degrees. These values lie well within the benchmark target for wind direction of MAE <30 degrees given in **Table 1**. In fact the largest 12-km surface-layer MAE for any individual 5 1/2-day segment is 30.4 degrees. This is actually a fairly demanding standard because surface winds are only reported by the NWS data transmission codes to the nearest 10 degrees. Furthermore, in statistical evaluations of surface mesonet wind data over Oklahoma, it has been found that wind directions at closest neighboring sites (~20 km) over mostly flat terrain are on the order of 20-25 degrees (J.M. Fritsch, personal communication). Since a model with 12-km resolution cannot resolve any features smaller than 24-48 km (2-4 Δx), it is clear that the model is fitting the data at about the limit that can be expected in complex terrain, even with FDDA.

Of course, most of the regional transport of atmospheric constituents does not take place in the surface layer, even though it may be the source of most pollutants. Vertical mixing by boundary layer turbulence carries surface emissions and secondary chemical species throughout the boundary layer. Although the bulk of the trace pollutants (gases and aerosols) remain in the PBL, other processes can carry substantial quantities higher into the free troposphere in certain circumstances. However, for most purposes on time scales of several days we can assume that the majority of the pollutants remain in the PBL with a smaller quantity being injected into the lower free troposphere. **Table 21** also shows that in the 12-km solutions the four-month average

MAEs for the nominal PBL and free troposphere are 14.9 and 11.1 degrees, respectively. The monthly and segment MAEs do not deviate much from these average values, indicating overall temporal consistency in the directional errors all the way from 30 m to 5000m. This is a very favorable result, given the influence of turbulence in the boundary layer. Thus, the average instantaneous local errors in these layers are quite small. Given these MAEs and the small biases (MEs) reported earlier in **Table 22** the direction of transport on all scales represented by the 12-km MM5 simulated winds should quite accurate.

Lastly, we compare the results from the 12-km wind-direction evaluations to the statistical results on the 36-km domain, within the portion that is coincident with the 12-km domain. **Tables 23-25** show that the wind direction errors on the 36-km domain are consistently larger for all three types of statistics and at all levels. The most important difference is found in the MAEs. **Tables 21 and 24** indicate that the four-month 36-km wind direction MAE = 29.5 degrees in the surface layer, while it was only 22.1 degrees on the 12-km domain. The 33% greater error in the 36-km solutions is too large to be explained by the absence of an independent data set in the 12-km case, so that the effects of model resolution and obs-nudging are expected to be dominant. The same effect is noted aloft, where the directional MAEs are more than twice as large in the 1500-5000 m layer on the 36-km domain, compared to the 12-km domain.

The rather dramatic differences in the MAEs for wind direction between the 12-km and 36-km solutions do not mean, by themselves, that the 36-km solutions cannot be used for estimating regional and inter-regional transport in air-quality applications. The 36-km mean errors (MEs) for direction shown in **Table 25** remain rather small at all levels, compared to the benchmark, even though they are somewhat greater than those found in the 12-km solutions (compare to **Table 22**). Even in the 30-1500 m layer, where the 36-km biases are largest, the four-month ME_{36} = -3.1 degrees and most 5 1/2-day segments have a bias < 5 degrees. Thus, the effect of the larger MAEs on the 36-km domain are not especially great for long-range transport.

4. Summary

The MM5 model with four-dimensional data assimilation (FDDA) has been applied to the region surrounding the Big Bend National Park as part of the BRAVO study on three nested-grid domains having grid resolutions of 36-, 12- and 4-km. The 36- and 12-km domains were run for the period from 1 July to 31 October 1999. All grids were configured with 35 layers in the vertical direction, having greater resolution near the surface and in the boundary layer, with deeper layers aloft. Additional runs were made using the 4-km domain for two 10-day Intensive Periods in mid-August and mid-October. The study period was modeled using 5 1/2 day segments, with the model being restarted with initial conditions and lateral boundary conditions supplied from NCEP analyses. Data were assimilated into each model run using analysis-nudging on the 36-km and 12-km domains and obs-nudging on the 12-km and 4-km domains. Special observations available during the BRAVO study consisted mostly of hourly radar wind profiler data at 10 sites in the 12-km domain. Two of these profilers were located within the 4-km domain at Eagle Pass and Big Bend. Additional observations from surface sites and radiosondes were also assimilated. All data fed to the FDDA system were carefully quality checked before being assimilated and questionable data were discarded.

Model output was validated by visual inspections of plotted fields for all predictive variables and selected diagnostic variables, plus extensive statistical evaluations. Given the length of the BRAVO study period, the emphasis was placed on statistical evaluations for the root mean square error (RMSE), mean absolute error (MAE) and mean error (ME), (or bias). The statistics were calculated over the 36-km, 12-km and 4-km domains for each 5 1/2-day segment and were compiled in tables by segment, intensive periods, month and for the full four-month BRAVO study period.

Evaluation of the statistics in the tables, along with examination of plotted hourly statistics and spatial fields of the model variables led to the following major conclusions:

1. **Examination of results from the August and October Intensive Periods indicates that the MM5 simulations for the 12-km domain have consistently smaller errors than those occurring on the 4-km domain.**

   This result is partly due to the different size of the domains and the fact that the 4-km domain contains terrain that is on average much more complex, while the 12-km domain includes wide areas of the Great Plains. Also, the greater resolution of the 4-km grid allows considerably more fine-scale structure to develop in the model solutions, especially near the surface.

   Temperature and moisture errors on the 4-km domain are larger than on the 12-km domain, in part, because the land-use types in the former are heavily dominated by arid and semi-arid climates. While the MM5 recognizes these land-use categories, it can be inferred from the results that the soil moisture availability for arid land- use types was specified to be too high, resulting in a pattern of higher-than-observed mixing ratios in the surface layer over arid areas and cooler temperatures.

2. **The model simulations of the Intensive Periods indicate that having only 12-km and 36-km MM5 solutions for the full four-month BRAVO period is not a handicap. The 12-km fields have generally low errors for wind, temperature and mixing ratio, compared to fields from the 4-km domain, and they contain sufficient detail to capture the regional flow.**

3. **The four-month MM5 simulations on the 12-km domain have errors for surface temperature and moisture that are well within the standard targets for accuracy established independently by ENVIRON Corp. Consequently, these fields should be suitable for use in air-quality studies.**

4. **The biases (MEs) found on the 12-km domain in the wind speed and direction for all layers and in all model run segments are small and fall within the standard targets for accuracy. This demonstrates that the 12-km wind fields are suitable for air-quality studies, including regional and inter-regional transport investigations.**

5. **For the 12-km domain, the small values of MAE for wind direction and RMSE for wind speed in the nominal PBL (30-1500 m AGL) and the lower free troposphere (1500-5000 m) are well within the standard targets for accuracy at all levels.**

   The RMSE and MAE wind speed and direction statistics reveal that the instantaneous local wind errors remain quite modest over all averaging periods from 5 1/2 days to 4 months. This is a favorable result for modeling regional and inter-regional transport because the majority of trace gases and aerosols are transported in these layers.

6. **On the 36-km domain, evaluation of errors within the same region covered by the 12-km domain indicates that wind speed and wind direction errors generally are larger than those found in the 12-km solutions. The differences are substantial and definitely are not due solely to the lack of an independent data set for validating the 12-km solutions (which benefit from obs-nudging based on wind data that are assimilated on that domain).**

   The loss of accuracy in the 36-km solutions is rather large for both wind speed and direction. Nevertheless, the directions simulated on the 36-km domain are accurate enough to fall within the benchmark values for most layers and most segments. Wind speed MEs and RMSEs above the surface in the 36-km solutions are greater than the benchmarks, so that the effect on regional and inter-regional transport must be considered significant. In the surface layer, however, the 36-km RMSE for speed is within the benchmark. Therefore, the 36-km winds are only marginally suitable for use in air-quality applications. In general, the 12-km wind fields should provide more accurate solutions for transport calculations.

7. **The 36-km temperature fields have, in general, somewhat larger errors than those found in the 12-km temperature fields. However, the 36-km solutions have slightly smaller errors for the water-vapor mixing ratio. The differences are not significant in either field.**

   Since the differences in the 36-km and 12-km solutions are not very large for temperature or mixing ratio, it is concluded that both are acceptable for air-quality applications. However, the 12-km solutions are preferred because of the impact of temperature on air chemistry and they should have more fine-scale detail than the 36-km solutions.

REFERENCES

Alapaty, K., N.L. Seaman, D.S. Niyogi, and A.F. Hanna, 2000: Assimilating Surface Data to Improve the Accuracy of Atmospheric Boundary Layer Simulations. Accepted for *J. Appl. Meteor.*, **39**, 15 pp.

Ardao-Berdejo, J.A., and D.R. Stauffer, 1996: On the relative contribution of the Newtonian relaxation term in a non-hydrostatic mesoscale model used for dynamic analysis. Preprints, 11th Conf. On Num. Wea. Prediction, Amer. Meteor. Soc., Norfolk, VA, 19-23 August, 200-202.

Dudhia, J., 1989: Numerical study of convection observed during the winter monsoon experiment using a mesoscale two-dimensional model. *J. Atmos. Sci.,* **46**, 3077-3107.

Grell, G. A., J. Dudhia and D. R. Stauffer, 1994: A description of the fifth generation Penn State/NCAR Mesoscale Model (MM5). NCAR Tech. Note, NCAR TN-398-STR, 138 pp.

Kain, J. S., and J. M. Fritsch, 1990: A one-dimensional entraining/detraining plume model and its application in convective parameterization. *J. Atmos. Sci.,* **47**, 2784-2802.

_____, and J. M. Fritsch, 1993: Convective parameterization in mesoscale models: the Kain-Fritsch scheme. I*n the representation of cumulus convection in numerical models, A.M.S. Monograph, K.A. Emanuel, and D. J. Raymond, EDS.*, 165-170.

Michelson, S.A. and N.L. Seaman, 2000: Assimilation of NEXRAD-VAD Winds in Meteorological Simulations over the Northeast U.S. *J. Appl. Meteor.*, **39**, 367-383.

Seaman, N.L., 2000: Meteorological Modeling for Air-Quality Assessments. *Atmospheric Environment*, **34**, 2231-2259.

Seaman, N.L., D.R. Stauffer and A.M. Lario-Gibbs, 1995: A Multi-Scale Four-Dimensional Data Assimilation System Applied in the San Joaquin Valley During SARMAP: Part I: Modeling Design and Basic Performance Characteristics. *J. Appl. Meteor.*, **34**, 1739-1761.

Seaman, N.L. and S.A. Michelson, 2000: Mesoscale Meteorological Structure of a High-Ozone Episode during the 1995 NARSTO-Northeast Study. *J. Appl. Meteor.*, **39**, 384-398.

Shafran, P.C., N.L. Seaman and G.A. Gayno, 2000: Evaluation of Numerical Predictions of Boundary-Layer Structure during the Lake Michigan Ozone Study (LMOS). *J. Appl. Meteor.*, **39**, 412-426.

Stauffer, D.R., R.C. Munoz and N.L. Seaman, 1999: In-cloud turbulence and explicit microphysics in the MM5. Preprints, Ninth PSU/NCAR MM5 Moldeing System Users' Workshop, Boulder, Colorado, June 23-24, 177-180.

Stauffer, D.R. and N.L. Seaman, 1990: Use of Four-Dimensional Data Assimilation in a Limited-Area Mesoscale Model. Part I: Experiments with Synoptic-Scale Data. *Mon. Wea. Rev.*, **118**, 1250-1277.

Stauffer, D.R., N.L. Seaman and F.S. Binkowski, 1991: Use of Four-Dimensional Data Assimilation in a Limited-Area Mesoscale Model. Part II: Effects of Data Assimilation Within the Planetary Boundary Layer. *Mon. Wea. Rev.*, **119**, 734-754.

Stauffer, D.R., N.L. Seaman, T.T. Warner and A.M. Lario, 1993: Application of an Atmospheric Simulation Model to Diagnose Air-Pollution Transport in the Grand Canyon Region of Arizona, *Chemical Engineering Publications*, **121**, 9-26.

Stauffer, D.R. and N.L. Seaman, 1994: On Multi-Scale Four-Dimensional Data Assimilation. *J. Appl. Meteor.*, **33**, 416-434.

Wang, W. and N.L. Seaman, 1997: A Comparison Study of Convective Parameterization Schemes in a Mesoscale Model. *Mon. Wea. Rev.*, **125**, 252-278.

Zhang, D.-L., and R.A. Anthes, 1982: A high-resolution model of the planetary boundary layer -- sensitivity tests and comparisons with SESAME-79 data. *J. Appl. Meteo.*, **21**, 1594-1609.